HIGGS SEARCH

Conveners: P.J. Franzini and P. Taxil

Working Group: M. Drees, L. Roszkowski, G. Chiefari, G. Coignet, P. Janot, V. Innocente, P. Lebrun and J.-P. Martin

The Higgs sector remains one of the most elusive (and perhaps unsatisfactory) features of the standard model. Certainly one of the most important questions we may hope to shed light on at LEP I is that of the nature of the electroweak symmetry breaking mechanism. Many excellent, and in some cases encyclopedic, reviews of Higgs physics have been recently published (see for example the works of Cahn;[1] Dawson, Gunion, Haber and Kane;[2] Chanowitz;[3] and references therein); it is our purpose in this work to give a concise summary of Higgs physics and search prospects during the first phase of LEP. In Part I we concentrate on the Higgs sector as predicted in the Minimal Standard Model (one Higgs doublet only), and in Part II on various extensions of this minimal scenario.

PART I: Standard Model Higgs

1. Introduction and General Structure

We begin by recalling briefly the standard model Higgs mechanism, i.e., the introduction of masses via spontaneous symmetry breaking, preserving renormalizability, in a gauge invariant theory originally requiring massless chiral fermions and gauge bosons. The Lagrangian is

$$\begin{aligned} &\mathcal{L} = (D_\mu\phi)^\dagger(D^\mu\phi) - \frac{1}{4}F^{\mu\nu}F_{\mu\nu} - V(\phi), \qquad V(\phi) = \mu^2\phi^\dagger\phi + \lambda(\phi^\dagger\phi)^2 \\ &D_\mu = \partial_\mu - ig\vec{W}_\mu\cdot\vec{T} - ig'\frac{Y}{2}B_\mu \qquad\qquad - ig\vec{T}\cdot\vec{F}_{\mu\nu} = [D_\mu, D_\nu] \end{aligned} \tag{1.1}$$

where D_μ is the covariant derivative, in terms of the gauge fields $\vec{W}_\mu$ associated with the generators T_i of $SU(2)$ and B_μ associated with the generator Y of the $U(1)$.

Here the scalar field ϕ is the complex doublet under weak $SU(2)$

$$\phi = \begin{pmatrix} \phi^+ \\ \phi^0 \end{pmatrix} \qquad \text{with VEV} \quad <\phi> = \begin{pmatrix} 0 \\ v/\sqrt{2} \end{pmatrix} \tag{1.2}$$

(where VEV stands for vacuum expectation value). Picking this arbitrary alignment of the degenerate vacuum spontaneously breaks the symmetry, giving mass to three of the gauge bosons. The Higgs is the leftover degree of freedom, the surviving physical scalar H ($\phi_3 - <\phi_3>$, where ϕ_3 is the real part of the neutral scalar). We can read off the mass terms from

$$(D_\mu <\phi>)^\dagger(D^\mu <\phi>) = \frac{v^2}{8}\left[g^2(W_{1\mu}^2 + W_{2\mu}^2) + (gW_{3\mu} - g'B_\mu)^2\right]. \tag{1.3}$$

The combinations $(W_1 \pm iW_2)/\sqrt{2}$ are the $W^\pm$, with mass $M_W^2 = g^2v^2/4$. The combination $(gW_3 - g'B)/\sqrt{g^2+g'^2}$ is the Z, with mass $M_Z^2 = (g^2+g'^2)v^2/4$, and the orthogonal $(g'W_3 + gB)/\sqrt{g^2+g'^2}$ is the γ, remaining massless. Thus the VEV is determined

$$v = 2M_W/g = 2^{-1/4}G_F^{-1/2} = 246\,\text{GeV} \tag{1.4}$$

but the Higgs mass — given by $\sqrt{2\lambda v^2}$ — is undetermined.

The Higgs-vector boson couplings are given by the full covariant derivative term:

$$\frac{g^2}{4}(v+H)^2\left(W_\mu^+ W^{-\mu} + Z_\mu Z^\mu/2\cos^2\theta\right). \tag{1.5}$$

Thus we have the coupling gM_W for the HWW vertex; $gM_Z/\cos\theta_W$ for the HZZ vertex; $g^2/2$ for $HHWW$ and $g^2/2\cos^2\theta_W$ for the $HHZZ$ vertex. The weak interaction couplings of fermions are obtained by expanding the term $\bar{\psi}(iD_\mu\gamma^\mu - M)\psi$.

The fermion masses come from terms such as

$$g_{\phi dd}\left[\begin{pmatrix}\bar{u}_L & \bar{d}_L\end{pmatrix}\begin{pmatrix}\phi^+\\ \phi^0\end{pmatrix} d_R + \bar{d}_R\begin{pmatrix}\phi^- & \bar{\phi}^0\end{pmatrix}\begin{pmatrix}u_L\\ d_L\end{pmatrix}\right] \tag{1.6}$$

invariant under weak isospin. The parts coming from $<\phi>$ give the mass terms

$$\frac{v}{\sqrt{2}}(g_{\phi dd}\bar{d}d + g_{\phi uu}\bar{u}u) \tag{1.7}$$

where the g's are (unfortunately) arbitrary (if the masses are not measured) couplings. Similarly, with H instead of $<\phi>$, we get the couplings of the Higgs —

$$\frac{H}{\sqrt{2}}(g_{\phi dd}\bar{d}d + g_{\phi uu}\bar{u}u) = H(m_d\bar{d}d + m_u\bar{u}u)/v \tag{1.8}$$

giving the Higgs-fermion couplings $gm_f/2M_W$. All the Feynman diagrams containing Higgses, including those for the trilinear and quadrilinear self-couplings not discussed above, can be found, for example, in ref. 2.

The rest of this Part is organized as follows: in Chapter 2 we discuss Higgs decay – in Sec. 2.1 the partial widths to 2-body partonic modes (with no radiative corrections); in Sec. 2.2 we discuss QCD corrections to these decays. In Sec. 2.3 we discuss the hadronic decays of light Higgses. Chapter 3 covers the current limits on Standard Model Higgses — experimental (Sec. 3.1) and theoretical (Sec. 3.2). In Chapter 4 we concentrate on the production and decay of Higgses.

2. Higgs decay

2.1 Partial Widths (no radiative corrections)

We will not discuss decays such as $H \to W^+W^-, Z^0Z^0$ and $H \to W^\pm f\bar{f}', Z^0 f\bar{f}$ which are not relevant for Higgs masses small enough to be produced at LEP I; for a discussion of such decays see for example refs. 1-5.

$\underline{H \to f\bar{f}}$ The partial width to any fermion channel is

$$\Gamma(H \to \bar{f}f) = \frac{N_c g^2 m_f^2 M_H}{32\pi M_W^2}\beta_f^3 \tag{2.1}$$

where N_c is the color factor, 1 for leptons and 3 for quarks and $\beta_f = (1 - 4m_f^2/M_H^2)^{1/2}$ is the usual kinematic factor.

$H \to \gamma\gamma$ Another decay mode of the Higgs relevant at LEP I energies, for light Higgses, is the decay into two γ's. This does not occur at tree level, but is induced via one-loop corrections involving quarks, charged leptons and W bosons. For completeness we include the formula for contributions from charged scalars in the loop. (Fig. 1.)

(a) Triangle diagram for $H \to \gamma\gamma$ – with charged particles of spin-0, 1/2 or 1 in the loop

(b) Bubble diagram for $H \to \gamma\gamma$ – with charged particles of spin-0 or spin-1 in the loop

Figure 1

The width is given by[7]

$$\Gamma(H \to \gamma\gamma) = \frac{\alpha^2 g^2}{1024\pi^3}\frac{M_H^3}{M_W^2}\left|\sum_i e_i^2 N_{ci} F_i\right|^2, \quad \text{or}$$

$$\Gamma_{SM}(\text{in GeV}) = 1.0 \times 10^{-13} M_H^3(\text{in GeV}^3)\left(\frac{1}{3}\sum_{d,s,b} F_{1/2} + \frac{4}{3}\sum_{u,c,t} F_{1/2} + F_{1(W)}\right), \tag{2.2}$$

where i is an index referring to the sum over all relevant particles, of spin-0, spin-1/2, and spin-1; N_{ci} is again a color factor; e_i is the electric charge in units of e; and

$$\begin{aligned} F_0 &= \tau(1 - \tau f(\tau)), \\ F_{1/2} &= -2\tau[1 + (1-\tau)f(\tau)], \\ F_1 &= 2 + 3\tau + 3\tau(2-\tau)f(\tau), \end{aligned} \tag{2.3}$$

where $\tau = 4m_i^2/M_H^2$ (assuming that coupling of a particle to the Higgs is proportional to its mass, which is not always true for scalars in extended models). The complex function $f(\tau)$ is given by

$$f(\tau) = \left[\sin^{-1}\left(\sqrt{\frac{1}{\tau}}\right)\right]^2, \quad \tau \geq 1; \qquad f(\tau) = -\frac{1}{4}\left[\ln\left(\frac{\eta_+}{\eta_-}\right) - i\pi\right]^2, \quad \tau < 1 \tag{2.4}$$

where

$$\eta_\pm \equiv (1 \pm \sqrt{1-\tau}). \tag{2.5}$$

In Fig. 2 we show $F_{1/2}$, which will also come into $\Gamma(H \to gg)$. We note the large τ (i.e. loop particle much heavier than the Higgs) limits of the F_i

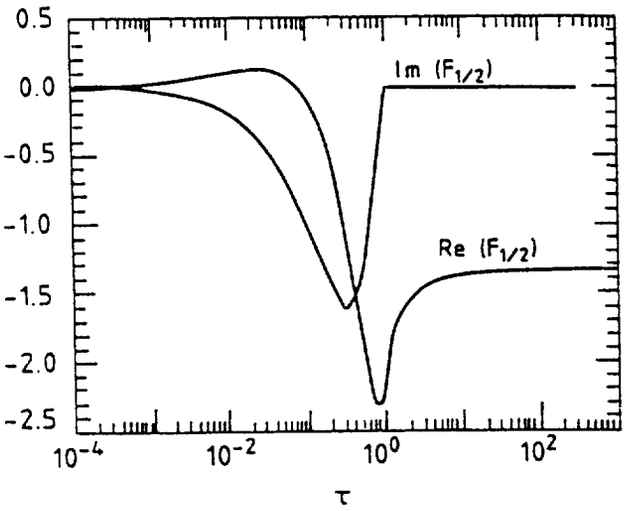

Figure 2. The loop factor $F_{1/2}$ appearing in the decays $H \to \gamma\gamma$ and $H \to gg$.

$$F_0 \to -\frac{1}{3}, \qquad F_{1/2} \to -\frac{4}{3}, \qquad F_1 \to 7, \tag{2.6}$$

illustrating the dominant W contribution, the smallness of the scalar contribution, and the opposite sign of the fermion and W terms. Once the loop particle is heavier than the Higgs, varying the loop particle mass has essentially no effect. As τ goes to zero, of course, these functions vanish.

For a light Higgs (lighter than the strange quark and the muon) the contribution from the heavy fermions (i.e. everything except e, u, and d) in the large τ limit is $-7.\overline{11}$, almost exactly cancelling the contribution from the W. Thus the 2γ decay is highly suppressed, and its magnitude is strongly dependent on the masses chosen for the light quarks. A large enhancement is therefore possible in a model with four generations; a extra generation, composed of particles of arbitrary masses large compared to the Higgs mass, gives a contribution of $\frac{32}{9}$. In Fig. 3 we show the partial widths for a Higgs decaying to two photons, illustrating the variation possible due to different choices for the light quark masses, and the enhancement due to a fourth generation, from a branching ratio for $H \to \gamma\gamma$ of $\approx 10^{-3}$ for the three generation case to as much as 35% in the four generation case for $M_H = 200$ MeV. Note that the cancellation, and hence the enhancement, only occurs for light Higgses ($M_H \lesssim 2m_s$); for heavier Higgses the predicted partial width in a four generation model can even lie below that for a three generation model.

$\underline{H \to gg}$ The Higgs decay to two gluons can be described by eqs. (2.2)-(2.6) by keeping only quark loops and replacing $\alpha^2 e_i^4 C_{fi}^2$ by $2\alpha_s^2$:

$$\Gamma(H \to gg) = \frac{\alpha_s^2 g^2}{512\pi^3} \frac{M_H^3}{M_W^2} \left| \sum_i F_{1/2i} \right|^2 . \tag{2.7}$$

Except in small windows, it is the heavy quarks that make the main contributions to $\Gamma(H \to gg)$ (since there is no W term to cancel the fermion contributions); thus a reasonable approximation is:

$$\Gamma(\text{in GeV}) = 1.5 \times 10^{-10} M_H^3(\text{in GeV}^3) n_h^2 \left(\frac{\alpha_s}{0.15}\right)^2 \tag{2.8}$$

where n_h is the number of quark flavors heavier than the Higgs. This expression can only be trusted for Higgs sufficiently heavy that α_s is small, above around 1 GeV.

In Fig. 4 we display the approximate partial decay widths of the Higgs – to photons, gluons, leptons and quarks. For the quarks we take current masses on the assumption that the pole of

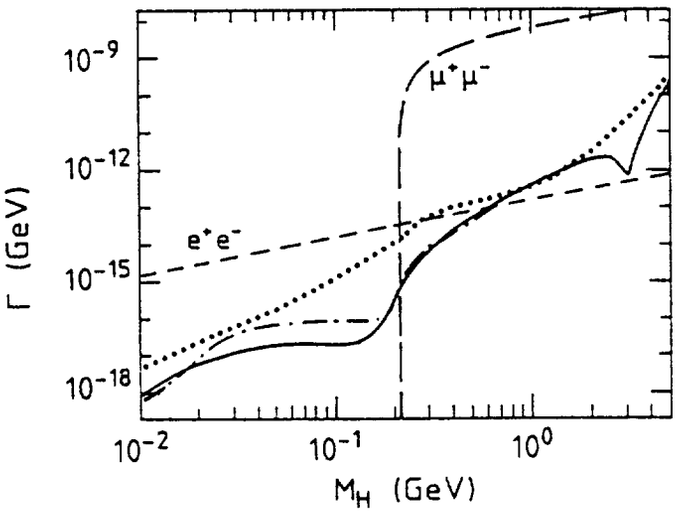

Figure 3. The partial decay widths of H to $\gamma\gamma$, and for comparison, to e^+e^- and $\mu^+\mu^-$ (both dashed). The solid line is for a three generation model, with $m_u = 5$ MeV, $m_d = 10$ MeV and $m_s = 150$ MeV; the dotdashed line is also for a three generation model, with $m_u = 10$ MeV, $m_d = 10$ MeV and $m_s = 200$ MeV; and the dotted line is for a four generation model, with $m_u = 5$ MeV, $m_d = 10$ MeV and $m_s = 150$ MeV.

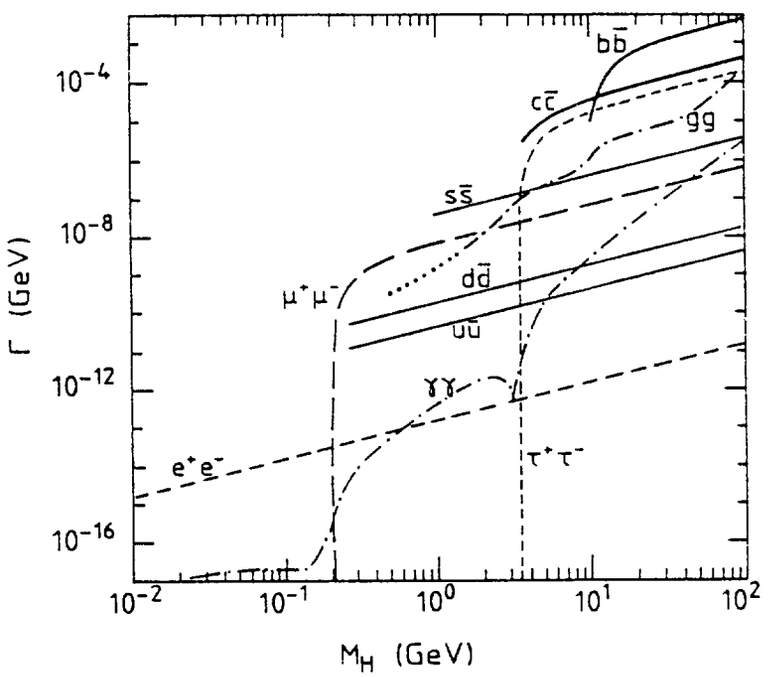

Figure 4. The approximate partial decay widths of H to all 2-body partonic decay modes. We use $m_u = 5$ MeV, $m_d = 10$ MeV, $m_s = 150$ MeV, $m_c = 1.5$ GeV, $m_b = 5$ GeV, and $m_t = 60$ GeV. The dashed curves show decays to charged leptons, the solid curves the decay into hadrons as computed from the contributions to each quark separately. The dotdashed curves illustrate the two gluon and two photon decays; for gluons we use the constant value $\alpha_s = 0.15$, with the understanding that the partial width given should be scaled by $\left(\frac{\alpha_s(q)}{0.15}\right)^2$.

the free quark propagator is most appropriate for the Higgs coupling. We choose $m_u = 5$ MeV, $m_d = 10$ MeV, $m_s = 150$ MeV, $m_c = 1.5$ GeV, $m_b = 5$ GeV and $m_t = 60$ GeV (see footnote 7 of ref. 8 for a further discussion of the possible variation in $\Gamma(H \to \gamma\gamma)$ due to different choices for quark masses). Of course the u and d modes do not open up until $M_H > 2m_\pi$ and so on. In illustrating the partial width to gluons we avoid the questions of what $\Lambda_{\overline{MS}}$ to use in calculating α_s, and of what scale to evaluate α_s at for a given M_H, by picking the constant value $\alpha_s = 0.15$; the result can then trivially be scaled by the square of one's favorite value of α_s. In Fig. 5 we show the lifetime and total width of the Higgs versus its mass, based on these partial widths. All hadronic widths given here are not very meaningful up to $1 - 2$ GeV; see Sec 2.3. We also leave the discussion of the subtleties pertaining to branching ratios to pions and so on to Section 2.3. In the next section we discuss the effects of radiative corrections to the decay widths.

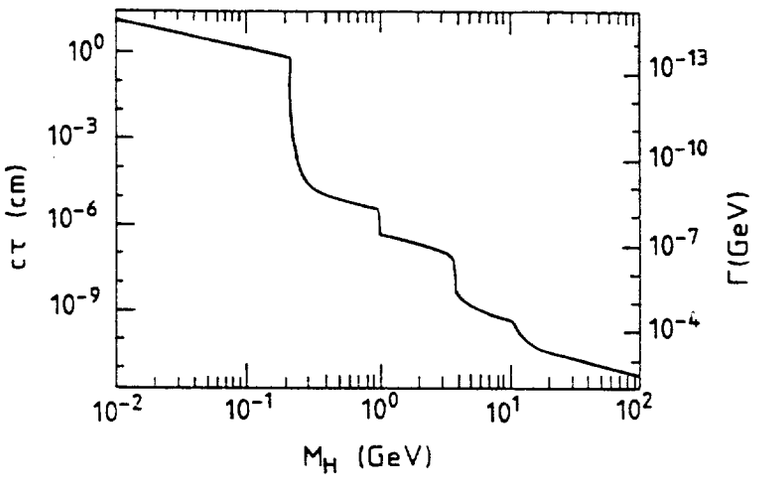

Figure 5. The lifetime and width of the Higgs versus its mass taking into account the decays displayed in Fig. 4. The "jumps" come from the imperfect treatment of the threshold — cutting off $q\bar{q}$ decays at the quarkonium mass. See Sec. 2.

2.2 QCD CORRECTIONS TO HIGGS BOSON DECAYS

The heavier Higgs bosons observable at LEP I, in the range very roughly speaking of 5 to 50 GeV, always have large or even dominant branching ratios for decays into heavy $q\bar{q}$ pairs. A quantitative prediction of the various branching ratios thus necessitates the inclusion of QCD corrections. We shall get a bit ahead of ourselves and discuss the decays of both the single Higgs H in the standard model, and a scalar H and pseudoscalar A^0 in an extended Higgs sector as well (see Chapters 6 and 7). For QCD corrections to the processes $H \to \gamma\gamma$, $H \to gg$ and $Z \to H\gamma$ we refer to Ref. 9.

For a scalar Higgs boson H, the 1-loop corrections have been computed[10] almost ten years ago, but a complete 1-loop calculation for the case of a pseudoscalar A^0 has only recently been performed.[11] The 1-loop corrections can be written in the general form

$$\Gamma_1(X \to q\bar{q}) = \Gamma_0(X \to q\bar{q}) \left[1 + \frac{4\alpha_s}{3\pi}\Delta_X(m_q, M_X)\right], \tag{2.9}$$

where X stands for H or A^0 and Γ_0 is the usual tree-level decay width. The functions Δ_X can be written as

$$\begin{aligned}\Delta_H &= \frac{1}{\beta_q}A(\beta_q) + \frac{1}{16\beta_q^3}(3+34\beta_q^2-13\beta_q^4)\ln\frac{1+\beta_q}{1-\beta_q} + \frac{3}{8\beta_q^2}(-1+7\beta_q^2)\\ \Delta_{A^0} &= \frac{1}{\beta_q}A(\beta_q) + \frac{1}{16\beta_q}(19+2\beta_q^2+3\beta_q^4)\ln\frac{1+\beta_q}{1-\beta_q} + \frac{3}{8}(7-\beta_q^2),\end{aligned} \tag{2.10}$$

with

$$\begin{aligned}A(\beta_q) = (1+\beta_q^2)\Bigg[&4\mathrm{Li}_2\left(\frac{1-\beta_q}{1+\beta_q}\right) + 2\mathrm{Li}_2\left(\frac{\beta_q-1}{1+\beta_q}\right) - 3\ln\frac{2}{1+\beta_q}\ln\frac{1+\beta_q}{1-\beta_q}\\ &-2\ln\beta_q\ln\frac{1+\beta_q}{1-\beta_q}\Bigg] - 3\beta_q\ln\frac{4}{1-\beta_q^2} - 4\beta_q\ln\beta_q.\end{aligned} \tag{2.11}$$

Here $\beta_q = (1-4m_q^2/M_X^2)^{1/2}$, and $\mathrm{Li}_2(x) = -\int_0^x \frac{\mathrm{d}t}{t}\ln(1-t)$ is the Spence function. The separate contributions from self-energy diagrams, real gluon emission, and virtual gluon emission can be found in Refs. 10 and 11.

It is interesting to consider the behavior of the QCD-corrections in the limiting situations $\beta_q \to 0$ or $\beta_q \to 1$. In the first case, corresponding to the region just above the $q\bar{q}$ threshold, one finds

$$\begin{aligned}\lim_{\beta_q\to 0}\Delta_H &= \frac{\pi^2}{2\beta_q} - 1 + \frac{\pi^2}{2}\beta_q + \mathcal{O}(\beta_q^2\ln\beta_q);\\ \lim_{\beta_q\to 0}\Delta_{A^0} &= \frac{\pi^2}{2\beta_q} - 3 + \frac{\pi^2}{2}\beta_q + \mathcal{O}(\beta_q^2\ln\beta_q).\end{aligned} \tag{2.12}$$

Note the occurrence of $\frac{1}{\beta_q}$ singularities with a positive sign. Very close to threshold, one would clearly have to add all terms of the form $(\alpha_s/\beta_q)^n$ in order to obtain a reliable result, even though the total one-loop result (2.9) is still finite as $\beta_q \to 0$; Schwinger[12] has shown for the case of QED that this summation is equivalent to the use of an $1/r$ potential to describe the interactions between the quark and the antiquark. In the case of QCD, these give rise[13] to a multitude of $q\bar{q}$ bound states and resonances; if $M_X \approx 2m_q$, these bound states will mix[14] with the Higgs boson, leading to a completely new phenomenology. We refer the reader to Ref. 11 for more details. Note, however, that the QCD-corrections remain positive out to $M_H \approx 4.3m_q$ and $M_{A^0} \approx 3.7m_q$, far outside the region where mixing effects are important. Indeed, eq. (2.9) should be trustworthy once the Higgs mass is 1 or 1.5 GeV above the physical open-flavor threshold.

In the opposite case $\beta_q \to 1$ one finds

$$\Delta_X \to 3\ln\frac{m_q}{M_X} + \frac{9}{4} \tag{2.13}$$

for $X = H$ or A^0. Notice the occurrence of a large negative logarithm, which would eventually even make the total decay width (2.9) negative. This is clearly unphysical. As already noticed

in Ref. 10, the solution is to sum these large logarithms to all orders, using renormalization-group techniques. We present here a formalism that can be used for all values of β_q (outside the resonance region, as discussed above). To this end, we sum the leading logs as in Ref. 10, but take care to keep the finite parts

$$\Gamma(X \to q\bar{q}) = \Gamma_0(X \to q\bar{q}) \left[\frac{\ln(2m_q/\Lambda)}{\ln(M_X/\Lambda)}\right]^{\frac{24}{33-2N_f}} \left[1 + \frac{4\alpha_s}{3\pi}(\Delta_X - 3\ln\frac{m_q}{M_X})\right], \qquad (2.14)$$

where Λ is the QCD scale parameter and N_f is the relevant number of flavors. The first term in square brackets is the renormalization group factor computed in Ref. 10; the second term in square brackets are the finite (for $\beta_q \to 1$) QCD corrections.

We also include the Higgs to gluons decay in our calculation. It can make a nonnegligible contribution to the total width even though it only proceeds via quark-antiquark (and, for the supersymmetric scalar, also by squark-antisquark) loops. Expressions for the relevant decay widths can be found in the previous section and Ref. 15.

We are now in a position to present detailed predictions for the various branching ratios of scalar and pseudoscalar Higgs bosons (Figs. 6-9). We have chosen the following values for the

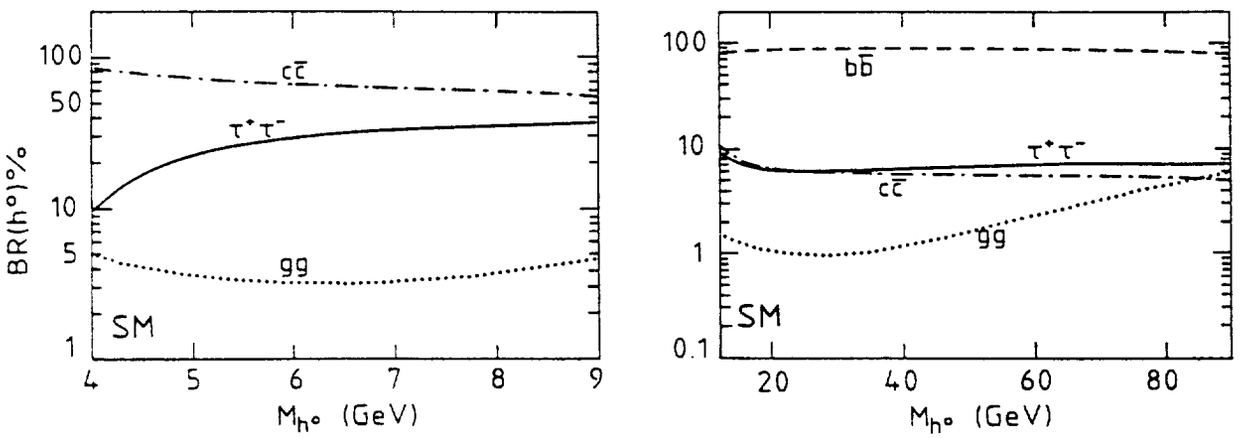

Figure 6. Branching ratios for a scalar Higgs in the standard model.

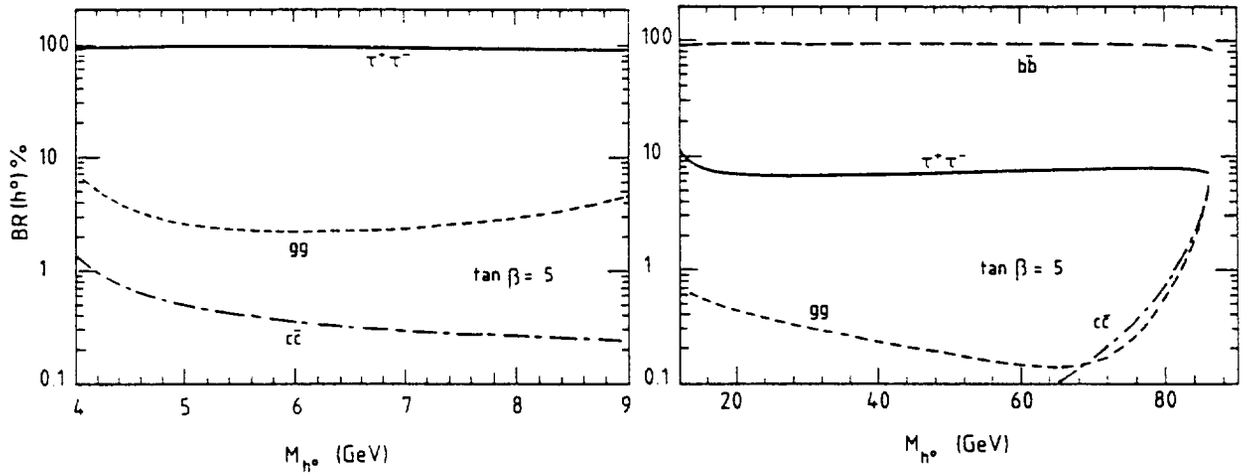

Figure 7. Branching ratios for a scalar Higgs in the minimal supersymmetric standard model (MSSM) with $\tan\beta = 5$.

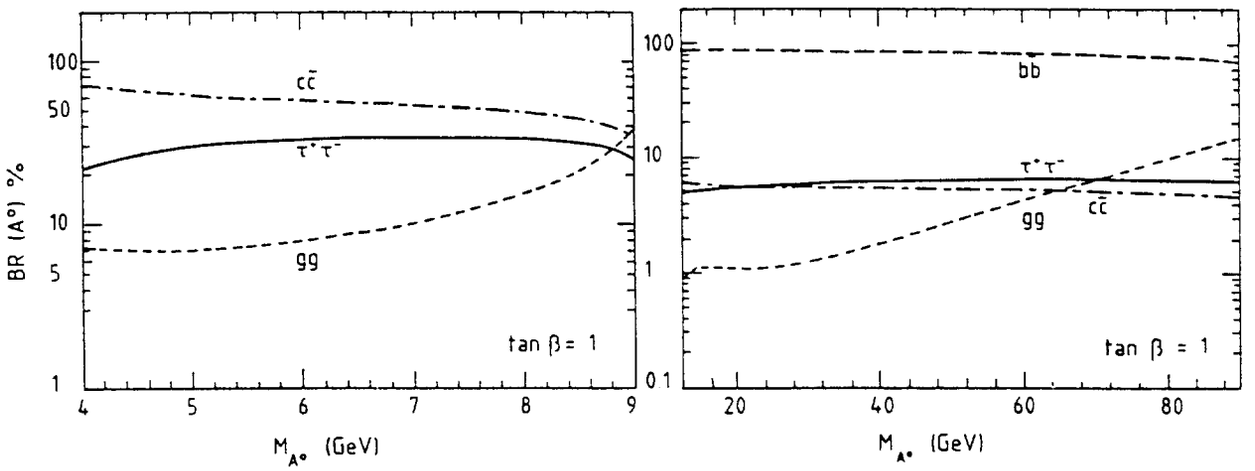

Figure 8. Branching ratios for a pseudoscalar Higgs in the MSSM with $\tan\beta = 1$.

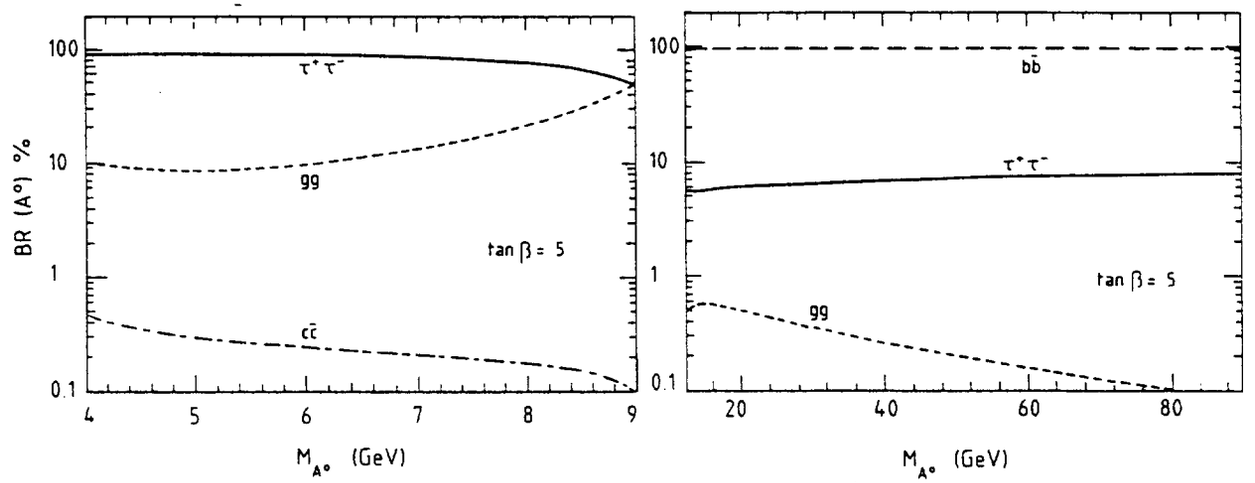

Figure 9. Branching ratios for a pseudoscalar Higgs in the MSSM with $\tan\beta = 5$.

relevant parameters: $m_c = 1.37$ GeV, $m_b = 4.5$ GeV, $m_t = 50$ GeV, $m_{\tilde{q}} = 100$ GeV, $\Lambda = 0.2$ GeV. The charm and bottom quark masses may seem rather low. However, the relevant mass here is the pole of the free quark propagator determined by perturbative methods, not the mass parameter of potential models, nor the mass of the lightest c or b flavored meson; the above values have been obtained in ref. 16 from QCD sum rules. On the other hand, the squark mass is so high that contributions to $H \to gg$ are insignificant. Finally, in order to avoid ugly kinks in our curves we use a phenomenological "running" N_f:

$$N_f = 3 + (1 - 4m_c^2/Q^2)\,\theta(Q^2 - 4m_c^2) + (1 - 4m_b^2/Q^2)\,\theta(Q^2 - 4m_b^2), \tag{2.15}$$

where Q^2 is the scale at which α_s is evaluated, and θ is the step function.

We cover the whole range of mass values (above the charm-threshold) relevant at LEP, except the region between 9 and 12 GeV, where the Higgs bosons mix[11,14] with $b\bar{b}$ bound states as described above. We included results for $\tan\beta = 1$, i.e., Standard Model-strength for all Yukawa couplings, and $\tan\beta = 5$ ($\tan\beta$ is defined in Sec. 6.1), but neglected the theoretically disfavored[17] region $\tan\beta < 1$; indeed, the top-quark Yukawa coupling will become non-perturbative if $\tan\beta \lesssim \frac{m_t}{175\ \mathrm{GeV}}$, i.e., $\tan\beta \lesssim 1/3$.

We see that one can always expect a healthy τ pair branching ratio below the beauty-threshold; for $\tan\beta > 1$ the decay into τ pairs quickly becomes dominant (see Figs. 7a and 9a). Even for larger Higgs masses (below $2m_t$) the branching ratio for $H, A^0 \to \tau^+\tau^-$ remains above 6%; this demonstrates the relevance of the QCD corrections, since without them this branching ratio would be below 5%. It might also be surprising that the gluonic branching ratio can be as large as 10% even without the inclusion of mixing effects (which are, however, responsible for the large $BR(A^0 \to gg)$ at $M_{A^0} = 9$ GeV, $\tan\beta = 5$). This shows that one can expect a sizeable fraction of Higgs events without any evidence for heavy quarks or leptons. Note, however, that the gluonic width is suppressed for heavier Higgs bosons if $\tan\beta > 1$, since this suppresses the Higgs-$t\bar{t}$ coupling (except in the region $M_H \gtrsim 70$ GeV in Fig. 7b, where one needs $M_{A^0} > M_Z$, which drives the couplings of H towards their Standard Model values). Notice finally how a P-wave threshold, QCD corrections and a fairly substantial $H \to gg$ width conspire to keep $BR(H \to b\bar{b})$ below 85% for the case of Standard Model couplings.

Before we leave the discussion of Higgs decays, two caveats are in order. First, as mentioned above, we have neglected Higgs$-(b\bar{b})$ mixing which for some combinations of parameters can result[11] in gluonic branching ratios of order 90%; this possibility to "hide" a Higgs boson should perhaps be kept in mind. Secondly, even though we have discussed a supersymmetric model, we have not included any supersymmetric decay modes of either Higgs boson. This is probably justified for charged sparticles whose lower bounds on the masses already approach 30 GeV, but branching ratios into neutralinos[18] or (for $\tan\beta \neq 1$) sneutrinos may be nonnegligible (although never dominant).

2.3 Hadronic decays of light Higgses

Below charm (or $\tau^+\tau^-$) threshold, the decays of the Higgs—predominantly to light hadrons made of u, d and s quarks—are not so readily understood (a first study of this process was done in Ref. 7). This is essentially because the masses of the light hadrons are not dominated by the "bare" or "current" quark masses that determine the Higgs coupling to fermions as discussed in Section 1. (We also recall the uncertainty in the partial width for $H^0 \to \gamma\gamma$ depending on the choice of quark masses involved in the loop.) Hence one cannot naively use these tiny masses ($m_u \approx 5$ MeV, $m_d \approx 10$ MeV) to estimate for example the partial width $\Gamma(H \to \pi\pi)$ from eq. (2.1). In the range $2m_\pi \lesssim M_H \lesssim 1$ GeV, which we will consider first, it would result certainly in an underestimation of this decay channel compared to the $\mu^+\mu^-$ channel which is of the utmost importance for Higgs detection in this mass range ($\Gamma(H \to \pi\pi)/\Gamma(H \to \mu\mu) \approx 3m_{u,d}^2/m_\mu^2 \approx 3 \times 10^{-2}$ in this approach).

It was pointed out by Voloshin[19] (following earlier investigations by other authors[20,21]) that the Higgs coupling to gluons via a triangle of heavy quarks (Fig. 10)

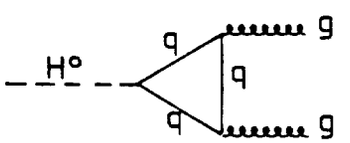

Figure 10. Triangle diagram contributing to Hgg interaction.

might be the dominant mechanism for the decay $H \to \pi\pi$, the difficulty being to convert the interaction Hgg into the interaction $H\pi\pi$. Adding the interaction with gluons (i.e., the contribution of n_h heavy quarks) and the direct interaction with the n_l light quarks constituting the light hadrons, one has to calculate

$$\langle \pi^+\pi^- | \mathcal{L}_{int} | H^0 \rangle \tag{2.16}$$

where

$$\mathcal{L}_{int} = -\frac{g}{2M_W}\left[\sum_{i=1}^{n_l} m_i \bar{\psi}_i \psi_i H^0 - \frac{2}{3}\frac{\alpha_s}{8\pi} n_h G^a_{\mu\nu} G^{\mu\nu a} H^0\right] \tag{2.17}$$

(the ψ's being quark fields and the G's gluon field strengths). Crucial use is made of the so-called conformal anomaly[22] allowing one to calculate the trace of the energy-momentum tensor in QCD

$$\theta^\mu_\mu = -\frac{b\alpha_s}{8\pi} G^a_{\mu\nu} G^{\mu\nu a} + \sum_{i=1}^{n_l} m_i \bar{\psi}_i \psi_i \tag{2.18}$$

where $b = 11 - \frac{2}{3}n_l$ is the first coefficient of the QCD beta function. Then, using standard techniques of chiral perturbation theory, one gets[7,19,21]

$$\langle \pi^+\pi^- | \theta^\mu_\mu | H^0 \rangle = M^2_{H^0} + 2m^2_\pi \tag{2.19}$$

Since PCAC gives

$$\langle \pi^+\pi^- | \sum_{i=u,d,s} m_i \bar{\psi}_i \psi_i | 0 \rangle \approx m^2_\pi \tag{2.20}$$

one gets for the decay amplitude[19] (with $n_l = n_h = 3$)

$$A(H^0 \to \pi^+\pi^-) = -\frac{g}{9M_W}\left(M^2_{H^0} + \frac{11}{2}m^2_\pi\right) \tag{2.21}$$

which leads to the ratio

$$R_{\pi\mu} \equiv \frac{\Gamma(H^0 \to \pi^+\pi^- + \pi^0\pi^0)}{\Gamma(H^0 \to \mu\mu)} = \frac{1}{27}\frac{M^2_{H^0}}{m^2_\mu}\left(1 + \frac{11}{2}\frac{m^2_\pi}{M^2_{H^0}}\right)^2 \frac{\beta_\pi}{\beta^3_\mu} \tag{2.22}$$

where β_i is the standard kinematic factor. Thus the Higgs branching ratio into $\mu^+\mu^-$ is suppressed in the range $2m_\pi \lesssim M_{H^0} \lesssim 1$ GeV ($R_{\pi\mu} \sim 4$ at $M_{H^0} \sim 1$ GeV). We present this branching ratio in Fig. 11. Another calculation[23] suggests that this branching ratio is severely suppressed in the range 0.95 to 1.1 GeV.

It has been pointed out[24] that the above formula is only reliable as an order of magnitude estimate since the knowledge of the full QCD beta function is in principle necessary to calculate

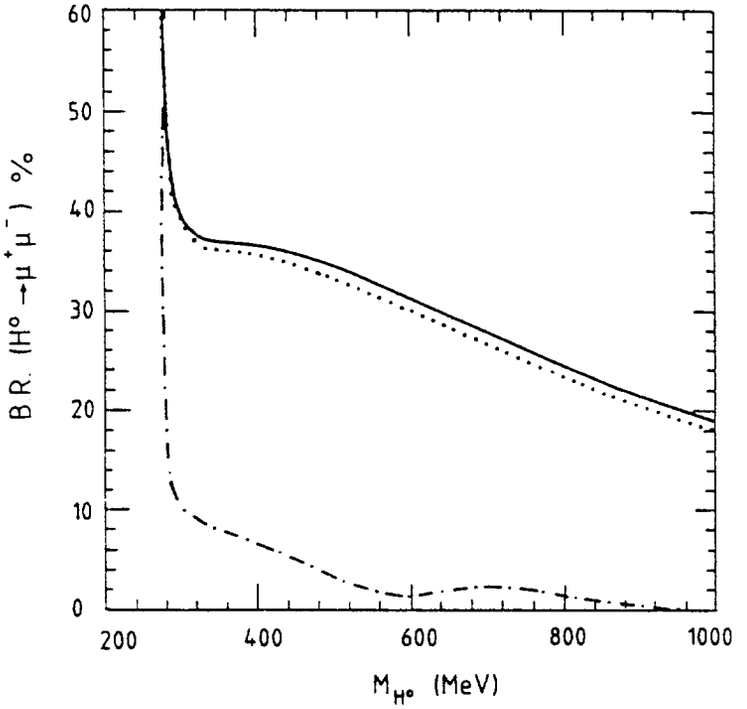

Figure 11. Branching ratio (%) for $H^0 \to \mu^+\mu^-$ according to eq. (2.22) (solid), with leading order QCD corrections—eq. (2.23)—(dots), and with resonance enhancement—eq. (2.24)—(dotdashed).

the trace anomaly (eq. (2.18)). Note however that the leading order QCD correction to the amplitude (eq. (2.21)) has been obtained recently[25] giving:

$$A(H^0 \to \pi^+\pi^-) = -\frac{g}{9M_W}\left[\left(1+\frac{\alpha_s}{\pi}\frac{35}{36}\right)M_{H^0}^2 + \frac{11}{2}\left(1-\frac{\alpha_s}{\pi}\frac{37}{198}\right)m_\pi^2\right]. \tag{2.23}$$

Obviously the correction is small for $0.1 \lesssim \alpha_s \lesssim 0.3$, resulting in at most a 5% decrease of the $\mu^+\mu^-$ branching ratio (see Fig 11).

An alternative approach has been considered by Grinstein et al;[26] using a chiral lagrangian they get a formula more general than eq. (2.21) but the sensitivity to two unknown strong interaction parameters makes the prediction uncertain.[27] In addition, taking into account the effects of final state $\pi\pi$ interaction as stressed by Raby and West[28] might lead to a dramatic increase of the ratio $R_{\pi\mu}$. This approach obliges us to deal with the complicated sector of $\pi\pi$ resonances — each resonance of mass M_R and width Γ_R which is taken into account causes $R_{\pi\mu}$ to be multiplied by an enhancement factor of

$$\frac{\left(M_R^2 + m_\pi\Gamma_R\right)^2}{\left(M_R^2 - M_{H^0}^2\right)^2 + M_{H^0}^2\beta_\pi^2\Gamma_R^2/4}. \tag{2.24}$$

We show in Fig. 11 the consequent suppression of the $\mu^+\mu^-$ branching ratio by a factor of 5 ($M_{H^0} \approx 300$ MeV) to 10 ($M_{H^0} \approx 700$ MeV) or more according to the phenomenological analysis performed in ref. 29.

The situation above $K\bar{K}$ threshold and below the τ or charm threshold is perhaps even more uncertain. Some authors[19] propose to use eq. (2.22) by simply substituting the masses of the mesons and multiplying by a factor of 4/3 for $K\bar{K}$ and 1/3 for $\eta\eta$ to take into account the number of states. However, others[1,2] point out that the accuracy of the low energy relations used to derive eq. (2.22) become suspect above 1 GeV. Then one may come back to a perturbative spectator approach — for instance a direct coupling to an $s\bar{s}$ pair with $m_s \sim 150$ MeV would give the decay into $K\bar{K}$ larger than into gg (which contributes to a variety of final states) if one follows the results displayed in Fig. 4. A recent analysis[30] has been performed taking into account the effect of a possible gluonium candidate G(1.6)[31] (named $f_0(1590)$ by the Particle Data Group[32]) which might enhance the $\eta\eta$ and $\eta'\eta$ modes around 1.6 GeV leading to a $\mu\mu$ branching ratio of $\sim 2\%$ in this region. In conclusion, a large uncertainty remains on this subject and the resulting $\mu\mu$ branching ratio is between 20% and 2% (possibly even smaller) in this range, according to various calculations.[1,2,26,30]

Higgs-nucleon coupling Similar techniques allow one to estimate[33] the Higgs-nucleon effective coupling, which is essential to set limits on a very light Higgs from nuclear physics experiments (see Sec. 3.1). The result may be written as

$$g_{H^0NN} = \frac{gM_N}{2M_W}\eta \tag{2.25}$$

where η parametrizes the difference from the naive result obtained if the nucleon is treated as fundamental like a quark. Analogous analyses to the ones we have summarized above give η between 0.2 and 0.5 to be probable, depending on the assumptions made on n_l, n_h. Note that if only the direct couplings of the Higgs boson to the u and d quarks in the nucleon were taken into account one would get a Higgs-nucleon coupling two orders of magnitude smaller.

3. Current limits

3.1 Summary of experimental limits and loopholes

Direct experimental constraints on the Higgs boson are currently few and far between, and suffer from considerable theoretical uncertainties, notably in the couplings to light hadrons as discussed in Sec. 2.3. In this section we briefly summarize some of the existing experimental results (see Refs. 1, 2, and 34, for example, for details). This is by no means a complete survey; rather we concentrate on the most recent or stringent results, e.g. those from SINDRUM,[35] RSC,[36] NA31,[8] CUSB,[37] and CLEO.[38]

Muonic x rays provide one of three limits extending down to arbitrarily small Higgs masses. A light Higgs boson could mediate an additional muon-nucleon interaction (too short-range to have effect if $M_H \gtrsim 10$ MeV). Beltrami et al[39] have measured the $3d_{5/2} - 2p_{3/2}$ X ray transition in ^{24}Mg and ^{28}Si muonic atoms, finding agreement with theoretical expectations to within 3 parts per million. In Fig. 12 we show the resultant bound on the coupling combination $|g_{HNN}g_{H\mu\mu}/e^2|$ versus the Higgs mass. On the righthand axis we give η, which parametrizes

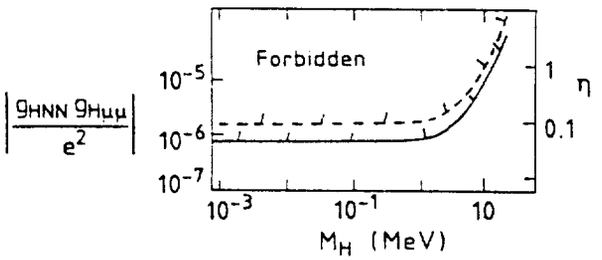

Figure 12. Limits on light Higgs bosons from muonic x-ray transitions (from Ref. 39). The solid line is the 1σ limit given in Ref. 39 and the dashed line is the 2σ limit.

the uncertainty in the calculation of g_{HNN}, as discussed in Sec. 2.3. For the conservative value $\eta = 0.2$, we find $M_H \gtrsim 3$ MeV (95% c.l.); for $\eta = 0.3$ the 1σ limit gives $M_H \gtrsim 8$ MeV. Note, however, that while no present theoretical calculation gives $\eta \lesssim 0.1$ (which would destroy this bound), given the uncertainties in such calculations, such a possibility cannot really be ruled out.

Another limit on extremely light Higgses is found by comparing electron-deuteron scattering experiments (relatively large 4-momentum transfer — $0.01 < t < 0.1$ GeV^2, t being the usual Mandelstam variable) with thermal electron-neutron scattering experiments (very small t). Adler et al[40] have noted that the presence of a scalar field will modify the electron-neutron Coulomb interaction, but can be ignored for the electron-deuteron scattering (the additional term in the potential is of the form $g_{Hee}g_{HNN}/(t - M_H^2)$). This gives the limit

$$M_H(\text{in MeV}) \gtrsim \frac{\sqrt{|g_{Hee}g_{HNN}/e^2|}}{5 \times 10^{-4}} = \frac{\sqrt{|g_{H\mu\mu}g_{HNN}/e^2|}}{7.19 \times 10^{-3}} = 0.55\sqrt{\eta}. \qquad (3.1)$$

This limit, while weaker than the previous one for expected η values, is notable in that it excludes a massless Higgs under any assumptions.

Finally, a limit on massless — and very light — Higgses comes from combining CUSB limits[41] on Υ decays to a photon plus a massless scalar ($BR(\Upsilon \to \gamma + scalar) < 0.59 \times 10^{-4}$ at 68.4% c.l.) with Crystal ball limits[42] on J/ψ decays to a photon plus a massless scalar ($BR(J/\psi \to \gamma + scalar) < 0.96 \times 10^{-5}$ at 68.4% c.l.). Using 1st order radiative corrections from Ref. 43, with $\alpha_s(m_b) = 0.174$ for Υ and $\alpha_s(m_c) = 0.25$ for J/ψ, the experimental product branching ratio is approximately four times smaller than the theoretical prediction for an infinitely long lived Higgs[44] (these radiative corrections are very large, however, and one must worry about what higher order corrections may bring). A very light Higgs is also constrained, since it has a high probability of living long enough to escape the detectors; the limit deduced is $M_H < 61$ MeV (90%).[44] Each measurement alone could also be used to give a limit; the Crystal Ball limit is somewhat stronger but even more subject to radiative correction uncertainties due to the larger α_s.

This limit can be very simply applied outside the standard model; in fact in the simplest extension ("Model II" in part II), this limit can be applied identically to the pseudoscalar Higgs because the two branching ratios change by equal and opposite factors. The scalar Higgs combined branching ratio unfortunately must be multiplied by the factor $\cos^2\alpha \sin^2\alpha / \cos^2\beta \sin^2\beta$ where α and β are mixing angles defined in part II.

In the mass range $2m_e \lesssim M_{H^0} \lesssim 20$ MeV both low energy neutron-nucleon scattering and certain $0^+ \to 0^+$ nuclear transitions would see the effect of a light Higgs. The neutron-nucleon scattering excludes the region[45]

$$1 \text{ MeV} \lesssim M_{H^0} \lesssim 13\sqrt{\eta} \text{ MeV}. \tag{3.2}$$

The $0^+ \to 0^+$ transitions, for $\eta = 0.3$,[46] exclude the region

$$2.8 \text{ MeV} \lesssim M_{H^0} \lesssim 11.5 \text{ MeV}. \tag{3.3}$$

The decay $\pi^+ \to e^+\nu$, with a Higgs emitted by the virtual W, gives limits on very light Higgses without problems with Higgs-nucleon couplings. One has (see, e.g., Ref. 34)

$$\frac{\Gamma(\pi^+ \to e^+\nu_e h^0)}{\Gamma(\pi^+ \to \mu^+\nu_\mu)} = \frac{\sqrt{2}G_F m_\pi^4 f(x)}{48\pi^2 m_\mu^2 (1 - m_\mu^2/m_\pi^2)^2} = 6.5 \times 10^{-9} f(x) \tag{3.4}$$

where $f(x) \equiv (1 - 8x + x^2)(1 - x^2) - 12x^2 \log x$ with $x \equiv M_{H^0}^2/m_\pi^2$. The SINDRUM[35] collaboration at PSI measures $\Gamma(\pi^+ \to e^+\nu_e e^+ e^-)/\Gamma(\pi^+ \to \mu^+\nu_\mu) = (3.2 \pm 0.5) \times 10^{-9}$. Taking into account M_H dependent acceptance and efficiency, they place an upper limit on $BR(\pi^+ \to e^+\nu_e H)$ shown in Fig. 13. Comparison with the theoretical prediction, also shown, excludes the region

$$10 \text{ MeV} \lesssim M_{H^0} \lesssim 110 \text{ MeV}. \tag{3.5}$$

This limit is easily applied outside the standard model by adjusting for the modified WWH coupling. In Fig. 13 we also show the analogous limit that can be deduced[36] from the BNL neutrino experiment RSC, which only excludes 10 MeV $\lesssim M_{H^0} \lesssim$ 40 MeV, but sets lower limits on $BR(\pi^+ \to e^+\nu_e H)$ in some of this range, of possible interest outside the standard model. Charged lepton decays (e.g., $\tau \to e\nu\bar{\nu}H$) are similarly free from theoretical uncertainty, but the branching ratios are too small for current experimental sensitivities.

Proceeding upwards in M_H, the next limit comes from a recent NA31[8] analysis. They search for the sequence of decays $K_L^0 \to \pi^0 H^0$ followed by $H^0 \to e^+e^-$. They see 3 candidates,

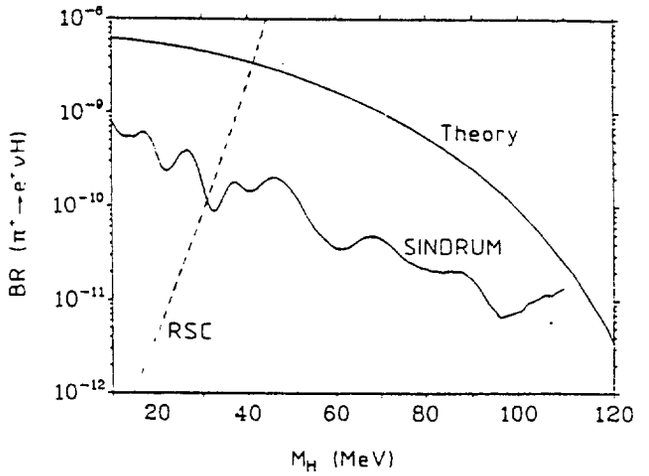

Figure 13. SINDRUM[35] and RSC[36] limits on $BR(\pi^+ \to e^+\nu_e H)$ vs M_H, and the theoretical prediction for this quantity.

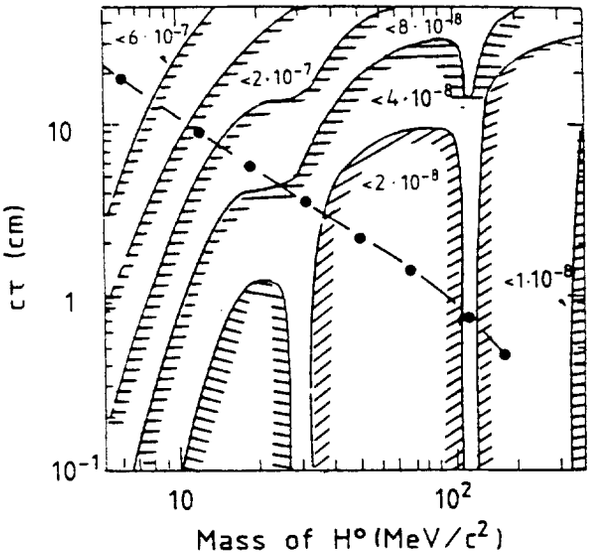

Figure 14. 90% confidence limits on $BR(K_L^0 \to \pi^0 H^0) BR(H^0 \to ee)$ from NA31 as a function of M_H and τ_H. Also shown (dot-dashed line) are the range of values for the lifetime as a function of mass for the Standard Model Higgs (from Ref. 8).

consistent with an expected background of 3.3. Their results, shown in Fig. 14, are given as contours of $BR(K^0 \to \pi^0 H^0) BR(H^0 \to e^+e^-)$ in the $M_H - \tau_H$ (Higgs lifetime) plane. (Slightly weaker bounds are found[47] by E731 at Fermilab; but "these limits depend on *a posteriori* analysis of experiments that were not designed to observe non-zero H^0 lifetimes."[8]) The line in this plane corresponding to the Standard Model is also shown; other models correspond to different lines. The theoretical situation is summarized by, among others, Ref. 2. They conclude

$$BR(K_L^0 \to \pi^0 H^0) \gtrsim 2.4 \times 10^{-5} \beta_{H^0} \tag{3.6}$$

where β_{H^0} is the standard kinematical factor (however, they have assumed three generations and a heavy top quark, i.e., $m_t > 80$ GeV). (In fact, lower limits on $m_t|V_{td}|$ from $B\bar{B}$ mixing measurements mean that these branching ratios may be expected to be 1-2 orders of magnitude larger.) Thus, for example, by following along the standard model line in Fig. 14, we see that the 90% confidence upper limit on $BR(K_L^0 \to \pi^0 H^0) BR(H^0 \to e^+e^-)$ is better than 2×10^{-8} for a Higgs of mass 100 MeV. This is to be compared with a theoretical estimate of order 10^{-5} from eq.(3.6) (note that β is of order 1 in the whole range of NA31 sensitivity, as is $BR(H^0 \to e^+e^-)$). However, there is still the possibility of a "fine-tuned" cancellation (see, e.g., the discussion in Ref. 34) which can make this branching ratio *arbitrarily* small. Thus the region 110 MeV to $2m_\mu$ is very unlikely, but not strictly excluded. The extension of these limits outside of the standard model is fairly complicated as both the $M_H - \tau_H$ curve and the predicted branching ratio must be recalculated, and do not change in a simple way.

Experimental limits on $K \to \mu^+\mu^-$ are roughly two orders of magnitude weaker than those for $K \to e^+e^-$ and make a Higgs between $2m_\mu$ and $2m_\pi$ "unlikely." More convincing limits in this region come from B physics. A consensus has been reached now on the decay width for the inclusive decay $B \to H^0 X$, and we have

$$BR(B \to H^0 X) = 0.36 \left(\frac{4.5\text{GeV}}{m_b}\right)^2 \left(\frac{m_t}{M_W}\right)^4 \left(1 - \frac{M_{H^0}^2}{m_b^2}\right)^2 \left|\frac{V_{ts}V_{tb}}{V_{cb}}\right|^2 . \tag{3.7}$$

as given in Ref. 2, using the experimental branching ratio for $B \to e\nu X$ of 0.123. Unitarity of the CKM matrix (in a three-generation model) gives the CKM factor to be ≈ 1. Then the TASSO limit[48]

$$BR(B \to \mu^+\mu^- X) < 0.02(95\% \text{ c.l.}) \text{ for } 2m_\mu < M_H \lesssim 5 \text{ GeV} \tag{3.8}$$

excludes the region $2m_\mu < M_H \lesssim 2m_\pi$ for $m_t \gtrsim 40$ GeV.

Note however that both TASSO and JADE (next paragraph) limits are really for $B \to \mu\mu X$, not for $B \to HX \to \mu\mu X$. They use final state particle distributions for three body final states, rather than for two step decays, with a two body intermediate state. This has been criticized many times.

Much stronger bounds on $BR(B \to \mu^+\mu^- X)$ are available for larger Higgs masses, e.g., from JADE[49] and CLEO[38] :

$$\begin{aligned} &BR(B \to \mu^+\mu^- X) < 0.007(95\% \text{ c.l.}) \text{ for } 0.3 < M_H \lesssim 5 \text{ GeV(JADE)} \\ &BR(B \to \mu^+\mu^- X) \lesssim 10^{-3} - 10^{-5}(90\% \text{ c.l.}) \text{ for } 1.0 \lesssim M_H \lesssim 3.5 \text{ GeV(CLEO)} \end{aligned} \tag{3.9}$$

These limits make a Higgs in the region 0.3 to 3.5 GeV rather unlikely; however the uncertainty in $BR(H \to \mu^+\mu^-)$ discussed in Sec. 2.3 precludes a solid limit. The exclusive channel $B \to KH$ excludes the same region[2,38] if we make the assumption

$$r_K \equiv \frac{BR(B \to KH)}{BR(B \to HX)} \gtrsim 0.01 \tag{3.10}$$

— a rather conservative estimate, but nonetheless not completely guaranteed.[2] These bounds, already highly dependent on theoretical estimates, become even more complicated outside the standard model.

The highest mass region is covered by measurements of the decay $\Upsilon \to H\gamma$ by the CUSB collaboration.[37] To lowest order one has[50]

$$\frac{\Gamma(\Upsilon \to H\gamma)}{\Gamma(\Upsilon \to \mu^+\mu^-)} = \frac{G_F m_b^2}{\sqrt{2}\pi\alpha}\left(1 - \frac{M_H^2}{M_\Upsilon^2}\right). \tag{3.11}$$

Unfortunately first order QCD corrections reduce this by about 50%.[43] Reanalysis in the $\overline{MS}$ scheme[51] finds the suppression to be somewhat smaller. However, one must worry about what higher order corrections might bring; moreover, further suppressions (or enhancements) may come from relativistic corrections to quarkonium decay.[52] In Fig. 15 we show the CUSB limit on $BR(\Upsilon \to \gamma + X)$ versus M_H, along with the theoretical predictions without radiative corrections, with those of Ref. 43, and with those of Ref. 51. We do not show possible effects of higher order radiative corrections (so far uncalculated) or relativistic corrections. Without these, a Higgs of up to 5 to 6 GeV is excluded. Limits are easily deduced for nonstandard models by

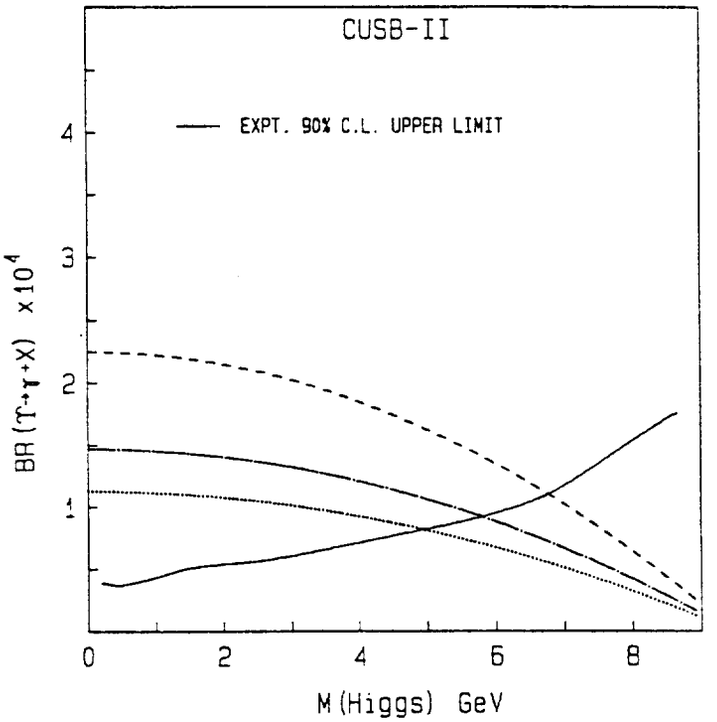

Figure 15. 90% confidence limits on $BR(\Upsilon \to \gamma + X)$ from CUSB (solid line) compared to the lowest order calculation (dashed line); the calculation with radiative corrections of Ref. 43 (dotted line); and radiative corrections of Ref. 51 (dotdashed line). From Ref. 37 (combined data sample, 800,000 Υ and 600,000 Υ'' events).

scaling the $BR(\Upsilon \to \gamma + X)$ as the square of the $Hb\bar{b}$ coupling (see Part II, for example eq. 7.6). ARGUS also excludes the Higgs from Υ radiative decays for $290 < M_H < 570$ MeV (through searches for H to $\pi\pi$).[53]

We conclude that, in the standard model a massless Higgs, and a Higgs with mass between 10 and 110 MeV, are excluded. A Higgs below 5-6 GeV is very unlikely — but a theoretical loophole exists to every experimental bound. In many of the cases described above, the most conservative theoretical estimate available preserves the bound; however one cannot with complete confidence state that the real answer could not be even "worse" than that estimate. Thus a LEP search in this region, which should be less plagued by theoretical uncertainty, is imperative to finally lay to rest these nagging doubts. Moreover, outside the standard model, where exclusions will probably have to be negotiated on a model by model basis, further limits on branching ratios and couplings are essential.

3.2 Theoretical limits

Upper and lower limits on Higgs masses can be derived by considering the constraints of vacuum stability and triviality. We do not pretend to go into all the subtleties of these arguments, but will instead try to give the basic flavor of the ideas involved, and of the kinds of bounds that can be extracted. For a detailed review of such physics the reader is referred to the forthcoming review by Sher.[54] These bounds, like their experimental counterparts, do not in general apply outside the minimal standard model, as we shall discuss in part II.

We first note that useful limits on M_H, unlike on m_t, cannot be placed by considering the contributions of the Higgs to radiative corrections, along with precision measurements of the electroweak ρ parameter and $\sin^2\theta_W$. This is because of the "screening" theorem[55] — at one loop the corrections go as $\frac{g^2}{16\pi^2}\log\left(\frac{M_H}{M_W}\right)$ while at two or more loops there are corrections of order $\left(\frac{g^2}{16\pi^2}\right)^2\left(\frac{M_H^2}{M_W^2}\right)$. Thus, for large Higgs masses, the theory is strongly coupled, but these effects are screened by an extra factor of g^2. A global fit to existing data gives $\sin^2\theta_W$ to an error of 0.0048, or 0.0064 if one simultaneously fits ρ, while the uncertainty in $\sin^2\theta_W$ due to Higgs effects with M_H unknown (10 GeV to 1 TeV) is 0.002.[56]

We now turn to limits deriving from considerations of vacuum stability and triviality. We recall from Chapter 1 that the Higgs mass is given by $\sqrt{2\lambda v^2}$ or thus $\lambda = g^2 M_H^2/8M_W^2$. It might seem therefore that arbitrarily low Higgs boson masses should be achievable. This is not so, as was shown by Linde[57,58] and by Weinberg.[59]

The limits from both vacuum stability and triviality can be discussed using the renormalization group equations at one loop. To be complete it is necessary to simultaneously consider the evolution of the $SU(3)_c \times SU(2)_W \times U(1)$ coupling constants g_s, g and g' (whose evolution is independent of fermion Yukawa couplings and λ); of fermion Yukawa couplings — only $g_t = m_t\sqrt{2}/v$ is relevant, the other fermions being too light — (this evolution depends on g_s, g and g', but is independent of λ) and of λ, whose evolution is given by[60,2]

$$\frac{d}{dt}\lambda = \frac{1}{16\pi^2}\left[12\lambda^2 + 6\lambda g_t^2 - 3g_t^4 - \frac{9}{2}\lambda g^2 - \frac{3}{2}\lambda g'^2 + \frac{3}{16}[2g^4 + (g^2+g'^2)^2]\right] \tag{3.12}$$

where $t = \log(Q^2/Q_0^2)$, Q being the energy scale and Q_0 some reference scale. For the vacuum stability bound, yielding a lower bound on M_H for $m_t < 80$ GeV, we may neglect the self-dependence in the evolution of λ (since for $M_H \lesssim 7$ GeV, $\lambda \lesssim 0.001g^2$) and write

$$\frac{d}{dt}\lambda = \frac{1}{16\pi^2}\left[-3g_t^4 + \frac{3}{16}[2g^4 + (g^2+g'^2)^2]\right] \equiv \beta_\lambda. \tag{3.13}$$

We refer the reader to, for example, refs. 60 or 2 for the renormalization group equations for the couplings g_s, g, g' and g_t. Approximating β_λ by a constant and integrating up to scales Q of order of the field ϕ itself gives (defining $\phi^2 \equiv \phi^\dagger\phi$),

$$\lambda(\phi) = \lambda(Q_0) + \beta_\lambda \log\frac{\phi^2}{Q_0^2}. \tag{3.14}$$

This can then be used to specify the one-loop effective potential[61]

$$V = \lambda(\phi)\phi^4 + \cdots = -\mu^2\phi^2 + \lambda(Q_0)\phi^4 + \beta_\lambda\phi^4\log\left(\frac{\phi^2}{Q_0^2}\right). \tag{3.15}$$

The VEV can then be determined by the extremal condition

$$\left.\frac{\partial V}{\partial\phi}\right|_{\phi=v/\sqrt{2}} = 0 \tag{3.16}$$

yielding

$$-\mu^2 + \lambda v^2 + \beta_\lambda v^2(\log(v^2/2Q_0^2) + 1/2) = 0 \tag{3.17}$$

as well as a solution at $v = 0$. The value of the potential at the extremum is then

$$V(v/\sqrt{2}) = -\frac{\lambda(Q_0)v^4}{4} - \frac{\beta_\lambda v^4}{4}\left(\log\frac{v^2}{2Q_0^2} + 1\right). \tag{3.18}$$

The mass of the Higgs particle is given by the coefficient of the H^2 term when we expand about the VEV: $\phi = v/\sqrt{2} + H$ or

$$M_H^2 = \frac{1}{2}\frac{\partial^2 V}{\partial\phi^2}\bigg|_{\phi=v/\sqrt{2}} = 2v^2\left[\lambda(Q_0) + \beta_\lambda\left(\log\left(\frac{v^2}{2Q_0^2}\right) + \frac{3}{2}\right)\right] = 2v^2\left[-\frac{4}{v^4}V\left(\frac{v}{\sqrt{2}}\right) + \frac{\beta_\lambda}{2}\right] \tag{3.19}$$

using eq. (3.17) to eliminate μ^2 and eq. (3.18) to eliminate $\lambda(Q_0)$. The requirement that the symmetry breaking vacuum be preferred, i.e., $V(v/\sqrt{2}) < V(0) = 0$, then yields the Linde-Weinberg bound

$$M_H^2 > \beta_\lambda v^2 = \frac{3}{16\pi^2 v^2}\left[2M_W^4 + M_Z^4 - 4m_t^4\right] \tag{3.20}$$

with no adjustment possible via negative values of $\lambda(Q_0)$. We will refer to this value as M_{LW}. This bound is valid up to $m_t^4(critical) = (2m_W^4 + m_Z^4)/4 = 80$ GeV; we will discuss bounds for greater values of m_t shortly. The m_t dependence of M_{LW} is illustrated in Fig. 16.

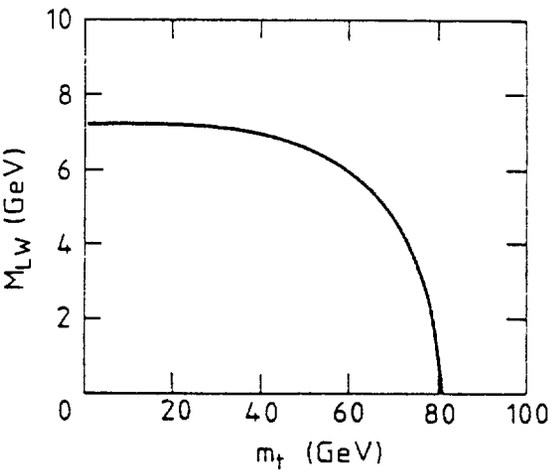

Figure 16. The lower limit on M_H, M_{LW}, as a function of m_t.

We note that since β_λ is given by eq. (3.13), and v is given by $v^2 = 4M_W^2/g^2$, there is only one independent parameter in the problem, which can be chosen, for example, to be the scale Q_0. If we define Q_0 to be the scale at which $\lambda(Q_0) = 0$ — a convenience, not a constraint — we can parametrize the system very simply in terms of $\lambda' = \lambda(v/\sqrt{2}) = \beta_\lambda \log\frac{v^2}{2Q_0^2}$:

$$\begin{aligned} M_H^2 &= 2v^2\left[\lambda' + \frac{3}{2}\beta_\lambda\right] \qquad V\left(\frac{v}{\sqrt{2}}\right) = -\frac{v^4}{4}[\lambda' + \beta_\lambda] \\ \mu^2 &= v^2\left[\lambda' + \frac{1}{2}\beta_\lambda\right] \qquad V = -v^2\left[\lambda' + \frac{1}{2}\beta_\lambda\right]\phi^2 + \lambda'\phi^4 + \beta_\lambda\phi^4\log\frac{2\phi^2}{v^2}. \end{aligned} \tag{3.21}$$

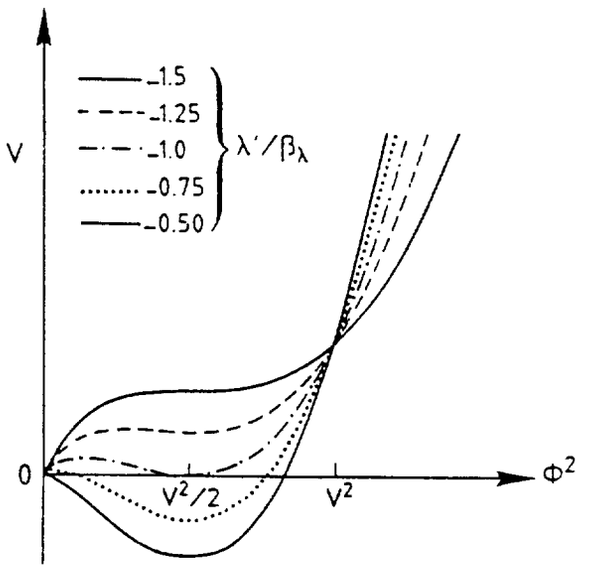

Figure 17. The Higgs potential V versus ϕ^2, for different values of the parameter λ'.

In Fig. 17 we show V versus ϕ^2 for a variety of values of λ'. With $\lambda' = -1.5\beta_\lambda$, which would give $M_H = 0$, we have as we might expect a potential which is flat at the symmetry breaking vacuum. The next curve is an intermediate example, and the third, with $\lambda' = -\beta_\lambda$, shows the limiting case yielding the Linde-Weinberg bound, with both vacua at equal levels. The fourth is another intermediate example, and the final curve shows the potential for $\lambda' = -.5\beta_\lambda$, where the $\phi = 0$ vacuum is no longer a local minimum. The potential now resembles the original Higgs potential without radiative corrections. This leads to a favored value for the Higgs mass, first demonstrated by Coleman and Weinberg,[61] $M_{CW} = \sqrt{2}M_{LW}$, the mass of the Higgs if the symmetry breaking is *generated* by radiative corrections.

This is not, however, quite the end of the story; there are two further points to be considered. The first is that the bound $M_H > M_{LW}$ might be loosened by allowing the vacuum at $\phi = v/\sqrt{2}$ to be higher than that at $\phi = 0$.[62,63] There is then a finite probability (if the initial state chosen by nature is the $\phi = v/\sqrt{2}$ vacuum) for quantum tunneling from this vacuum to the one of lower energy; or, in other words, quantum fluctuations may spontaneously generate a "bubble" where $\phi < v/\sqrt{2}$, which may then expand to fill the universe as ϕ decays to zero. If the lifetime of the metastable state is much longer than the age of the Universe, i.e., if the probability of forming such a bubble over the lifetime of the Universe is much less than one, such a metastable state yields an allowable scenario. This probability was first calculated by Frampton[63] who estimated that for $M_H \gtrsim M_{LW}/\sqrt{2}$ the number of such bubbles occurring in the lifetime of the universe is extremely small. The calculation was redone by Linde[58,64] who found that this bound is actually even an order of magnitude lower.

However, in the same papers he pointed out that it had been shown[65] that unless the Universe is extremely charge asymmetric (to the tune of 8 orders of magnitude larger leptonic than baryonic charge) then high-temperature effects restore the symmetry in the standard model at time $t \to 0$. Such a large charge asymmetry would be *extremely* pathological; all existing

models predict the leptonic and baryonic charges to be of the same order of magnitude. Thus it is now the metastability of the $\phi = 0$ vacuum (against, in this case, thermodynamic fluctuations) that must be considered, in the range $M_{LW} < M_H < M_{CW}$, and spontaneous symmetry breaking will only occur if the lifetime of the metastable $\phi = 0$ vacuum is much less than that of the universe. Linde[58,64] found this is the case only if $\mu^2 = d^2V/d\phi^2\Big|_{\phi=0}$ at vanishing temperatures is negative or extremely small ($\mu^2 \lesssim 0.1$ GeV^2); we see from eq. (3.21) that this occurs for $\lambda' \lesssim \beta_\lambda/2$, or in other words that the true bound on M_H is very close to M_{CW}. Further refinements (see for example Ref. 54 for a summary) may adjust this bound by at most a few percent.

For $m_t > 80$ GeV, or $\beta_\lambda < 0$, the potential we have specified in eq. (3.15) will, for sufficiently large ϕ, become unbounded from below, making the minimum at $V(\phi/\sqrt{2})$ rather superfluous (though it may be possible, if unlikely, that such a vacuum could be metastably long-lived enough ...[64]). Let us return to the full evolution equation for λ, eq. (3.12), and consider now the opposite approximation to what we have so far used; namely neglect all couplings other than λ; we then obtain a solution of the form

$$\lambda(Q) = \frac{\lambda(v)}{1 - \lambda(v)\frac{3}{4\pi^2}\log\frac{Q^2}{v^2}} \tag{3.22}$$

where we have evolved from some large scale Q down to v. The term triviality[66] refers to the fact that $\lambda(v)$ is driven to zero ($\rightarrow$ trivial non-interacting theory) if $\lim_{Q\to\infty}\lambda(Q)$ is not to blow up (as required for stability). However, we cannot expect to use 1-loop equations when $\lambda(Q)$ becomes too large, and may hope that higher-order or non-perturbative corrections will save the situation (e.g., by yielding a fixed point where β_λ vanishes, preventing growth of $\lambda(Q)$ beyond this point). We may then put an upper bound on M_H by requiring that the theory remain perturbative (e.g. $\lambda(\Lambda_0) = 1$) up to some scale Λ_0. For example, if we choose this scale to be the Planck scale (considering pure ϕ^4 theory so that $M_H^2 = 2v^2\lambda$) we find $M_H \lesssim 140$ GeV, a result rather insensitive to both exactly what low energy scale we evaluate λ at to calculate M_H and exactly where we cut off the perturbative domain (whether we use $\lambda(M_{PL}) = 1$ or ∞ for example). Similar results with a mild m_t dependence are found if we take into account the gauge and fermion couplings; since the bounds are at any rate well above the range of LEP I we do not go into further details but refer the reader to, for example, refs. 2, 54, 60 and references therein.

We now return to the lower limit on M_H for $m_t > 80$ GeV. Neglecting the Q^2 dependence of g_t, g and g' in eq. (3.12), we see that in this range of m_t the right-hand side has one negative and one positive root: $\lambda_- < 0 < \lambda_+$. For any initial value $\lambda(v)$ between 0 and λ_+, the right-hand side is negative and $\lambda(Q)$ becomes negative at some finite value of Q. Requiring then as stability condition that $\lambda(v) > \lambda_+$ results in the lower bound

$$M_H^2 > \sqrt{12m_t^4 - 6M_W^4 - 3M_Z^4 + \frac{9}{4}m_t^4} - \frac{3}{2}m_t^2, \tag{3.23}$$

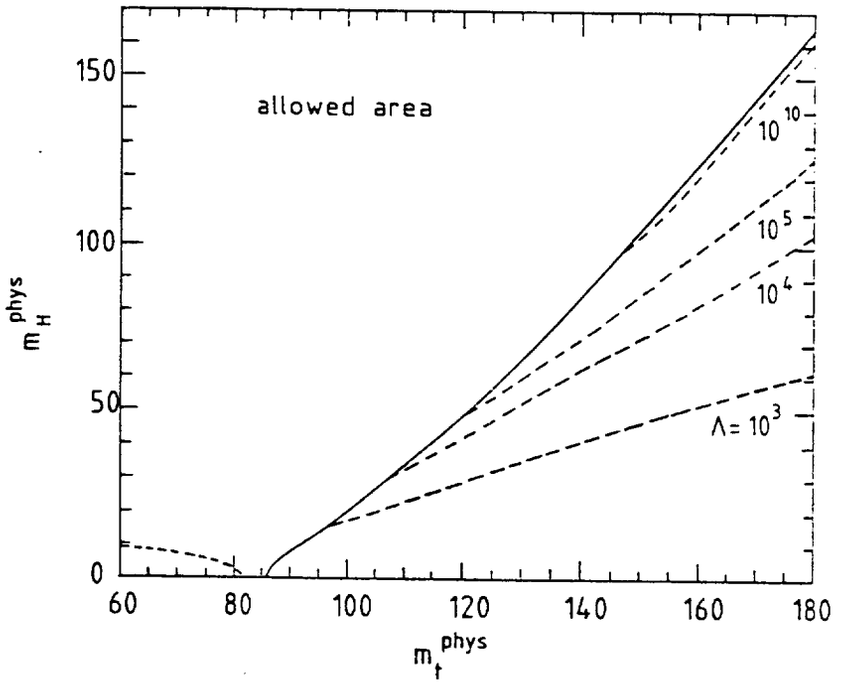

Figure 18. The vacuum stability bounds at the two loop level with one loop boundary conditions for different cutoff scales Λ. The solid line is for $\Lambda = 10^{15}$ GeV, and the dashed lines represent lower cutoffs. Systematic uncertainties are smaller than 1 GeV. The bound for smaller top quark masses ($\sim M_{CW}$) is also shown as a dashed line. From Ref. 68.

a more accurate version of the bound discussed in Ref. 67. In Fig. 18 we display the bound as calculated by Lindner, Sher and Zaglauer[68] using the full renormalization group equations valid to 2-loops, for different choices of cutoff scale.

We note that there may be a sort of competition between the $p\bar{p}$ colliders and LEP I in whether a lower bound on M_H via non-observation of the top quark can be placed with $p\bar{p}$ colliders before LEP I can place such a bound directly; this of course only holds for standard model Higgses.

An experimental violation of these theoretical bounds would clearly be very exciting. We conclude that the observation of a light Higgs is evidence for either 1) non-standard model physics; 2) a very large charge asymmetry in the Universe or 3) m_t very close to 80 GeV. The second case is very unlikely, and in any case would not explain an ultra-light Higgs (less than several hundred MeV).

4. Production and Detection

4.1 Introduction

We turn now to Standard Model Higgs production at LEP I. Three main processes have been considered:

Toponium decay: $t\bar{t} \to H\gamma$ The Wilczek process[50] involving toponium looked very promising in the past and has been discussed at length (see Refs. 4 and 5). Unfortunately, it appears now

that $t\bar{t}$ cannot be light enough for this process to be useful at LEP I, except in the presence of a light charged Higgs, a possibility we discuss in Chapter 9.

$\underline{Z^0 \to H^0\gamma}$ This process should have a clean signature thanks to the outgoing monochromatic photon. However, it only occurs through higher order loop diagrams where fermions and $W^{\pm}$ contribute (see Fig. 19). This process is analogous to $H^0 \to \gamma\gamma$ discussed in Section 2.1.

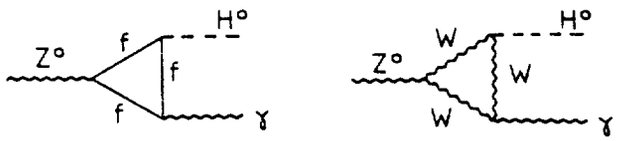

Figure 19. Triangle diagrams for $Z^0 \to H^0\gamma$.

The relative decay rate is given by[69]

$$\frac{\Gamma(Z \to H\gamma)}{\Gamma(Z \to \mu\mu)} = \frac{\alpha^2}{8\pi^2 \sin^2\theta_W}\left(1 - \frac{M_{H^0}^2}{M_Z^2}\right)^3 \frac{|A_f + A_W|^2}{1 + (1 - 4\sin^2\theta_w)^2} \tag{4.1}$$

where A_f and A_W are the contributions of the fermion loops and the W loop respectively. Complete analytic results (involving the complex function defined in eq. (2.4)) can be found in Refs. 71. The fermion loops receive contributions from massive fermions only and A_f approaches a constant limit as the fermion mass goes to infinity:

$$\lim_{m_f \to \infty} A_f = \sum_f \frac{2N_c Q_f (T_3^f - 2Q_f \sin^2\theta_W)}{3\cos\theta_W} \tag{4.2}$$

for a fermion of charge Q_f and weak isospin T_3^f (N_c = color factor again). The limiting values are 0.03, and 0.29 and 0.26 for a charged lepton and up and down type quarks respectively. An approximate formula for A_W is

$$A_W = -\left(4.55 + 0.31(M_H^2/M_W^2)\right) \tag{4.3}$$

— i.e., a much larger contribution. Note the destructive interference between the two terms, implying that extra generations will decrease the rate. Keeping only the W contribution, a good approximate expression for eq. (4.1) is (using $\alpha = 1/128$):

$$\frac{\Gamma(Z \to H\gamma)}{\Gamma(Z \to \mu\mu)} \approx 6.94 \times 10^{-5}\left(1 - \frac{M_H^2}{M_Z^2}\right)^3 \left(1 + 0.07\frac{M_H^2}{M_Z^2}\right)^2 . \tag{4.4}$$

The result of the exact calculation is displayed in Fig. 20. It shows that even with 10^7 Z's one ends up with at most 20 events (even for a very light Higgs), this production process becoming comparable to the Bjorken process (see below) for masses $M_H \gtrsim 60$ GeV in a region where the signal is too small to be visible at LEP. (Note however that the conventional background[6] from $e^+e^- \to f\bar{f}\gamma$ should be manageable.) One may conclude that if the Higgs particle happens

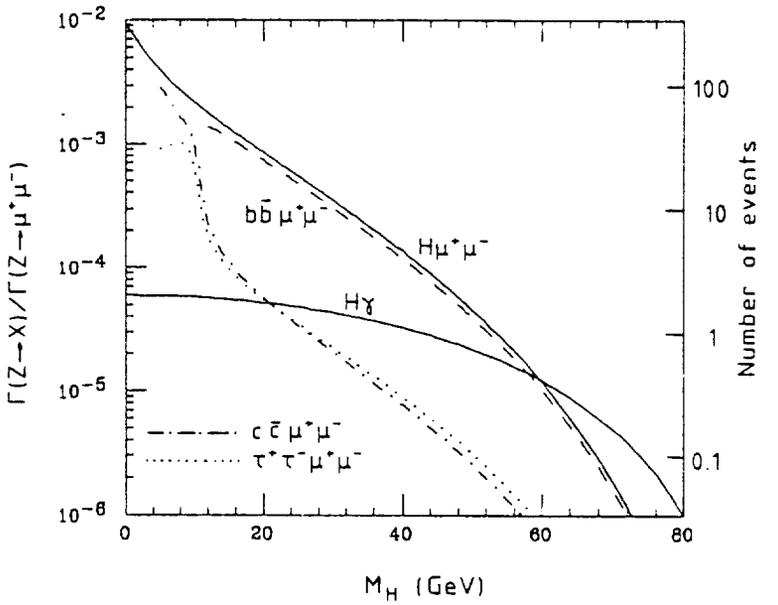

Figure 20. Branching ratios for $Z \to H\mu^+\mu^-$ and $Z \to H\gamma$ (for $m_t = 60$ GeV; the m_t dependence is almost negligible), relative to that for $Z \to \mu^+\mu^-$. For $Z \to H\mu^-\mu^-$ we give the breakdown for three two-fermion decays of the H - $Z \to H\mu^+\mu^- \to b\bar{b}\mu^+\mu^-$ (dashed), $Z \to H\mu^+\mu^- \to c\bar{c}\mu^+\mu^-$ (dotdashed), and $Z \to H\mu^+\mu^- \to \tau\bar{\tau}\mu^+\mu^-$ (dotted). On the righthand axis we translate branching ratio to number of events, given 10^6 Z^0's. We use $\alpha = 1/128$, $\sin^2\theta_W = 0.23$, $M_Z = 92$ GeV, $\Gamma_Z = 2.55$ GeV, and $BR(Z^0 \to \mu^+\mu^-) = 3.3\%$.

to be found in this mass region ($M_H \lesssim 60$ GeV) via another process, this mode is potentially interesting as a check of the Standard Model since all three gauge bosons vertices enter into the calculation of A_W. Also, as this decay occurs via a loop it is a probe of physics at a higher mass scale and one must keep in mind that the rate may be enhanced (or suppressed) by non-standard — e.g., supersymmetric — contributions (see section 7.4).

$\underline{Z^0 \to H^0 f\bar{f}}$

This process, encompassing the Bjorken process[72] $H^0 l^+ l^-$, is especially interesting thanks to the large ZZH coupling and to the favorable detection possibilities, and we will focus on it in the next two sections. It proceeds through $Z^0 \to H^0 Z^{0*}$, where Z^{0*} is an offshell Z^0, followed by $Z^{0*} \to f\bar{f}$. Detection and Higgs mass reconstruction is then achieved by studying the outgoing fermions and/or the decay product of the Higgs. In the following section we discuss the general features of this process, and in section 4.3 features specific to various mass ranges.

4.2 $Z^0 \to H^0 f\bar{f}$, GENERAL FEATURES

Rates: The differential decay rate, normalized to the $Z^0 \to f\bar{f}$ decay rate, is given by

$$\frac{1}{\Gamma(Z \to f\bar{f})}\frac{d\Gamma(Z^0 \to H^0 f\bar{f})}{dx} = \frac{\alpha}{4\pi \sin^2\theta_W \cos^2\theta_W}\frac{\left(1 - x + \frac{x^2}{12} + \frac{2r^2}{3}\right)\left(x^2 - 4r^2\right)^{1/2}}{(x - r^2)^2 + (\Gamma_Z/M_Z)^2} \qquad (4.5)$$

where $x = 2E_H/M_Z$ and $r = M_H/M_Z$, the kinematical limits being $2r \le x \le 1 - r^2$. The energy of the Higgs boson, E_H, is related to the invariant mass of the fermion pair $M_{f\bar{f}}$ (i.e., the mass of the virtual Z^*):

$$E_H = \left(M_Z^2 + M_H^2 - M_{f\bar{f}}^2\right)/2M_Z. \tag{4.6}$$

To get the total event rate in each channel, eq. (4.5) has to be integrated, e.g. numerically (the exact — and lengthy — expressions can be found in Ref. 73, and approximate expressions in Ref. 2). Obviously, the Bjorken process $Z^0 \to H^0\mu^+\mu^-$ is expected to be the cleanest; the production rate for this process, relative to $Z^0 \to \mu^+\mu^-$, is shown in Fig. 20. (In general, when we write μ, we mean, practically speaking, e or μ. Also, all rates are given for an ideal 100% acceptance.)

When M_H is close to zero, this relative rate can be as large as 10^{-2}. In table 1 we give the expected number of $Z^0 \to H^0\mu^+\mu^-$ events given 10^6 Z^0's (without radiative corrections, but using $\alpha = \alpha(M_Z) = 1/128$) assuming $BR(Z^0 \to \mu^+\mu^-) = 3.3\%$.

M_H (GeV)	10	15	20	25	30	35	40	45	50	55	60
no. of events	75	45	29	18	12	7.5	4.5	2.5	1.5	0.8	0.4

Table 1. Event rate for the process $Z^0 \to H^0\mu^+\mu^-$ given 10^6 Z^0's, using $\alpha = 1/128$, $\sin^2\theta_W = 0.23$, $M_Z = 92$ GeV, $\Gamma_Z = 2.55$ GeV, and $BR(Z^0 \to \mu^+\mu^-) = 3.3\%$.

Considering that looking also for $Z^* \to e^+e^-$ doubles the statistics these numbers would imply that roughly speaking a Higgs whose mass is as large as ~ 40 GeV (~ 60 GeV) might be seen at LEP given a sample of 10^6 (10^7) Z^0's. In this process initial state radiative corrections are known to be important.[73,4] A simulation has been performed, implementing the $\mathcal{O}(\alpha)$ initial state corrections giving low energy photons emitted for the most part close to the beam direction. Its effect is to lower the energy of the incoming electron and/or positron and thus to reduce substantially ($\sim 30\%$) the Higgs production cross-section. Event rates according to this simulation are shown in Fig. 21. Of course, initial state radiation has the same suppression

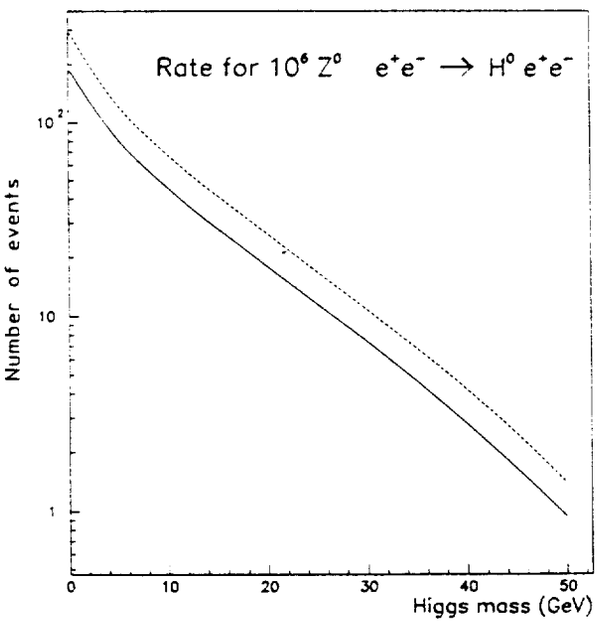

Figure 21. Event rate with (solid) and without (dashed) radiative corrections versus Higgs mass, using $\alpha = 1/137$, $\sin^2\theta_W = 0.23$, $M_Z = 92$ GeV, $\Gamma_Z = 2.5$ GeV, and $BR(Z^0 \to \mu^+\mu^-) = 3\%$ (for 10^6 "tree-level" Z's).

effect on the number of Z's *actually produced*; when we quote 10^6 (10^7) Z's we are referring to "tree-level" Z's, used as a convenient meterstick of luminosity.

Detection: The Higgs boson should be detectable without even observing the specific decay products of the Higgs itself; M_H can be reconstructed by measuring the four-momenta of the outgoing fermions from the Z^*. Let us first consider the case where f = lepton (e or μ). If $\theta_{l^+l^-}$ is the opening angle between the two leptons, and E_{l^+} and E_{l^-} their respective energies, M_H (for $s = M_Z^2$) is given by:

$$M_H = [M_Z^2 + 2E_{l^+}E_{l^-}(1 - \cos\theta_{l^+l^-}) + 2m_l^2 - 2M_Z(E_{l^+} + E_{l^-})]^{1/2}. \tag{4.7}$$

In addition, the invariant mass distribution of the leptons $M_{l^+l^-}$ is strongly peaked at very large values of the invariant mass[74] because the virtual Z^* boson is as close as possible to its mass shell. We plot in Fig. 22 the invariant mass spectrum.

Relevant formulae can be found in Refs. 74, 75 and 5 (see also 29), including formulae for the differential cross-sections, useful for building event-generators.

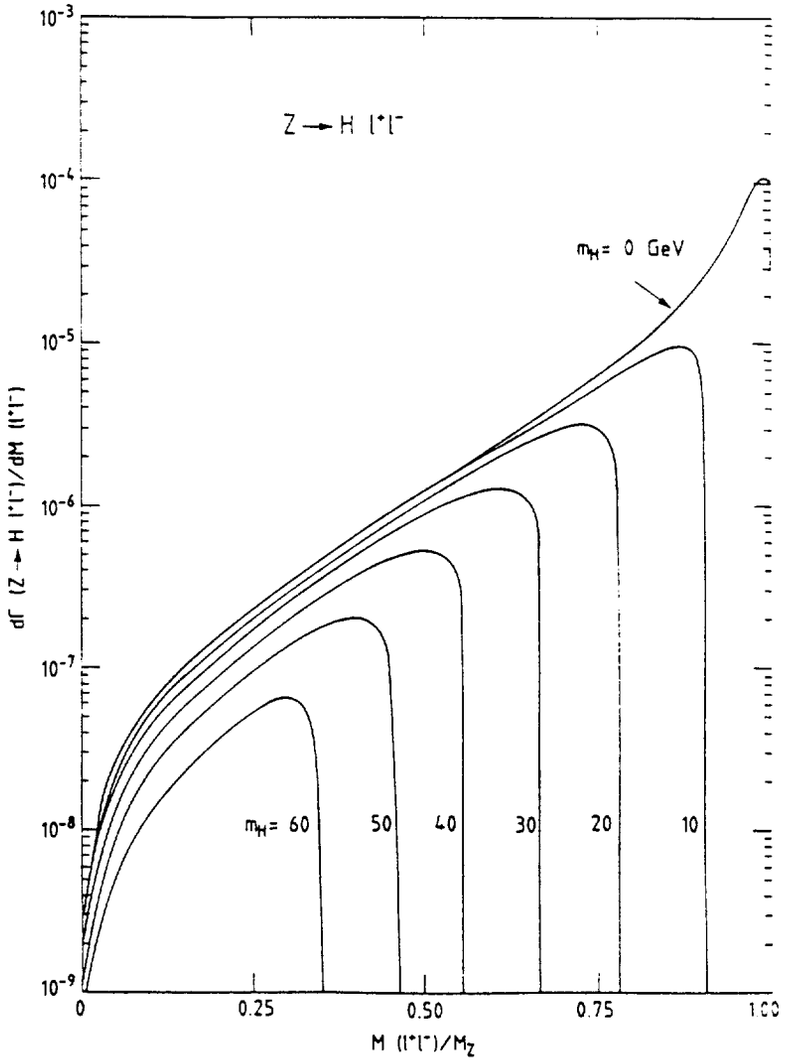

Figure 22. Shape of the $m_{\mu^+\mu^-}$ distribution in $Z^0 \to H^0 + \mu^+\mu^-$.

An interesting point is that in the electromagnetic production of hadrons plus an l^+l^- pair, which contributes part of the background, the l^+l^- pair will be peaked towards low invariant masses because it comes from a photon,[70] so even if this production is copious, a simple cut in $M_{l^+l^-}$ will be sufficient to eliminate most of this background. More severe might be the background from the weak semileptonic decay of heavy flavors: $Z^0 \to Q\bar{Q} \to \mu^+\mu^-$ or $e^+e^- + X$. In fact the "dominant" expected background from $Z \to t\bar{t}$ studied extensively in the recent past (Refs. 4, 76) is now irrelevant (however one must keep in mind the possible background from $b'\bar{b}'$ decay). Note that it was shown that this sort of background did not present real difficulties in extracting a clear signal with simple selection criteria (no missing energy in the event, etc.) leading to a 65% efficiency even in the presence of a t quark with mass below $M_Z/2$. For light Higgs bosons (below about 10 GeV) the recoiling leptons will have large momenta and the resolution with which the l^+l^- invariant mass and energies are measured will be degraded because ΔE_l increases with the lepton energy. Note that the exact behavior of ΔE_e and ΔE_μ is dependent on the experimental setup, and the claim made some years ago that "e better than μ" (Ref. 6) is no longer necessarily true. As a consequence, a study of the recoiling Higgs decay products has certainly to be performed in detail. However, as we have seen, the production rate, which is fairly large in this case (see Fig. 21) will greatly help.

If one keeps to techniques in which one triggers only on the Z^* channel one may be able to improve the Higgs search by examining choices other than l^+l^- for the Z^* final states. This has the advantage of increasing the event rate, but the background may also become much larger. It is obviously the case if one considers hadronic final states $Z^0 \to H^0 q\bar{q}$ since (if one includes all 5 flavors) the branching ratio is around 20 times that for $Z^0 \to \mu^+\mu^-$: the main problem will come from an overwhelming QCD multijet background. For purely hadronic final states, the only channel likely to be useful would be $Z^0 \to H^0 b\bar{b}$ followed by $H^0 \to b\bar{b}$ (for $M_{H^0} > 10$ GeV), the resulting $b\bar{b}b\bar{b}$ final state to be identified using a vertex detector.

An other interesting channel may be $Z^0 \to H^0\nu\bar{\nu}$ because of the increased statistics — $BR(Z^0 \to H^0\nu\bar{\nu})/BR(Z^0 \to H^0\mu\bar{\mu}) \approx 6$ summing over all kinds of neutrinos. The signal would be substantial missing energy together with hadronic jets from the Higgs decay, a very distinct signature. However, without identification of the charged lepton pair, reconstruction of these events must rely on the Higgs decay products themselves (which depend on the value of the Higgs mass); moreover, all ordinary events where energy is for some reason lost constitute a severe background. This background may come from energetic long lived neutrals (K_L^0, n, $\bar{n}$), semileptonic decays of heavy quarks giving high energy neutrinos, two-photon processes, and (mainly) energy losses due to the holes and limited efficiency of the detectors (note that the contributions of four fermion events to this background is very small since the branching ratio is at most $\sim 10^{-7}$.[70] Quite different assumptions (understandably so, being based on quite different detectors) have been made on this last point by the various studies[4,77,78] performed up to now, leading to somewhat different conclusions. Nevertheless, all the studies for a Higgs in the mass range 10 GeV $\lesssim M_H \lesssim$ 30 GeV agree more or less on the statement that the l^+l^- channel is superior for $M_H \gtrsim 20$ GeV or so due to the better mass resolution which becomes crucial as the production rate goes down. However, when M_H is not too far above the

$b\bar{b}$ threshold the signature of the events will be two jets and missing energy with a particular geometry (acolinearity, non-coplanarity) for the two-jet system which provides a powerful way to isolate these events.

Conclusions of the studies performed for $Z^0 \to H^0\nu\bar{\nu}$:

MARKII[77] : after Monte Carlo simulation of detector, cuts, severe selection criteria, they are not very optimistic: background above or comparable to the signal (e.g.. for 10^6 Z's, the background is 210 events, the signal is 60 events, for $M_H = 15$ GeV). They stress the necessity of a very good understanding of this background.

Yellow book 86[4] : More optimistic with less restrictive cuts and more hermetic detector — predicts clean signal above background for $M_H = 20$ or 30 GeV.

Duchovni, Gross and Mikenberg[78] : Claim (after cuts, etc.) that there is no serious background for 5 GeV $\lesssim M_H \lesssim$ 15 GeV. A comparison between $e^+e^- \to Z^0 - Z^*H$ with the subsequent decays $Z^* \to \nu\bar{\nu}$ and $H \to$ *jet jet* and the same process with $Z^* \to e^+e^-$ (two channels which are claimed to have comparable efficiency) implies that the $\nu\bar{\nu}$ channel is dominant up to $M_H \sim 20$ GeV.

An optimistic conclusion seems to be that with the neutrino process, 2×10^4 to 10^5 Z^0 events might be sufficient to either limit or observe the Higgs in the mass range 5 GeV$\lesssim M_H \lesssim$ 15 GeV. In the region below the charm threshold, a first analysis[77] gives a comparable signal and background. This region is under study by other groups.

4.3 Peculiarities of mass regions

Very light Higgs: $M_H \lesssim 200$ MeV As we have seen in Section 3.1, in spite of valiant efforts, it remains difficult to state with complete confidence that such a Higgs is ruled out. It will be highly valuable to search for the H^0 at LEP as far down in mass as possible because these limits should be free of the theoretical ambiguities discussed in Section 3.1 (as long as questions like Higgs decays into light hadrons can be avoided). We recall the general features of light Higgs search: high rates but difficulties in reconstructing M_H from the Z^* decay products, demanding a study of the Higgs decay system.

This mass region, below the muon threshold, is certainly the simplest one. since the decay into an e^+e^- pair (greatly dominating those into $\gamma\gamma$) is the only relevant process (ignoring the possibilities of decays into light exotic particles). In this case, the Bjorken process is $Z^0 \to H^0 + l^+l^- \to e^+e^-l^+l^-$, a simple 4-lepton process where the leptons coming from the Z^* are nearly back-to-back and carry almost all the energy, and the electron pair coming from the decay of the long-lived Higgs materializes at a large distance from the primary vertex. This event topology is very different from the one for an electromagnetically produced $e^+e^-l^+l^-$ event, which has a comparable branching ratio ($\sim 2 \times 10^{-4}$).[70] Note that the emission of a *real* γ from a lepton line in a simple $Z^0 \to l^+l^-$ interaction, followed by its conversion into an e^+e^- pair after an interaction with the material of the detector, does result in an event with

the same topology as the one we are interested in. Therefore it may be a potentially dangerous background whose quantitative estimate is detector dependent.

The mean values of the decay lengths are shown in Table 2 for M_H from 50 to 200 MeV together with the mean values of the opening angles of the two electrons. These decay lengths

M_H (MeV)	50	100	150	200
$< l >$ (cm)	175	55	22	13
$< \theta >$ (deg.)	1.7	3.0	5.0	6.7

Table 2. Mean values for decay lengths and electron opening angles.

imply that the Higgs decay will be seen in the central detectors. In this mass range the average energy of the Higgs ($< E_H > \sim$ 8 GeV) is of course very large compared to its mass; thus the electrons acquire their momentum from the Higgs momentum, and will have a substantial energy ($< E_e > \sim$ 3.5 GeV). In addition they will also have a small opening angle (see table) preserving the original direction of motion of the Higgs. Note also that for a very light Higgs the H^0 angular distribution is essentially flat[75,29] so one expects no particularly important losses in the forward direction where most of the experiments are blind.

If, in spite of the low decay rate, one is interested in the 2 photon decays, the kinematics are quite similar but one loses the information from the central tracking detector about the secondary vertex. Finally the reaction $Z^0 \to H^0 q\bar{q} \to e^+e^-$ *jet jet* suffers from the already mentioned advantages and disadvantages but may be worthwhile to look for.

Light Higgses above the two-pion threshold Higgs detection possibilities in this mass range have been explored in Ref. 29, in particular in the channel $Z^0 \to q\bar{q}H \to q\bar{q}\mu^+\mu^-$. As in the previous mass region, one takes advantage of the flat distribution, the still large momentum of the Higgs compared with its mass, and the small opening angle of the muons, which will have an invariant mass distribution sharply peaked at the Higgs mass. It is claimed that reasonable cuts may exclude all backgrounds, keeping an acceptance efficiency of $\sim$ 20% for signal events, leading to 20 to 40 Higgs events for 10^6 Z's. To get these numbers a branching ratio of 5% has been assumed for $H \to \mu\mu$. As we have seen in Section 2.3 the uncertainties concerning Higgs decay in this mass range will result in real trouble in setting definite limits on the Higgs mass, since the $\pi\pi$ branching ratio could be further enhanced, causing the above signal to disappear! Certainly more studies are needed, both theoretical, and experimental concerning detection with minimal cuts. The present estimates indicate that it should be fairly easy to improve on the limits that can be placed from B physics (where the main uncertainty is again the $H \to \mu^+\mu^-$ branching ratio) below $M_H \approx 1$ GeV (from JADE data, see eqs. (3.7) and (3.9)); above 1 GeV an improvement on the limit from B physics (CLEO, eq. (3.9)) will be more challenging to achieve.

Above 5-10 GeV

This is the cleanest region, where the study of Z^* decays alone should allow one to set conclusions on the Higgs search. In view of the problems discussed above with the $H \to \mu^+\mu^-$ branching ratio, it is important to push this region to as small M_H's as possible.

Of course, the isolation of candidate events would provide an opportunity to study the actual decays of the Higgs: mostly $H \to b\bar{b}$ if $M_H \gtrsim 10$ GeV resulting in a hadronic system having a rather low momentum (since the lepton pair from the Z^* tends to have a large invariant mass) thus resembling the final state of a $b\bar{b}$ event at $\sqrt{s} = M_H$.

One may wonder what will be the effect of radiative emission from the final state Z^* leptons on the shape of the reconstructed Higgs mass. Note that, in some cases, the photon energy could be high enough and the photon emitted at relatively large angle from the beam direction in such a way that it could modify the event topology. This could lead to a reconsideration of the event selection criteria and therefore of the reconstruction strategy.

This study was performed in the case of a perfect detector, introducing no energy nor angular dispersion in the measurement. In order to estimate the effect of the final state radiation, we used a routine created by R. Kleiss[79] for gluon emission, and modified with his help for the photon radiation case. The energy spectrum of the photons emitted by the final state leptons has a shape similar to the one obtained in the case of initial state radiation, but with a tail extending to higher energy. The mean energy value has a slight dependence on the Higgs mass. These photons are nearly collinear with the outgoing leptons and will be detected for the most part, unlike the photons radiated in the initial state, which are emitted close to the beam direction and therefore escape detection.

The effect of these final state radiated photons is to lower the effective energy of the outgoing leptons and to slightly change their opening angle so that the reconstructed Higgs mass (eq. (4.7)) is shifted towards higher mass values as shown in Fig. 23 for $M_H = 20$ GeV. This effect

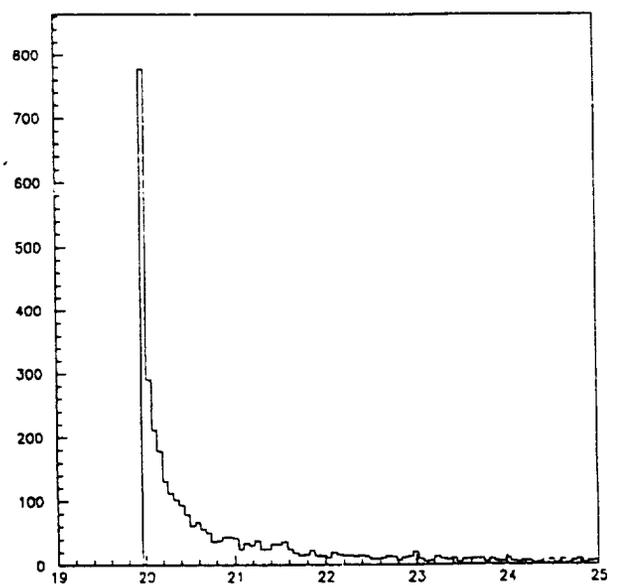

Figure 23. Reconstructed Higgs mass (GeV), according to eq. (4.7), for $M_H = 20$ GeV, with $\delta M_H = 60$ MeV binning, for 1000 events generated.

will be smeared when the angular and energy resolution of the real detector is taken into account, and the relative importance of the radiative distortion in the mass resolution will decrease. The impact of this effect on the reconstruction could be slightly worse for the muon than for the electron pair final states since in the electron case the energy of the photons emitted at small angles will be registered along with the electron energy by the electromagnetic detector.

In any case, these final state radiation effects will only affect slightly the overall Higgs mass reconstruction.

In conclusion, concerning the maximum attainable limit of LEP I, it seems that there are no qualitative problems in this region and that it is only a question of rates, which drop with M_H. Reasonable limits after taking into account initial state radiative corrections and detector efficiencies are around $M_H^{max} = 35$ GeV for 10^6 "tree-level" Z's, 55 for 10^7 "tree-level" Z's.

PART II: Beyond the Minimal Standard Model Higgs

5. Introduction

Since we have no experimental information concerning the Higgs sector, it is clearly a good idea to explore some implications of a more complicated symmetry breaking structure, which could be present either as a minimal extension of the standard model, or as one aspect of a more complicated extension such as supersymmetry. We will not attempt here to enter into a discussion of the motivations of such models; a list of appropriate references can be found for example in ref. 4.

Among the various extensions the most natural one is that of models with 2 or more Higgs *doublets* (for a discussion of more complicated Higgs sectors see for example ref. 2 and references therein). These models have the virtue of satisfying automatically the important constraint $\rho_{tree} = M_W^2/M_Z^2 \cos^2\theta = 1$, and for 2 doublets the absence of flavor-changing neutral currents at tree level can be easily and naturally arranged. Such a structure (2 doublets) is also required in the important case of the minimal supersymmetric extension of the standard model (MSSM), which we shall discuss in Chapter 7. We will focus on the simplest examples, models with only two Higgs doublets. In Sec. 6.1 we introduce the general structure of two-Higgs doublet models; in Sec. 6.2 we discuss the bounds that may be derived from $B\bar{B}$ mixing physics. In Chapter 7 we concentrate on the MSSM, outlining its general structure in Sec. 7.1, discussing the phenomenology of the complementary processes $Z^0 \to h^0 l^+ l^-$ and $Z^0 \to h^0 A^0$ in Sec. 7.2, the signals from the decay $Z \to h^0 A^0$ and subsequent Higgs decays in Sec. 7.3, and other channels in Sec 7.4. In Chapter 8 we discuss briefly some of the physics of a "minimal" extension of the MSSM. Finally, we discuss charged Higgses in Chapter 9. For a discussion of more complicated Higgs sectors, such as those present in left-right symmetric models, composite, hypercolor and technicolor scenarios, we refer to the literature on the subject.[80]

6. Two-Higgs doublet models

6.1 General structure

Introducing two complex $Y = 1$ $SU(2)_L$ doublets,

$$\phi_1 = \begin{pmatrix} \phi_1^+ \\ \phi_1^0 \end{pmatrix} \qquad \phi_2 = \begin{pmatrix} \phi_2^+ \\ \phi_2^0 \end{pmatrix}, \tag{6.1}$$

the Higgs potential becomes

$$\begin{aligned} V(\phi_1,\phi_2) = {} & \lambda_1(\phi_1^\dagger\phi_1 - v_1^2)^2 + \lambda_2(\phi_2^\dagger\phi_2 - v_2^2)^2 \\ & + \lambda_3\left[(\phi_1^\dagger\phi_1 - v_1^2) + (\phi_2^\dagger\phi_2 - v_2^2)\right]^2 \\ & + \lambda_4\left[(\phi_1^\dagger\phi_1)(\phi_2^\dagger\phi_2) - (\phi_1^\dagger\phi_2)(\phi_2^\dagger\phi_1)\right] \\ & + \lambda_5\left[\mathrm{Re}(\phi_1^\dagger\phi_2) - v_1 v_2\cos\xi\right]^2 \\ & + \lambda_6\left[\mathrm{Im}(\phi_1^\dagger\phi_2) - v_1 v_2\sin\xi\right]^2 \end{aligned} \tag{6.2}$$

where the λ_i are real parameters and ξ a phase that can be rotated away by a redefinition of fields if $\lambda_5 = \lambda_6$, as is the case for example in the MSSM. We will set $\xi = 0$ henceforth, which incidentally yields a CP invariant Higgs sector. The quantities v_1 and v_2 are the VEV's of ϕ_1 and ϕ_2 respectively (along the real parts of the neutral scalars). Of the eight degrees of freedom present in eq. (6.2), three are "eaten" to give the $W^\pm$ and Z^0 mass, leaving five physical Higgs bosons: two charged states $H^\pm$,

$$H^\pm = -\phi_1^\pm\sin\beta + \phi_2^\pm\cos\beta \tag{6.3}$$

where β is given by $\tan\beta = v_2/v_1$, and three neutral states — the scalars

$$\begin{aligned} H^0 &= \sqrt{2}\left[(\mathrm{Re}\phi_1^0 - v_1)\cos\alpha + (\mathrm{Re}\phi_2^0 - v_2)\sin\alpha\right] \\ h^0 &= \sqrt{2}\left[-(\mathrm{Re}\phi_1^0 - v_1)\sin\alpha + (\mathrm{Re}\phi_2^0 - v_2)\cos\alpha\right] \end{aligned} \tag{6.4}$$

where H^0 is the heavier scalar, by convention; the mixing angle α specifies the rotation necessary to diagonalize the neutral scalar Higgs mass matrix; and

$$A^0 = \sqrt{2}\left[-\mathrm{Im}\phi_1^0\sin\beta + \mathrm{Im}\phi_2^0\cos\beta\right] \tag{6.5}$$

a CP-odd scalar commonly referred to as a pseudoscalar (see ref. 2 for a discussion, and the expressions for α and the Higgs masses in terms of the λ_i and v_i).

We have thus gone from the one free parameter of the standard model Higgs sector to six: four Higgs masses, the VEV ratio $\tan\beta$, and the mixing angle α of the neutral scalar sector. The W mass fixes $v_1^2 + v_2^2 = (246\ \text{GeV})^2/2 = 1/(G_F 2\sqrt{2})$. For phenomenological studies it is clearly very important to reduce the number of parameters by picking a more specific model, as will be done in Chapter 7 where we discuss the MSSM. Nonetheless, there are some useful things to be said about two-doublet models in general.

The couplings of the H^0 and h^0 to the vector bosons are suppressed compared to the couplings of the minimal standard model Higgs; they satisfy the sum rule

$$g^2_{H^0VV} + g^2_{h^0VV} = \left(g^{SM}_{HVV}\right)^2 \tag{6.6}$$

(here V stands for W or Z) or in terms of α and β

$$\frac{g_{H^0VV}}{g^{SM}_{HVV}} = \cos(\beta-\alpha) \qquad \frac{g_{h^0VV}}{g^{SM}_{HVV}} = \sin(\beta-\alpha). \tag{6.7}$$

Note also that the couplings $Z^0Z^0A^0$ and $W^+W^-A^0$ are absent; the couplings of a Z to a pair of identical Higgses are forbidden by Bose symmetry; and the couplings $Z^0A^0h^0$ and $Z^0A^0H^0$ are allowed. The couplings of the Higgses to fermions are more model dependent, and will be discussed for the specific case of the MSSM in Chapter 7.

In the two Higgs doublet models generally discussed, flavor changing neutral currents at tree-level are avoided by having only one doublet couple to a given type of quarks (and leptons) — either (in what we will refer to as Model I) by having only one Higgs doublet couple to all quarks and leptons, and decoupling the second Higgs doublet from the fermions[81] or (Model II), as required for the MSSM, by having one doublet couple only to the up-type quark and leptons and the other only to the down-type fermions.[82]

For the theoretical lower bounds on the mass of a light Higgs, it is often claimed that in any multiple Higgs model one can in general only place a lower bound only on the sum $\sum_i M^2_{H^0_i}$, which allows the lightest scalar to have an arbitrarily small mass (independently of the t quark mass). However stronger statements can be made;[54] in particular in a two-doublet model one has

$$M^2_{H^0}\cos^2(\alpha-\beta) + M^2_{h^0}\sin^2(\alpha-\beta) \gtrsim M^2_{CW'} \tag{6.8}$$

where $M_{CW'}$ is defined analogously to M_{CW} in Section 3.2, but may be larger, since now massive scalars may be included in the sum in eq. (3.20) (with contributions 1/3 that of the vector bosons). Referring to eq. (6.7) we see that an h^0 with SM couplings to the vector bosons ($\sin(\beta-\alpha)=1$) must be heavier than the CW mass as defined in the standard model. However, if the h^0 has couplings "slightly" smaller than standard model — and therefore may be experimentally indistinguishable from a standard model Higgs boson — the H^0 couplings are large enough to satisfy the bound with a massive H^0 alone. For example, consider a model with three Higgses ($H^\pm$ and A^0) of mass 150 GeV; then $M_{CW'} \sim 20$ GeV. If the observed $\Gamma(Z^0 \to h^0 l^+ l^-)$ is 90% of the expected standard model value, then a H^0 of 70 GeV is sufficient to satisfy the bound (6.8) with no constraints on h^0.

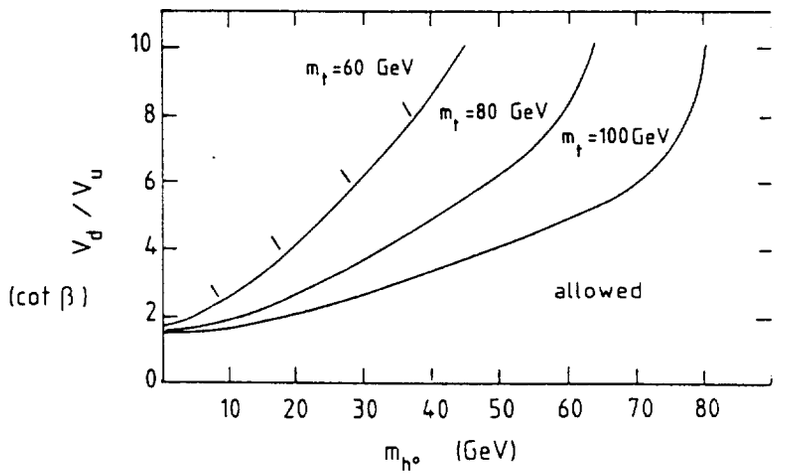

Figure 24. Georgi-Manohar-Moore bound on the VEV ratio in a two-Higgs-doublet model. From Ref. 54.

Theoretical upper bounds are not strong enough to concern us here. One other theoretical bound, that of Georgi, Manohar and Moore[83] applies in the case $v_u << v_d$. Since the Yukawa coupling of the t quark is enhanced over the Standard Model by the ratio v_d/v_u, it is very large and can destabilize the potential of the light scalar in the low-energy theory. The resultant bound is of course stronger for heavier m_t. In Fig. 24 we show this limit.

Experimental constraints need to be considered limit by limit and model by model. In Sec. 3.1 we mention for each limit considerations for extending it outside the standard model. The current bound on the charged Higgs boson is obtained at PEP and PETRA from the failure to observe the $H^\pm$ in $e^+e^- \to \gamma^*, Z^* \to H^+H^-$, giving $M_{H^\pm} \gtrsim 17$ GeV.[84] This limit is anticipated to be improved to $M_{H^\pm} \gtrsim 25 - 30$ GeV at Tristan.

Another source of limits comes from various low-energy experiments. The best limits come from the measurements of $B\overline{B}$ mixing, and we shall discuss this process as an illustrative case in the next section. Rare decays such as $b \to s\gamma$, $b \to sl^+l^-$, $K \to \pi\nu\overline{\nu}$ and $B \to X_s\nu\overline{\nu}$ may also prove promising.[85]

6.2 Limits from $B\overline{B}$ mixing[88]

In a two-Higgs doublet model, additional box diagram contributions to $B\overline{B}$ mixing are obtained by replacing one or both of the W lines by physical charged Higgses (Fig. 25). We will use a combined value based on ARGUS[89] and CLEO[90] measurements of

$$r_d \equiv \frac{P(B_d^0 \to l^+\nu X^-)}{P(B_d^0 \to l^-\overline{\nu}X^+)} = 0.20 \pm 0.06; \qquad \text{or } x_d = \frac{\Delta M_{B_d-\overline{B}_d}}{\Gamma_{B_d}} = 0.71 \pm 0.14. \tag{6.9}$$

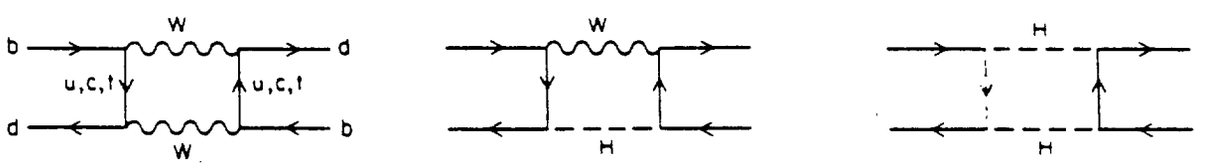

Figure 25. Box diagrams for $B\overline{B}$ mixing in a two-Higgs-doublet model. H is a physical, charged Higgs boson.

To excellent approximation we may neglect the contributions of box diagrams with u or c quarks and consider only t quark contributions. Then x_d is given by

$$x_d = \frac{G_F^2}{6\pi^2} m_t^2 \tau_{B_d} B_{B_d} f_{B_d}^2 M_{B_d} |V_{td} V_{tb}^*|^2 \left[A_{WW} + A_{WH} + A_{HH}\right]$$

$$A_{WW} = \left[\frac{1}{4} + \frac{9}{4}\frac{1}{1-z_t} - \frac{3}{2}\frac{1}{(1-z_t)^2} - \frac{3}{2}\frac{z_t^2 \ln z_t}{(1-z_t)^3}\right] \eta_{QCD} \tag{6.10}$$

$$A_{WH} = m_t^2 \cot^2\beta \; (32 M_W^2 I_2 + 8 I_3) \qquad A_{HH} = m_t^2 \cot^4\beta \; 4 I_1 / M_W^2$$

where I_1, I_2 and I_3 are integrals that can be found for example in Refs. 87 and 2. Here B_B is the bag factor; f_B is defined analogously to the pion or kaon decay constants, f_π and f_K; τ_B and M_B are the B meson lifetime and mass (we take $M_B = 5.275$ GeV); the V_{ij} are Cabibbo-Kobayashi-Maskawa matrix elements; and η_{QCD} is a well-calculated QCD correction factor that we take to be equal to 0.85. We neglect the QCD corrections for the Higgs terms. Eqs. (6.10) are valid both in Model II where $v_1(v_2)$ is the VEV of the Higgs giving mass to the down (up) type quarks and in Model I where v_2 is the VEV of the only Higgs field coupling to fermions.

The uncertainty in the calculation of x_d comes mainly from m_t, and the combinations $B_B f_B^2$ and $\tau_B |V_{td}|^2$ ($|V_{tb}|^2 \approx 1$, from the unitarity of the 3×3 CKM matrix). We choose

$$B_{B_d}^{1/2} f_{B_d} = 160 \pm 40 \text{ MeV} \tag{6.11}$$

which is meant to imply that the whole range of "conceivable" possibilities is within about twice the quoted error. For $\tau_B |V_{td}|^2$ we take the approximate parametrization[92]

$$V = \begin{pmatrix} V_{ud} & V_{us} & V_{ub} \\ V_{cd} & V_{cs} & V_{cb} \\ V_{td} & V_{ts} & V_{tb} \end{pmatrix} \approx \begin{pmatrix} 1 - \frac{1}{2}\lambda^2 & \lambda & A\lambda^3 \rho e^{i\phi} \\ -\lambda & 1 - \frac{1}{2}\lambda^2 & A\lambda^2 \\ A\lambda^3(1 - \rho e^{-i\phi}) & -A\lambda^2 & 1 \end{pmatrix}, \tag{6.12}$$

$$\text{giving} \qquad |V_{td}| \approx \lambda \sqrt{1 + \rho^2 - 2\rho\cos\phi}\; |V_{cb}|, \tag{6.13}$$

where $\lambda = \sin\theta_c = 0.221$. V_{cb} is reasonably well-determined by the semileptonic branching ratio $B_{SL} = B(b \to e\nu X)$:[93,32]

$$\tau_B |V_{cb}|^2 = (2.9 \pm 0.6) \times 10^{-15}\text{s}. \tag{6.14}$$

The limit $R = \Gamma(b \to X_u e\nu)/\Gamma(b \to X_c e\nu) < 0.04$ implies a bound $\rho < 0.6$ (see e.g. Ref. 94). With essentially no bounds on $\cos\phi$ (although for small m_t one should probably be more careful and consider bounds from the measurement of the CP violation parameter ϵ_K), particularly for $m_t > 50$ GeV, this yields

$$\tau_B |V_{td}|^2 = (0.18 \text{ to } 4.4) \times 10^{-16}\text{s}. \tag{6.15}$$

We choose three illustrative cases (note that cases 1 and 3 are not truly maximal):

1. a case allowing a large charged Higgs contribution:
$B_{B_d}^{1/2} f_{B_d} = 120$ MeV, $\tau_B |V_{td}|^2 = 0.5 \times 10^{-16}$s, and $x_d = 0.85$ (dashed)

2. a central case:

$B_{B_d}^{1/2} f_{B_d} = 160$ MeV, $\tau_B |V_{td}|^2 = 2.0 \times 10^{-16}$s, and $x_d = 0.71$ (solid)

3. a case leaving little room for charged Higgs contributions:

$B_{B_d}^{1/2} f_{B_d} = 200$ MeV, $\tau_B |V_{td}|^2 = 3.5 \times 10^{-16}$s, and $x_d = 0.57$. (dotted)

In Figs. 26 and 27 we show the value of $\tan\beta$ as a function of $M_{H^\pm}$ that yields the experimental $B\bar{B}$ mixing assumed in each of the three cases, for several values of m_t. For case 1 we

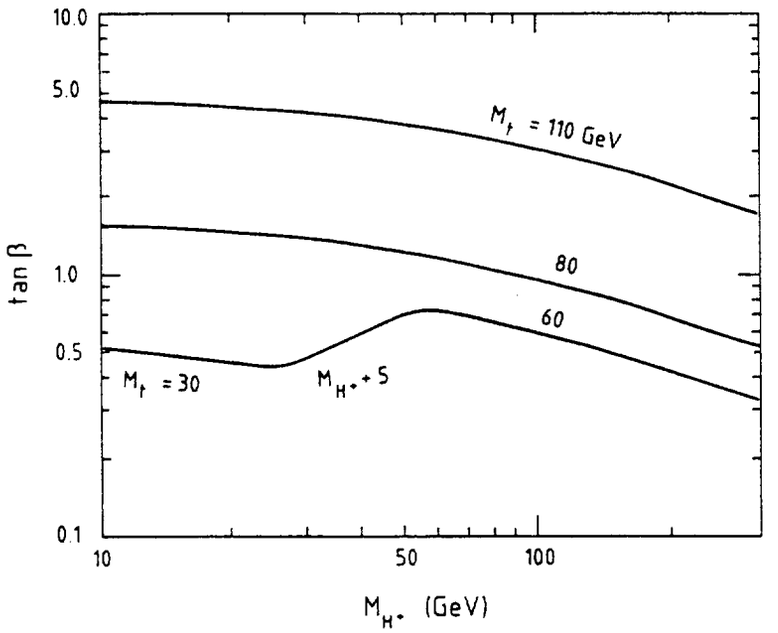

Figure 26. The value of $\tan\beta$ required to obtain the central experimental $B\bar{B}$ mixing result for central standard model parameters (case 2 above), as a function of $M_{H^\pm}$, for various m_t values.

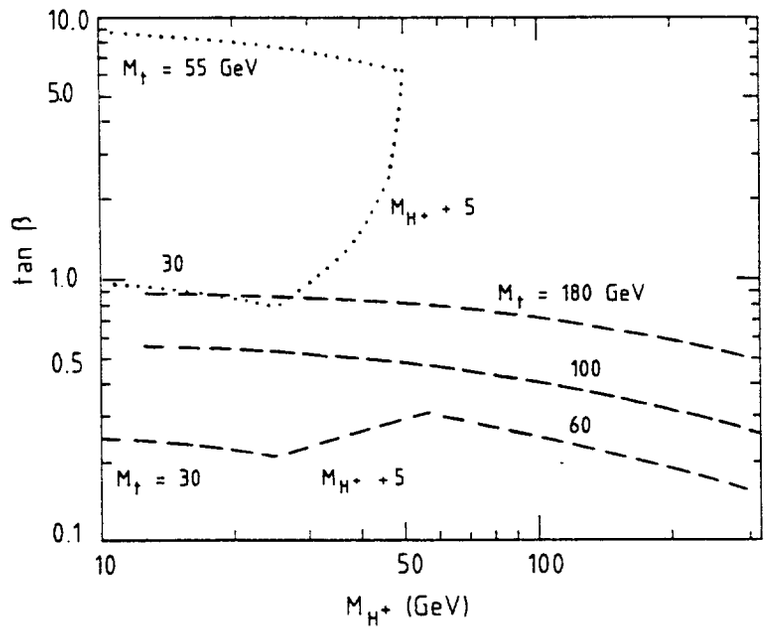

Figure 27. The value of $\tan\beta$ required to obtain the extreme experimental $B\bar{B}$ mixing result for extreme standard model parameters (cases 1 (dashed) and 3 (dots) above) as a function of $M_{H^\pm}$, for various m_t values.

show curves for $m_t = 60$, 100 and 180 GeV, and for case 2 curves for $m_t = 60, 80$ and 110 GeV. We have chosen our minimal value of m_t to be 60 GeV, since recent $p\bar{p}$ collider results have indicated that m_t below 60 GeV is "quite unlikely."[95] However, one possible caveat to this bound is the presence of a light $H^{\pm}$ dominating the decays of the top quark (as will be discussed in Chapter 9) and thus for $M_{H^{\pm}} < 55$ GeV we extend our 60 GeV curves by curves calculated for $m_t = M_{H^{\pm}} + 5$ GeV. For $M_{H^{\pm}} < 25$ GeV we use $m_t = 30$ GeV. For case 3 we show curves for m_t minimized in the above fashion, and for $m_t = 55$ GeV, only for light enough Higgses. Note that all of this fine tuning will be unnecessary when we consider the MSSM, where $M_{H^{\pm}}$ is required to be larger than $M_{W^{\pm}}$.

Until the t quark is found, no upper bounds on $\tan\beta$ can be placed, despite what Figs. 26 and 27 may seem to indicate, since—except for extreme cases like 1—we can always take m_t large enough so that the standard model contribution saturates the observed $B\bar{B}$ mixing (this occurs for $m_t = 460, 120$ and 56 GeV for cases 1, 2, and 3 respectively). The lower bounds are promising, especially as the limits on m_t improve in the near future. (Actually, in A_{WH} and A_{HH} (eq. (6.10)), we have neglected effects of the m_b contribution to the $H^+b\bar{t}$ coupling (see eqs. 9.1 and 9.2). In Model I these contributions are proportional to $\cot\beta$ like those from m_t, and hence are always negligible. In Model II, however, the m_b contributions go as $m_b \tan\beta$, thus lowering slightly the curves for $\tan\beta > 1$ shown in Figs. 26 and 27, *and* definitively excluding sufficiently large $\tan\beta$.)

We look forward to improved constraints on m_t, and the combinations $B_B f_B^2$ and $\tau_B |V_{td}|^2$, as being highly constraining for charged Higgs bosons.

7. Minimal Supersymmetric Extension of the Standard Model

7.1 General structure

Supersymmetric theories currently provide the only known way to avoid the problems of fine-tuning, naturalness (or rather unnaturalness...), and hierarchy[96] and to describe a relatively light fundamental Higgs boson free from quadratic divergences. The minimal supersymmetric extension of the Standard Model is a particular case of two Higgs doublet models of opposite hypercharge, the $Y = -1$ ($Y = 1$) doublet coupling only to down-type (up-type) quarks and leptons. This choice is required in order to give masses to both types of particles. In our notation v_2 (v_1) will be the VEV of the Higgs giving mass to the up (down) type quarks.

Supersymmetry imposes symmetry relations between the parameters of the Higgs potential (6.2) and the Higgs sector is now more tightly constrained, depending on only two independent parameters. As a consequence a number of relations exists between the masses, the ratio of the VEV's, $\tan\beta$, and the mixing angle α. Thus

$$M^2_{H^0,h^0} = \frac{1}{2}\left[M^2_{A^0} + M^2_{Z^0} \pm \sqrt{\left(M^2_{A^0} + M^2_{Z^0}\right)^2 - 4M^2_{A^0} M^2_{Z^0} \cos^2 2\beta}\right] \tag{7.1}$$

giving

$$M_{h^0}^2 + M_{H^0}^2 = M_{A^0}^2 + M_{Z^0}^2. \tag{7.2}$$

We have also

$$M_{H^\pm}^2 = M_{A^0}^2 + M_{W^\pm}^2 \tag{7.3}$$

and

$$\tan 2\alpha = \tan 2\beta \left(\frac{M_{A^0}^2 + M_{Z^0}^2}{M_{A^0}^2 - M_{Z^0}^2} \right) \tag{7.4}$$

fixing the value of α. This expression only determines α to within an ambiguity of $\pi/2$, which is resolved by the additional definition $\cos 2\alpha = -\cos 2\beta \, (M_{A^0}^2 - M_{Z^0}^2)/(M_{H^0}^2 - M_{h^0}^2)$ or by always respecting the conventions $0 \leq \beta \leq \pi/2$ and $-\pi/2 \leq \alpha \leq 0$. Other useful relations are easily derived, and may be found for example in Refs. 2 and 15, along with all Higgs boson couplings and Feynman rules.

From the above equations it is obvious that $M_{H^0} \geq M_{Z^0}$ and $M_{H^\pm} \geq M_{W^\pm}$, implying that these Higgs bosons are not of interest at LEP I. Conversely, we point out that the observation of charged Higgs bosons at LEP would rule out the MSSM. We are therefore left with the light scalar Higgs h^0, whose mass is constrained by

$$M_{h^0}^2 \leq \cos^2 2\beta \; M_{Z^0}^2 \tag{7.5}$$

i.e., restricted to be lighter than the Z^0, and the "pseudoscalar" A^0 whose mass is arbitrary if $\tan\beta = v_2/v_1$ is not fixed. We see that M_{h^0} is also constrained to be less than M_{A^0} (in fact $M_{h^0}^2 \leq \cos^2 2\beta \; M_{A^0}^2$.)

The couplings of the MSSM Higgs bosons to up-type and down-type fermions. relative to the SM Higgs couplings, are

$$\begin{aligned} h^0 u\bar{u}: &\quad \frac{\cos\alpha}{\sin\beta} \qquad h^0 d\bar{d},\; h^0 l\bar{l}: \quad -\frac{\sin\alpha}{\cos\beta} \\ A^0 u\bar{u}: &\quad \cot\beta \qquad A^0 d\bar{d},\; A^0 l\bar{l}: \quad \tan\beta \end{aligned} \tag{7.6}$$

(these relations, in fact, are not restricted in validity to the MSSM, but hold in general for Model II). Also of particular use to us in the following is the coupling $Z^0 A^0 h^0$, with Feynman rule factor

$$\frac{g\cos(\beta-\alpha)}{2\cos\theta_W}(p+p')^\mu \tag{7.7}$$

where p and p' are the Higgs momenta.

It is usually assumed that the VEV v_2, which gives mass to the top quark. is bigger than v_1, which gives mass to the bottom quark, giving $\tan\beta > 1$.[97] In this case $\pi/4 \leq \beta \leq \pi/2$ and $-\pi/2 \leq \alpha \leq -\pi/4$ in the ideal case for phenomenology where both h^0 and A^0 are lighter than the Z^0 ($-\pi/4 \leq \alpha \leq 0$ if A^0 is heavier than Z^0.) Nevertheless, one should not ignore the range $0 < \tan\beta < 1$ and in our figures we show results for the whole range. In general bounds are symmetric about $\tan\beta = 1$, that is, for $\tan\beta \leftrightarrow \cot\beta$.

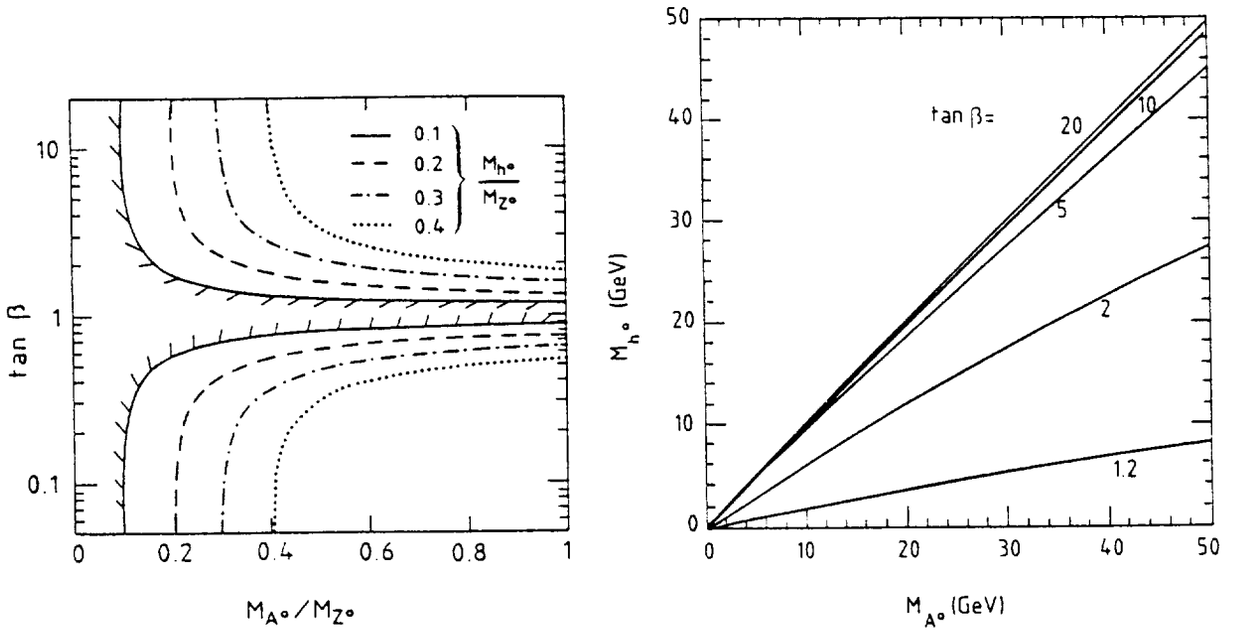

Figure 28. Contours of constant M_{h^0} in $\tan\beta - M_{A^0}$ parameter space, and contours of constant $\tan\beta$ in $M_{h^0} - M_{A^0}$ parameter space.

We see from eq. (7.1) that if $\tan\beta \to 1$ then $M_{h^0} \to 0$ while M_A can take on any value. Large values of $\tan\beta$, on the other hand, imply that h^0 and A^0 are approximately degenerate in mass (for A^0 lighter than the Z^0; otherwise h^0 and Z^0 are approximately degenerate in mass). In Fig. 28 we show the interrelation of M_A, M_h and $\tan\beta$.

Finally, we comment on how to recover the standard model with one Higgs doublet from the MSSM.[2] To recover the SM couplings it suffices to set $\tan\beta = 1$. However, this forces $M_{h^0} = 0$, so one must set the Higgs masses by hand (M_{h^0} to a non-zero value and the rest to ∞). More rigorously, one takes the limit $M_{A^0} \to \infty$. This forces $M_{H^\pm}$ and M_{H^0} to ∞ as well, and

$$\sin 2\beta = -\sin 2\alpha = \sqrt{1 - M_{h^0}^2/M_Z^2}; \qquad \cos\alpha = \sin\beta \tag{7.8}$$

which may be demonstrated to yield the SM couplings from Eq. (7.6); note that $M_{h^0} = 0$, $\tan\beta = 1$ is a special case of Eq. (7.8).

7.2 Phenomenology — $Z^0 \to h^0 l^+ l^-$ and $Z^0 \to h^0 A^0$

We will focus now on the situation which is the most fruitful for phenomenology at LEP, namely when both h^0 and A^0 are lighter than the Z^0, and we will see below that the two decays $Z^0 \to h^0 l^+ l^-$ and $Z^0 \to h^0 A^0$ are complementary processes which deserve a careful study. Note that the decay $Z^0 \to A^0 l^+ l^-$ is forbidden. This section is based in part on work of Giudice.[98]

First, according to eq. (6.7) the decay $Z^0 \to h^0 l^+ l^-$ is suppressed with respect to the Standard Model decay of a Higgs of the same mass

$$\frac{\Gamma(Z^0 \to h^0 l^+ l^-)}{\Gamma(Z^0 \to H^0_{SM} l^+ l^-)} = \sin^2(\beta - \alpha) \tag{7.9}$$

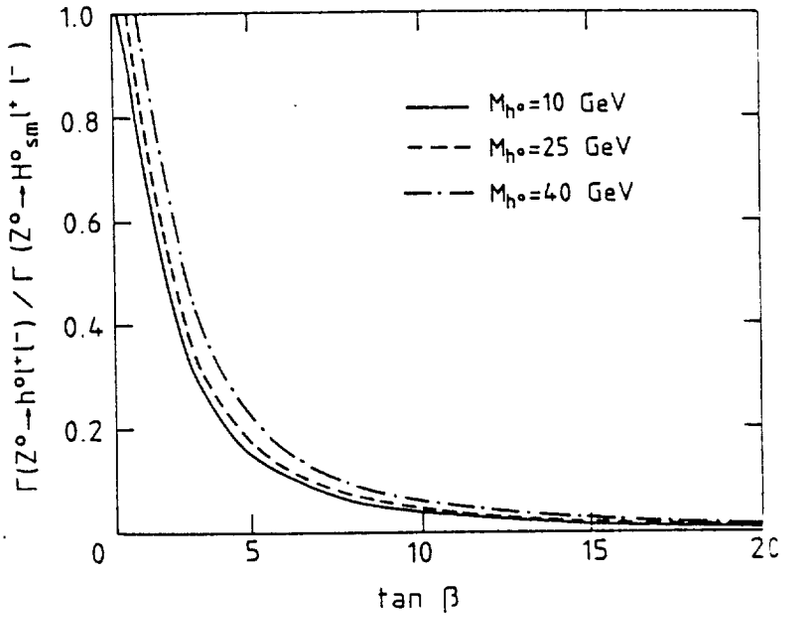

Figure 29. The value of $\Gamma(Z^0 \to h^0 l^+ l^-)/\Gamma(Z^0 \to H^0_{sm} l^+ l^-)$ as a function of $\tan\beta$, for various values of M_h^0 (taken from Ref. 98).

where

$$\sin^2(\beta - \alpha) = \left(1 - \frac{M_h^2}{M_A^2}\right)\left(\frac{M_A^2 - M_h^2 + M_Z^2}{M_A^2 - 2M_h^2 + M_Z^2}\right). \tag{7.10}$$

The effect of this suppression is displayed in Fig. 29, where we show the ratio $\frac{\Gamma(Z^0 \to h^0 l^+ l^-)}{\Gamma\, Z^0 \to H^0_{SM} l^+ l^-)}$ as a function of $\tan\beta$, for various values of M_h^0. In Fig. 30 we show contours of this ratio versus $\tan\beta$ and M_A, or in other words, the limits on the $\tan\beta - M_A$ parameter space that can be placed given limits on this ratio (see Fig. 39 for similar contours in the $M_{h^0} - M_{A^0}$ plane).

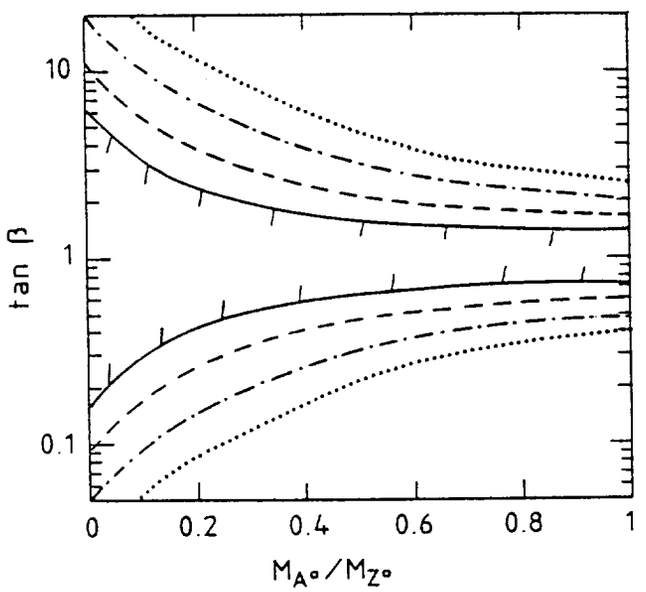

Figure 30. Limits on the $\tan\beta - M_A$ parameter space, given limits on the branching ratio of $Z \to h\mu^+\mu^-$: $BR(Z^0 \to h^0\mu^+\mu^-) < 3 \times 10^{-5}$ (solid), 1×10^{-5} (dashed), 3×10^{-6} (dotdashed) and 1×10^{-6} (dotted).

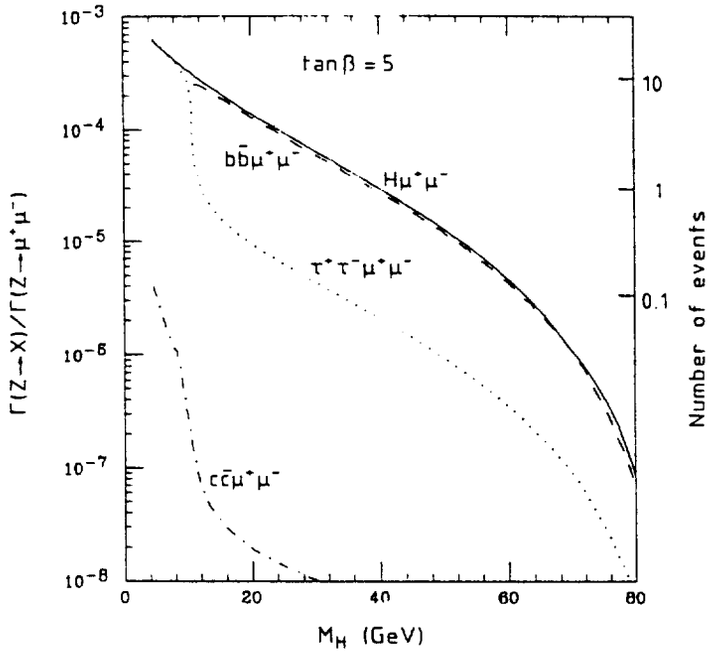

Figure 31. Branching ratio for $Z \to H\mu^+\mu^-$ relative to that for $Z \to \mu^+\mu^-$ in the MSSM, for $\tan\beta = 5$. We also give the breakdown for three two-fermion decays of the H: $Z \to H\mu^+\mu^- \to b\bar{b}\mu^+\mu^-$ (dashed), $Z \to H\mu^+\mu^- \to c\bar{c}\mu^+\mu^-$ (dotdashed), and $Z \to H\mu^+\mu^- \to \tau\bar{\tau}\mu^+\mu^-$ (dotted). On the righthand axis we translate branching ratio to number of events, given 10^6 Z^0's (again, we use an ideal 100% acceptance, and μ means, practically speaking, μ or e).

In Fig. 31 we show the equivalent of Fig. 20 (i.e., the branching ratios for $Z \to h^0\mu^+\mu^-$ and for this process followed by h^0 decaying to $b\bar{b}$, $c\bar{c}$ or $\tau^+\tau^-$) for the MSSM, having chosen $\tan\beta = 5$ as a representative example. Again on the right-hand axis we give the expected number of events for 10^6 Z's.

Between the number of events (which may be translated to an equivalent mass M_H^e that would generate the same number of events in the standard model) and the observed kinematic mass, we should in principle have a handle on $\tan\beta$ (in the MSSM). In Fig. 32 we show contours

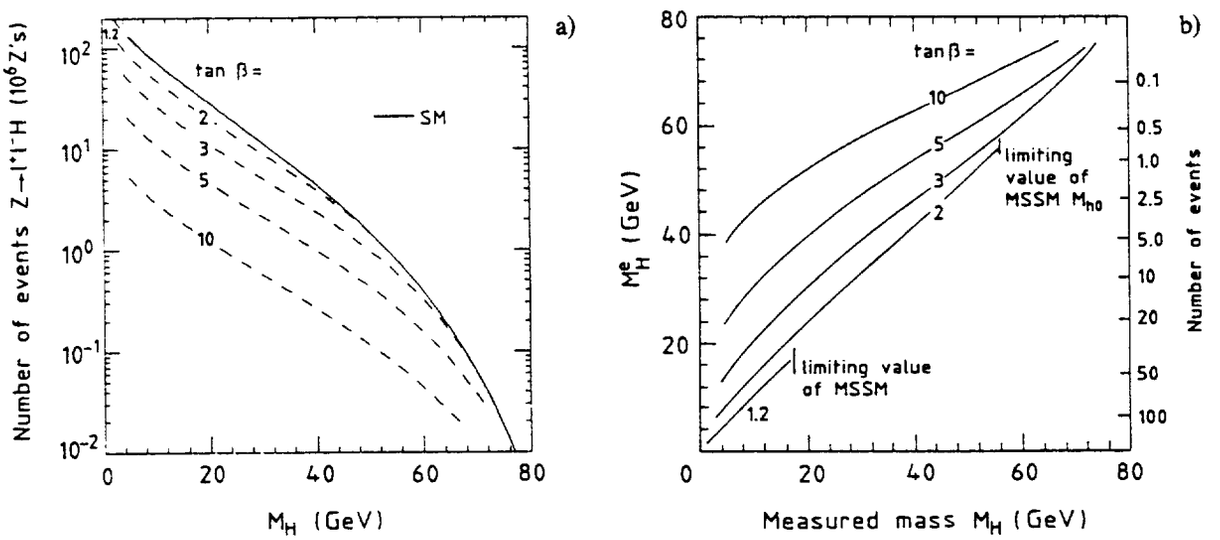

Figure 32. Contours in various $\tan\beta$ values in the plane of number of $Z \to l^+l^-H$ events versus the measured Higgs mass (a) or in equivalent mass M_H^e versus measured mass (b). $\tan\beta$ and $1/\tan\beta$ are equivalent here. l stands for μ or e.

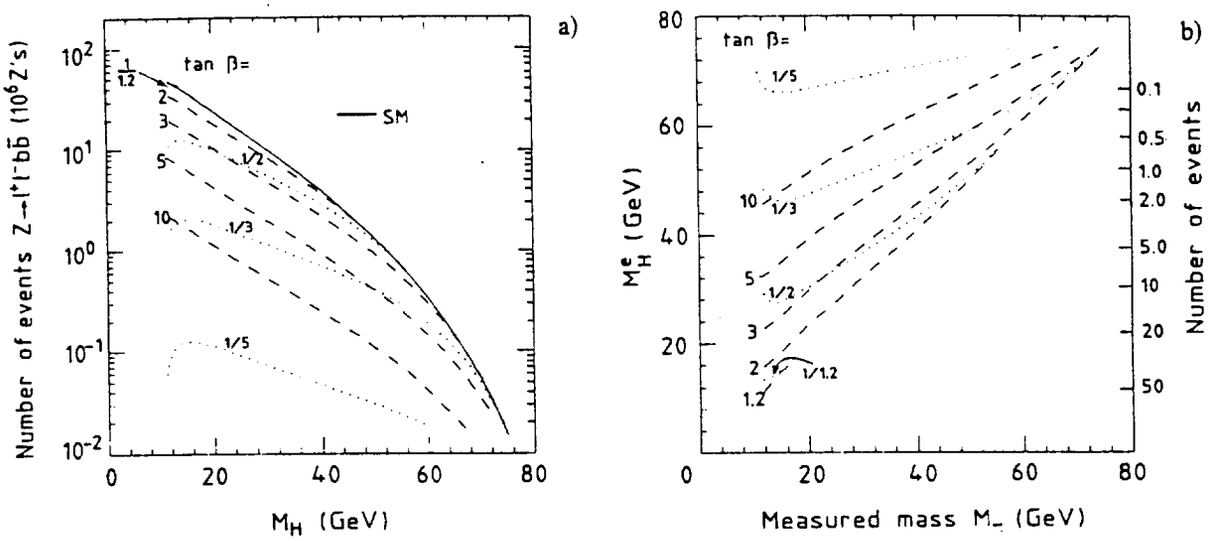

Figure 33. Contours in various $\tan\beta$ values in the plane of number of $Z \to l^+l^- H \to l^+l^- b\bar{b}$ events versus the measured Higgs mass (a) or in equivalent mass M_H^e versus measured mass (b). l stands for μ or e.

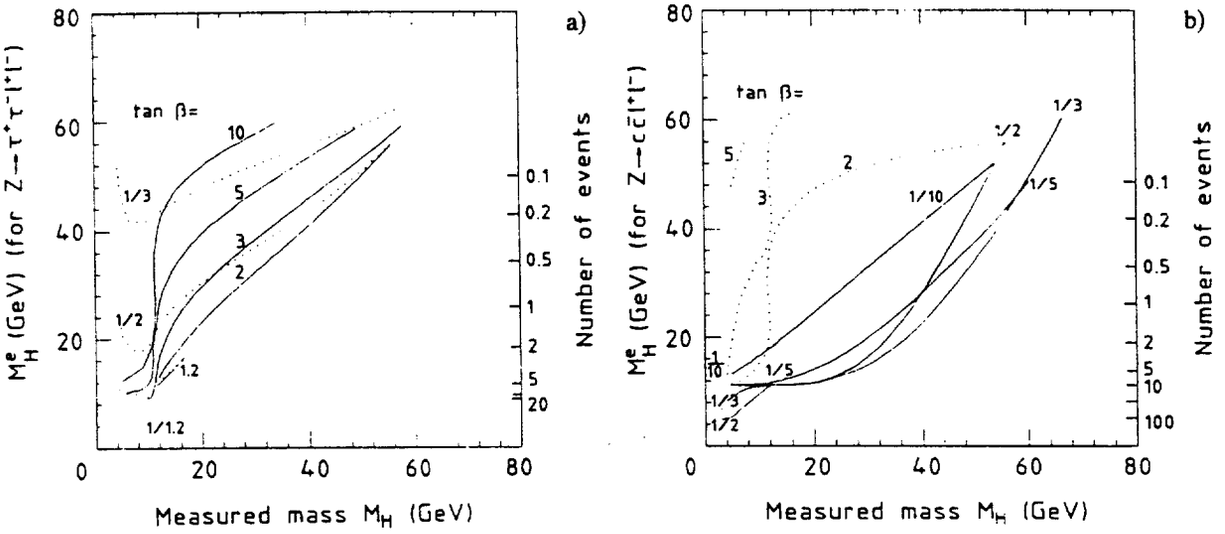

Figure 34. Contours in various $\tan\beta$ values in the plane of equivalent mass M_H^e for $Z \to l^+l^- H \to l^+l^- c\bar{c}$ events versus the measured Higgs mass (a) and in the plane of equivalent mass M_H^e for $Z \to l^+l^- H \to l^+l^- \tau^+\tau^-$ events versus the measured Higgs mass (b). l stands for μ or e.

in various $\tan\beta$ values in the plane of number of $Z \to l^+l^- H$ events versus the measured Higgs mass (Fig. 32a) or in equivalent mass M_H^e versus measured mass (Fig. 32b). In Fig. 33 we show the equivalent contours for $Z \to l^+l^- H \to l^+l^- b\bar{b}$, and in Fig. 34 the contours (in the $M_H^e - M_H$ plane only) for $Z \to l^+l^- H \to l^+l^- c\bar{c}$ and $Z \to l^+l^- H \to l^+l^- \tau^+\tau^-$ (note that for this last the contours for $\tan\beta = 3$, 2, and 1.2 get truncated for low M_H because the event rate gets higher than in the standard model for any M_H as the $\tau^+\tau^-$ channel gets enhanced relative to $c\bar{c}$ — see eq. (7.6)).

To summarize, if $\tan\beta \to 1$, h^0 will behave like the Standard Model Higgs and it will be difficult to distinguish it from H^0_{SM}; if on the contrary $\tan\beta$ is large ($\gtrsim 5$) (favored in supergravity models in the case of a heavy top quark) the rapid suppression of the decay $Z^0 \to$

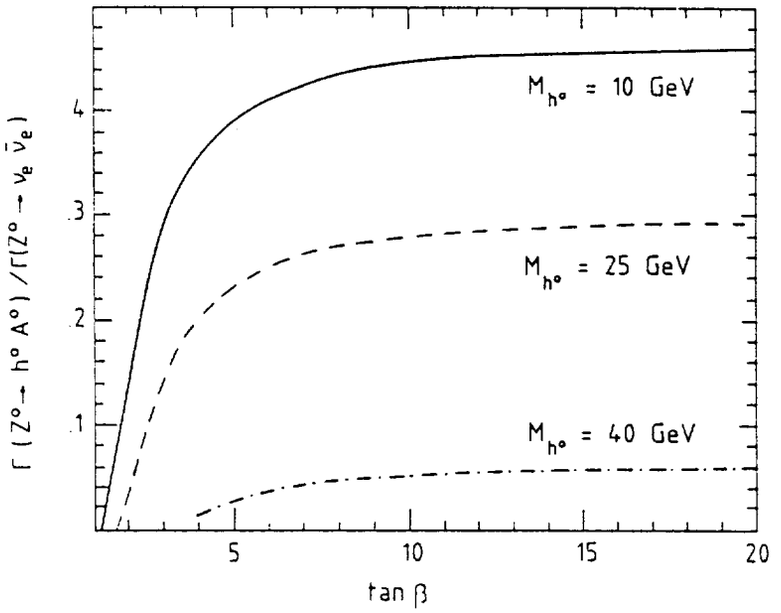

Figure 35. The value of $\Gamma(Z^0 \to h^0 A^0)/\Gamma(Z^0 \to \nu_e \overline{\nu}_e)$ as a function of $\tan\beta$, for various values of M_h^0 (from Ref. 98).

$h^0 l^+ l^-$ makes this process hopeless for the detection of a light SUSY Higgs at LEP I. Fortunately, if $\tan\beta$ is large and h^0 light, A^0 becomes light too and the branching ratio for the complementary process $Z^0 \to h^0 A^0$ increases dramatically. The rate for this decay compared to the standard model process $Z^0 \to \nu_e \overline{\nu}_e$ is

$$\frac{\Gamma(Z^0 \to h^0 A^0)}{\Gamma(Z^0 \to \nu_e \overline{\nu}_e)} = \frac{1}{2}\cos^2(\beta - \alpha)\,\lambda^3\left(1, \frac{M_{h^0}^2}{M_Z^2}, \frac{M_{A^0}^2}{M_Z^2}\right) \tag{7.11}$$

where λ is the usual kinematic factor

$$\lambda(a,b,c) = \left((a-b-c)^2 - 4bc\right)^{1/2} \tag{7.12}$$

and the differential cross-section has a $\sin^2\theta$ angular dependence.

This relative branching ratio is shown in Fig. 35, as a function of $\tan\beta$, for various values of M_{h^0}. In Fig. 36 we show contours of this ratio versus $\tan\beta$ and M_A, or in other words, the limits on the $\tan\beta - M_A$ parameter space that can be placed given limits on this ratio.

In Fig. 37 we illustrate the complementarity of these processes by displaying together two of the bounds from Figs. 30 and 36. Comparing this figure with Fig. 28 we see that the combined excluded region is sufficient to exclude $M_{h^0} \lesssim .2 M_{Z^0}$ and $M_{A^0} \lesssim .3 M_{Z^0}$, while each measurement alone would not exclude any values of M_{h^0} or M_{A^0}.

For comparison, in Fig. 38, we show the $B\overline{B}$ mixing bounds of Figs. 26 and 27 redrawn in the $\tan\beta - M_A$ plane.

The question of the decay modes of these Higgs bosons now becomes critical. For the mass range of interest to us the only interesting tree level modes are heavy quark or lepton pairs.

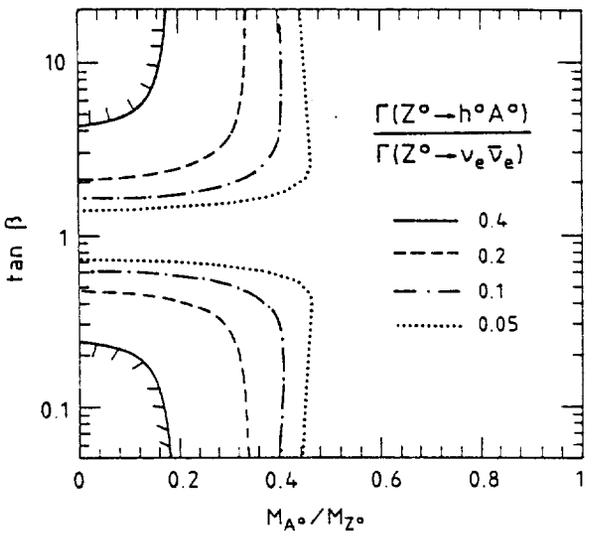

Figure 36. Limits on the $\tan\beta - M_A$ parameter space, given limits on the branching ratio of $Z \to h^0 A^0$.

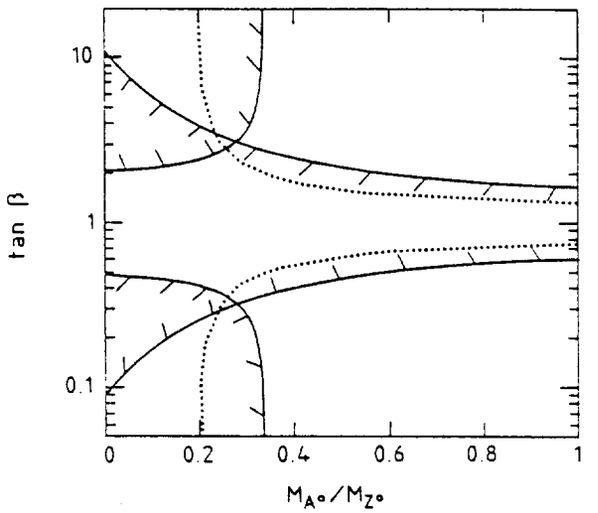

Figure 37. Excluded region of $\tan\beta - M_A$ parameter space, given the limits $BR(Z^0 \to h^0\mu^+\mu^-) < 1 \times 10^{-5}$ and $\Gamma(Z^0 \to h^0 A^0)/\Gamma(Z^0 \to \nu_e\bar{\nu}_e) < 0.2$. For comparison, we show the dotted line representing $M_{h^0}/M_{Z^0} = 0.2$, which we see is excluded.

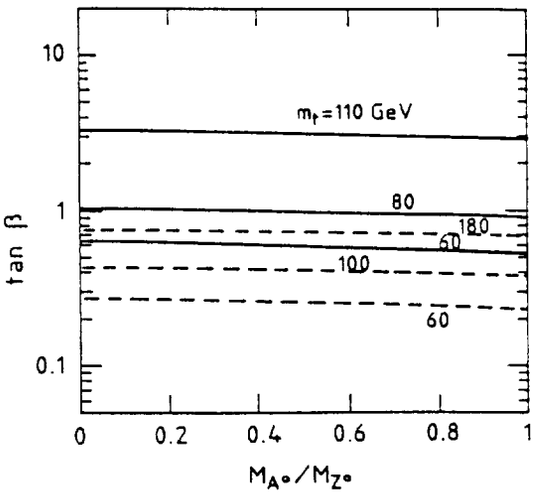

Figure 38. Limits on $\tan\beta - M_A$ parameter space from $B\overline{B}$ mixing (solid, case 2 of previous section; dashed, case 1 of previous section).

Each Higgs tends to decay into the heaviest possible particles, but the effects of the mixing of the original Higgs doublets introduces new factors.

7.3 Signals from $Z \to h^0 A^0$ decay

We now wish to discuss the signals that may emerge from the decay of the Z boson into a pseudoscalar A^0 and scalar h^0, which may be an extremely copious process. The solid lines in Fig. 39 show lines of constant $BR(Z \to h^0 A^0)$ in the $M_{h^0} - M_{A^0}$ plane (like Fig. 36 in a different parameter space). Fixing M_{h^0} and M_{A^0} still leaves the ambiguity $\tan\beta \leftrightarrow \cot\beta$; however the $Z^0 h^0 A^0$ and $Z^0 Z^0 h^0$ couplings are fixed uniquely (see eq. (7.10)). We see that the branching ratio can be quite large, unless either $M^2_{h^0} << M^2_{A^0}$ (corresponding to $\tan\beta$ near 1; see Figs. 28 and 36), or kinematic constraints become severe. We also show in Fig. 39 lines of constant $BR(Z^0 \to \mu^+\mu^- h^0)$, the complementary process. While this branching ratio is small relative to $Z \to hA$, the characteristic energy and invariant mass distribution of the lepton pair gives a clear Higgs signal without having to resort to special decay modes of the Higgs boson.

Unfortunately, the $Z \to h^0 A^0$ decay does not immediately provide a striking signature for Higgs production (unlike the Bjorken process), if both Higgs bosons decay hadronically and the efficiency for identifying heavy quarks, especially b quarks, is low. In this case one would basically see a fairly spherical event, with usually some amount of missing energy due to semileptonic decays in the decay chain $b \to c \to s$. Any pair production of hadronically decaying heavy particles will look qualitatively similar. Also, if b quarks cannot be identified efficiently, all QCD multijet events contribute to the background. For a clear Higgs signal one therefore probably has to require one of the two Higgs bosons to decay into a $\tau^+\tau^-$ pair. In Fig. 40 we show lines of constant branching ratio for $Z \to h^0 A^0 \to \tau^+\tau^- X$ in the $M_{h^0} - M_{A^0}$ plane, where we now have to specify $\tan\beta \geq 1$. Comparison with Fig. 39 shows that the loss in rate is not as large as one might have feared; even if both h^0 and A^0 are well above $2m_b$, one loses only about a factor of 7 (10, if QCD corrections had not been included). In contrast, if we require that X is not just one photon (to suppress the radiative τ pair background), then requiring the event to

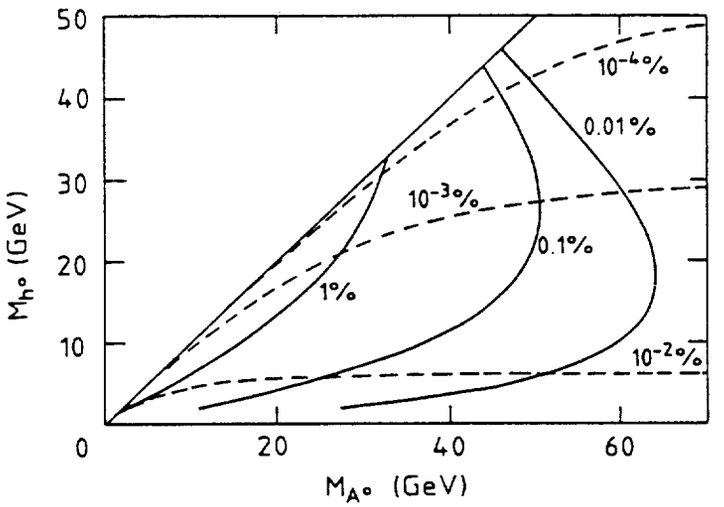

Figure 39. Lines of constant $BR(Z \to h^0 A^0)$ (solid) and $BR(Z \to \mu^+\mu^- h^0)$ (dashed) in the $M_{h^0} - M_{A^0}$ plane, using $M_Z = 93$ GeV, $\Gamma_Z = 3$ GeV and assuming $M^2_H >> \Gamma^2_Z$.

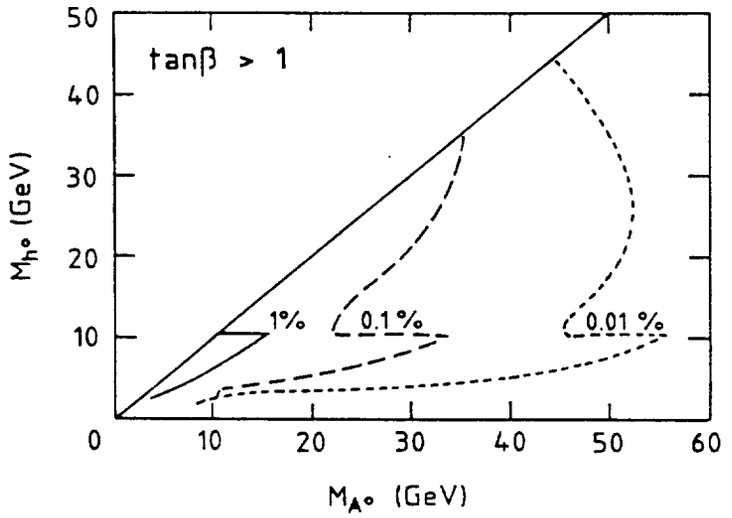

Figure 40. Lines of constant $BR(Z \to h^0 A^0 \to \tau^+\tau^- X)$ in the $M_{h^0} - M_{A^0}$ plane.

contain a τ pair reduces background by a factor $(\alpha/\alpha_s)^2 \approx 10^{-2}$ even for perfect b identification, and by a still larger factor without a good b trigger. Thus losing 85% of the events is not too high a price to pay. A procedure for identification of these events — with appropriate cuts — has already been discussed in Ref. 4 where Monte Carlo simulation is shown with optimistic conclusions.

The process $Z \to h^0 A^0 \to b\bar{b}b\bar{b}$ may be of particular interest since, if it is possible to identify leptons inside jets, the process 2 leptons + 4 jets (the leptons coming from semi-leptonic decays of 2 of the b's) may be competitive with $Z \to h^0 A^0 \to \tau^+\tau^-$ + jets. The experimental outlook is optimistic, but there may be difficulties in identification if M_{h^0} and M_{A^0} are relatively large, since the A^0 and h^0 will be nearly at rest and the decay products will be widely distributed. Trouble may also occur if $M_{h^0} \lesssim 2m_\tau$ and/or if $M_{A^0} \lesssim 2m_b$. In general low masses (i.e., below $\tau^+\tau^-$ threshold) together with large $\tan\beta$ may lead to difficulties in detection.

Note the spikes at $M_{h^0} \approx 2M_B$, which are due to the opening of the $h^0 \to$ beauty decay channel. In this figure we have neglected all mixing effects, which would substantially complicate the situation around $M_{h^0,A^0} \approx 10$ GeV.

It should be stressed that even though a b-quark identification does not seem to be necessary to extract a clean Higgs signal if $\tan\beta > 1$, it would still be very useful: requiring, e.g., h^0 to decay into $\tau^+\tau^-$, one could then measure the various branching ratios of A^0 as predicted in Figs. 8-9, and vice versa. Note that within the minimal model all rates and branching ratios are fixed once M_{h^0} and M_{A^0} are known (e.g., kinematically); each measured cross-section is then an additional check on the model.

In Figs. 41 and 42, we show the distribution of τ pair opening angles in the process $Z \to h^0 A^0 \to \tau^+\tau^- A^0$ for several choices of the h^0 and A^0 masses.

Finally, despite strong theoretical arguments in favor of $\tan\beta > 1$, the opposite possibility should not be totally forgotten. In this case the $h^0, A^0 \to \tau^+\tau^-$ branching ratios are severely suppressed. (Recall that couplings to both leptons and down-type quarks are suppressed for

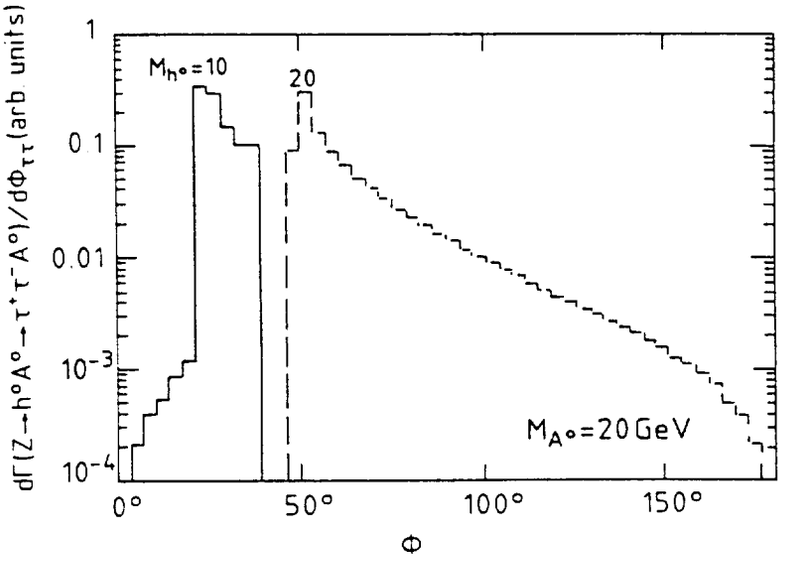

Figure 41. The distribution of τ pair opening angles in the process $Z \to h^0 A^0 \to \tau^+\tau^- A^0$ for $M_{A^0} = 20$ GeV and several choices of the h^0 mass.

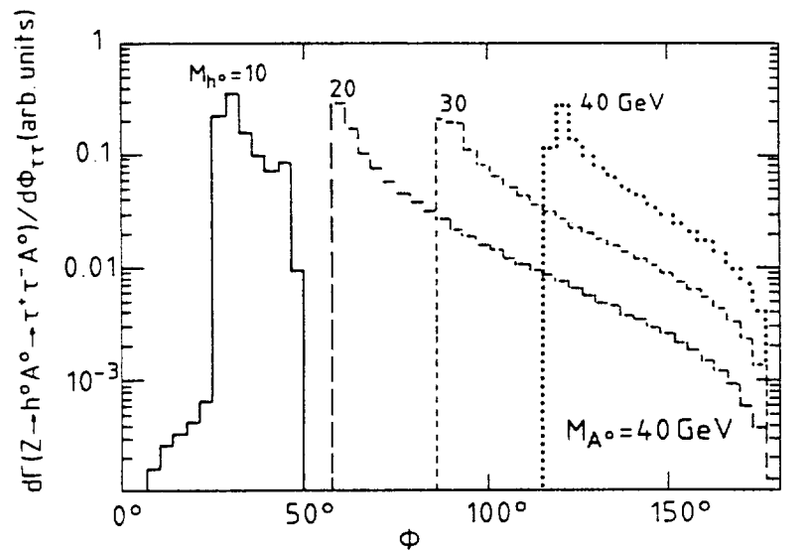

Figure 42. The distribution of τ pair opening angles in the process $Z \to h^0 A^0 \to \tau^+\tau^- A^0$ for $M_{A^0} = 40$ GeV and several choices of the h^0 mass.

$\tan\beta < 1$.) However, as long as $\tan\beta > 1/3$, sufficiently heavy Higgs bosons will still dominantly decay into $b\bar{b}$; b quark identification might then be crucial to extract an unambiguous Higgs signal. The $c\bar{c}$ decay widths with respect to those for $b\bar{b}$, derived from eq. (7.6), are

$$\begin{aligned}
\frac{\Gamma(h^0 \to c\bar{c})}{\Gamma(h^0 \to b\bar{b})} &= \frac{m_c^2}{m_b^2} \cot^2\alpha \cot^2\beta \frac{(1-4m_c^2/M_h^2)^{3/2}}{(1-4m_b^2/M_h^2)^{3/2}} \\
\frac{\Gamma(A^0 \to c\bar{c})}{\Gamma(A^0 \to b\bar{b})} &= \frac{m_c^2}{m_b^2} \cot^4\beta \frac{(1-4m_c^2/M_h^2)^{1/2}}{(1-4m_b^2/M_h^2)^{1/2}}.
\end{aligned} \tag{7.13}$$

The ratios for $c\bar{c}$ versus $\tau^+\tau^-$ are trivially obtained by $m_b \to m_\tau$ and multiplying by a color factor of 3. Note the different phase space dependences for h^0 and A^0 decays.

Parts of the $M_{h^0} - M_{A^0}$ plane can already be probed[99] at Tristan, but the higher energy at LEP obviously allows us to extend this region. Furthermore, if a signal is seen either at Tristan or at LEP, the vastly larger event rate at LEP will probably be necessary to study the properties of the Higgs bosons in detail.

7.4 Other Channels

The decays $Z^0 \to h^0\gamma$, $A^0\gamma$ These decays occur at the one-loop level, with charged particles running inside the loop as already discussed in Section 4.1 for the standard model case $Z^0 \to H^0_{SM}\gamma$. Modifications to this process come about in two ways — the couplings of the Higgses to quarks, leptons and W's are modified and also new particles (SUSY partners) may run in the loop. A study of these processes has been carried out in Ref. 100, and the conclusions are as follows.

$Z^0 \to h^0\gamma$ The contributions of quarks and leptons remain very small. SUSY only changes their couplings to the Higgses by the factors displayed in eq. (7.6), which are not large except in some extreme cases. Scalar partners of quarks and leptons contribute even less than ordinary matter fermions. The contribution of charged Higgses heavier than the W is bounded in any case, and small. The W contribution remains the dominant term, even if somewhat suppressed by the factor $\sin(\beta - \alpha)$ (see sections 6.1 and 7.1).

Charginos, the fermionic partners of the W's, contribute at the same level as the W's; thus interference between these two terms plays an important role. Unfortunately, the situation with the chargino sector is complicated by the fact that physical states are mixtures of pure Wino and Higgsino states[96] and it is impossible to analyze what happens without introducing extra parameters related to the supersymmetry breaking pattern. Contour plots for $\Gamma(Z^0 \to h^0\gamma)/\Gamma(Z^0 \to H^0_{SM}\gamma)$ with respect to these parameters are shown in ref. 100 for a light h^0. The conclusion is that this ratio can be enhanced by constructive interference or suppressed by destructive interference, by a factor of 1 to 3, the influence of the values of m_{h^0} and $\tan\beta$ being not very important. Conversely, the measurement of this decay rate at LEP would enable one to constrain the supersymmetry breaking parameters involved.

$Z^0 \to A^0\gamma$ There is no longer any contribution by $W^\pm$, $H^\pm$ or scalar partner loops, due to CP invariance. Only charged fermionic states contribute. There are no drastic differences in the matter fermionic loops (enhancement or suppression by factors of $\cot\beta$ or $\tan\beta$ according to eq. (7.6)). The chargino exchange, which is dominant, yields a ratio $\Gamma(Z^0 \to A^0\gamma)/\Gamma(Z^0 \to H^0_{SM}\gamma)$ between 0.25 and 2 (see ref. 100); consequently this decay may be observed at LEP. Note however that this process is less favorable kinematically since A^0 is required to be heavier than h^0.

The SUSY decay $Z^0 \to \tilde{\chi}^{0\prime}\tilde{\chi}^0$, $\tilde{\chi}^{0\prime} \to \tilde{\chi}^0 h^0$ Here $\tilde{\chi}^{0\prime}$ and $\tilde{\chi}^0$ are neutralinos (mass eigenstate combinations of fermionic partners of neutral gauge bosons and Higgs bosons). $\tilde{\chi}^0$ is the lightest supersymmetric particle (LSP), which is thus stable and escapes detection, so we are concerned with $Z^0 \to h^0$ + missing energy events, whose Standard Model "background" is $Z^0 \to H^0\nu\bar{\nu}$. Again the situation is model-dependent due to the various possible mixings which occur in the

neutralino sector.[96] For example the decay[101] $Z^0 \to \tilde{\chi}^{0\prime}\tilde{\chi}^0$ depends strongly on the mixing properties because the Z^0 boson only couples to the Higgsino component of the neutralinos. Nevertheless a sizable branching ratio for this decay (if kinematically allowed) may be obtained for an important range of the relevant parameters.[101] Moreover the subsequent decay[102] $\tilde{\chi}^{0\prime} \to h^0\tilde{\chi}^0$ (or $A^0\tilde{\chi}^0$) is dominant because if $\tilde{\chi}^{0\prime}$ is lighter than the Z^0, and also than the sleptons and squarks, there are no other two-body decay modes at tree level. Note however that this decay is forbidden if the LSP is a pure photino (a case presently considered very unlikely although often discussed in the literature). Keeping these uncertainties in mind, the whole cascade process has been studied in ref. 103 (see also ref. 104) and it is claimed that a branching ratio as large as 0.1% to 1% could be obtained for m_{h^0} up to $40 - 50$ GeV and for a certain range of the SUSY parameters. This would lead to a sizable enhancement of the rate for $Z^0 \to h^0 +$ missing energy, since these branching ratios are $10^2 - 10^3$ times larger than those of $Z \to h^0\nu\bar{\nu}$ (whose SUSY version is suppressed by a factor $\sin^2(\beta - \alpha)$ according to eq. (7.9)). Hence, apart from the discovery of the Higgs boson itself, this mode would distinguish SUSY from the standard model in a dramatic way. This process may be quite important because one might observe effects of slightly heavier Higgses even if they are a bit too heavy to detect in the processes we have concentrated on previously.

8. Beyond the Minimal SUSY Model - Remarks

The Minimal Supersymmetric Standard Model (MSSM) is certainly the most popular and well-explored supersymmetric theory of direct interest to experimentalists. This is due in large part to its 'minimality', being the simplest SUSY extension of the SM. It also gives rather definite predictions for the masses and couplings of the Higgs bosons, e.g., one neutral scalar Higgs always lighter than the Z^0, and $M_{H^\pm} > M_{W^\pm}$. One should, however, keep in mind that these and other features of the MSSM are *not* of general validity in supersymmetric models. In fact, one can build a variety of more complicated, or less 'minimal', models in which many predictions of the MSSM are relaxed or even completely violated. Typical supergravity and superstring models provide us with much richer scenarios, by introducing new fields and/or extending the gauge group. Here we give but one example of such a model,[105] which we call a Minimal Non-Minimal Supersymmetric Standard Model, going beyond the MSSM in a minimal way by adding to the necessary two Higgs doublets a complex scalar field N which is a singlet of the SM gauge group. (In this minimal extension we do not allow for any additional gauge group at low energy.)

There are rather strong theoretical motivations for exploring the phenomenological structure of such a model. First of all, in superstring based models one typically finds one or more singlet Higgs fields (consider, e.g., the so-called 'flipped $SU(5)$' model[106]). Secondly, as explained in ref. 105, introducing a singlet provides a dynamical mechanism for generating the mass parameter in the Higgs potential of the MSSM, whose origin is otherwise unknown. In addition, it gives a mass parameter of the correct order of magnitude, yielding in this way a simple solution to the Naturalness Problem: why is the electroweak scale ($\propto M_{W^\pm}$) so much smaller than some unification scale M_X, in turn expected to be somewhere between 10^{16} GeV and the Planck scale.

The most general trilinear superpotential for the Higgs sector with one singlet field is

$$W = \lambda N H_1 H_2 - \frac{k}{3} N^3. \tag{8.1}$$

(The singlet cubic term is necessary since otherwise there would be an unacceptable axion present in the model.) The Higgs potential reads

$$\begin{aligned} V = &\mid \lambda H_1 H_2 - kN^2 \mid^2 + \lambda^2(\mid H_1 \mid^2 + \mid H_2 \mid^2) \mid N \mid^2 + \frac{1}{8}(g^2 + g'^2)(\mid H_2 \mid^2 - \mid H_1 \mid^2)^2 \\ &+ m_1^2 \mid H_1 \mid^2 + m_2^2 \mid H_2 \mid^2 + m_N^2 \mid N \mid^2 - (\lambda A_\lambda N H_1 H_2 + \text{h.c.}) - (\frac{k A_k}{3} N^3 + \text{h.c.}) \end{aligned} \tag{8.2}$$

where the second line contains soft-SUSY breaking terms. The resulting physical Higgs spectrum consists of a pair of charged Higgs $H^\pm$, two neutral pseudoscalars P_1 and P_2, and three neutral scalars S_1, S_2 and S_3 (increasing index in the order of increasing mass).

One finds now six independent parameters (to be contrasted with two in the MSSM), and accordingly more freedom. It is not our purpose here to make a full survey of all the possibilities but rather to point out some of the departures from the MSSM.

First, the sum rules, eqs. 7.2 – 3, are in general not obeyed. In the present model they are

$$\begin{aligned} m_{S_1}^2 + m_{S_2}^2 + m_{S_3}^2 &= M_{Z^0}^2 + m_{P_1}^2 + m_{P_2}^2 + 4k(kx^2 - A_k x - \lambda v_1 v_2) \\ m_{H^\pm}^2 &= M_{W^\pm}^2 + m_{P_1}^2 + m_{P_2}^2 - [\lambda^2(v_1^2 + v_2^2) + \lambda A_\Sigma \frac{v_1 v_2}{x} + 3k(\lambda v_1 v_2 - A_k x)] \end{aligned} \tag{8.3}$$

where $x =< N >$ is the singlet vacuum expectation value and $A_\Sigma = A_\lambda + kx$.

Obviously, due to the minus sign in eq. (8.3b), it is now possible for the charged Higgs to be lighter than the W, depending on the relative values of the parameters. One region of the parameter space where $H^\pm$ is invariably lighter than the W is when $x << v_1, v_2$. On the other hand, for $x >> v_1, v_2$ *all* the Higgs bosons can be heavier than the Z and some of them can even be in the TeV region. Secondly, the Higgs couplings to vector bosons pairs can be substantially different from the MSSM case, as well as the couplings to quarks and other matter fields. In particular, for some choices of parameters the lightest scalar S_1 can share only very small couplings to W^+W^- and Z^0Z^0, in contrast to the minimal supersymmetric case. Thirdly, since the singlet N does not couple to the ordinary matter, it will be rather hard to produce and detect those physical scalars which have a substantial N component.

In order to give the flavor of a typical scenario that one can expect in this model, we give the example of a representative choice of parameters resulting from solving the Renormalization Group Equations with the plausible assumption that the (universal) gaugino mass is the only source of SUSY breaking at the unification scale. The values for the six independent parameters are

$$\begin{aligned} &\tan\beta = 2.04 \quad x/\sqrt{v_1^2 + v_2^2} = 0.64 \quad \lambda = 0.128 \quad k = 0.097 \\ &A_\lambda = 28.6 \text{ GeV} \quad A_k = 0.7 \text{ GeV}. \end{aligned} \tag{8.4}$$

The corresponding masses of the Higgs bosons are given in Table 3.

Particle	S_1	S_2	S_3	P_1	P_2	$H^{\pm}$
Mass (GeV)	15	38	95	31	39	86

Table 3. Higgs boson masses for the choice of parameters given in (8.4).

In addition, the top mass is 83 GeV, and the squark and gluino masses are 177 GeV and 204 GeV, respectively. The lightest supersymmetric partner (LSP) can be either the sneutrino or the lightest neutralino, both having mass of 23 GeV.

The results are clearly encouraging — many particles are predicted to have masses within the LEP range — the two lightest scalars, as well as both pseudoscalars, are considerably lighter than the Z. This opens up the possibility of not only single scalar production but also of a scalar-pseudoscalar pair production from Z decays. More detailed study confirms this conjecture.[105]

The presence of a light scalar in SUSY theories seems to be their general feature.[107] This can be illustrated by several specific examples. In a superstring inspired model[108] based on the E_6 unification group with the low-energy gauge group containing an additional $U(1)$, the lightest scalar can be in principle substantially heavier than the Z. However, by requiring that various parameters remain in the perturbative regime one can restrict it to lie below about 108 GeV.[109] In this model the charged Higgs can also be lighter than the W but never less than about 54 GeV.[109,110] The Higgs mass spectrum is highly constrained with several Higgs bosons almost degenerate in mass and one Higgs nearly degenerate in mass with the extra neutral gauge boson.

In a supersymmetric left-right model[111] resulting from the E_6 superstring model the lightest neutral scalar can never be heavier than $\sqrt{2}m_W$. A detailed survey of various supersymmetric (as well as non-supersymmetric) extensions of the MSSM can be found in Ref. 2.

As we have seen, it is quite probable that the lightest scalar is light enough to be discovered at LEP. One should not, however, forget that it is not impossible, although perhaps a bit unnatural, in SUSY models, to have all the Higgs bosons even beyond the reach of LEP II. In conclusion, in searching for the Higgs one should certainly not restrict oneself to the SM or its simplest SUSY extension.

9. Charged Higgs

So far we have concentrated on neutral Higgses, particularly in the context of the Minimal Supersymmetric Standard Model, where the charged Higgses are required to be heavier than the W boson, and hence are unobservable at LEP I. However, the search for a light charged Higgs, which can be carried out at LEP I, is of undeniable importance, both on general grounds and because the observation of such a particle would immediately rule out the MSSM. Moreover, current bounds on the top quark mass, from hadron colliders,[95] can be invalidated by the existence of a light charged Higgs,[112] as will be discussed below in detail.

We will consider only Model I and Model II, as described in Section 2.1. The couplings of the charged Higgs to fermions are then given by the lagrangian:

$$\mathcal{L}_{H^+f'\overline{f}} = \frac{g}{2\sqrt{2}M_W}\Big[H^+\overline{U}\Big(\cot\beta M_u V(1-\gamma_5) - \cot\beta V M_d(1+\gamma_5)\Big)D \\ - H^+\overline{N}\cot\beta M_l(1+\gamma_5)L + \text{h.c.}\Big] \tag{9.1}$$

for Model I, where v_2 (in $\tan\beta \equiv v_2/v_1$) is the VEV of the only Higgs field coupling to fermions, and

$$\mathcal{L}_{H^+f'\overline{f}} = \frac{g}{2\sqrt{2}M_W}\Big[H^+\overline{U}\Big(\cot\beta M_u V(1-\gamma_5) + \tan\beta V M_d(1+\gamma_5)\Big)D \\ + H^+\overline{N}\tan\beta M_l(1+\gamma_5)L + \text{h.c.}\Big] \tag{9.2}$$

for Model II, where v_2 (v_1) is the VEV of the Higgs field coupling only to up-type (down-type) fermions. In these equations U and D are column matrices consisting of three generations of quark fields; N and L are column matrices consisting of three generations of neutrinos and charged leptons; V is the CKM matrix, and M_u, M_d and M_l are the diagonal mass matrices for the up-type quarks, down-type quarks, and charged leptons respectively. Also essential to our study of charged Higgs is the vertex $Z^0H^+H^-$, given by

$$\frac{-ig\cos 2\theta_W}{2\cos\theta_W}(p+p')^\mu \tag{9.3}$$

where p and p' are the Higgs momenta. At tree level, the vertices $H^+W^-\gamma$ and $H^+W^-Z^0$ vanish. The $H^+W^-\gamma$ vertex is zero as a consequence of the conservation of the electromagnetic current. The vanishing of the $H^+W^-Z^0$ vertex is more model dependent but turns out to be a general feature of all models with only Higgs doublets and singlets.[113]

The existence of a charged Higgs boson light enough to be detected at LEP I is intimately tied to the search for a top quark via its characteristic semi-leptonic decays at the $p\bar{p}$ colliders. If $M_{H^\pm}$ is less than $m_t - m_b$, the dominant decay mode of the top quark becomes $t \to H^+ + b$ (for $m_t < M_W + m_b$). The decay width, for a general coupling of the form $\bar{u}(x + \gamma_5 y)dH$, is

$$\Gamma(t \to H^\pm b) = \frac{1}{16\pi m_t}\lambda\left(1, \frac{m_b^2}{m_t^2}, \frac{M_{H^\pm}^2}{M_t^2}\right)\left[(x^2+y^2)(m_t^2+m_b^2-M_{H^\pm}^2) + 2(x^2-y^2)m_t m_b\right] \tag{9.4}$$

giving for Models I and II[114] respectively

$$\Gamma = \frac{G_F\sqrt{2}}{8\pi}\left[\left[\cot^2\beta m_t^2 + \cot^2\beta m_b^2\right](m_t^2+m_b^2-M_{H^\pm}^2) - \cot^2\beta(2m_b m_t)^2\right]\lambda(m_t^2, m_b^2, M_{H^\pm}^2)/m_t^3$$

$$\Gamma = \frac{G_F\sqrt{2}}{8\pi}\left[\left[\cot^2\beta m_t^2 + \tan^2\beta m_b^2\right](m_t^2+m_b^2-M_{H^\pm}^2) + (2m_b m_t)^2\right]\lambda(m_t^2, m_b^2, M_{H^\pm}^2)/m_t^3 \tag{9.5}$$

assuming $V_{tb} = 1$. The width in Model I can become arbitrarily small as $\tan\beta$ increases, but in Model II, which we will concentrate on for illustrative purposes, the quantity in the inner square brackets cannot be smaller than $2m_t m_b$. In this minimal situation, for $m_t - M_H - m_b = 0.3$ GeV, we already have $\Gamma \geq .4$ MeV (if instead $\tan\beta = 1$, $\Gamma \gtrsim 1$ MeV), far larger than the weak interaction width of

$$\Gamma = \frac{9G_F^2 m_t^5}{192\pi^3} = .04 \text{ MeV} \tag{9.6}$$

for $m_t = 45$ GeV. Moreover, the $B\bar{B}$ mixing measurements (see Figs. 26,27) tend to require small values of $\tan\beta$ to accommodate a light top quark, and hence we expect even larger decay widths for $t \to H^+ + b$.

Thus the discovery of the top quark via its semi-leptonic decays would exclude $M_{H^\pm} \lesssim m_t - 5$ GeV. In fact, at the time of writing of Refs. 4, 5, the possibility of a charged Higgs light enough to be detected at LEP I was considered rather dubious due to the "discovery" of the top quark at around 40 GeV. Now instead the problem is the reverse — in order for $t \to H^\pm + b$ to be a useful production mode for $H^\pm$ we require a top quark light enough to be pair produced at LEP I — almost certainly excluded now in the Standard Model. *However*, it is precisely this decay which, by possibly swamping the expected semi-leptonic rate, provides the only serious doubt to the $p\bar{p}$ collider limits; thus it is not only possible, but peculiarly appropriate, to search for the charged Higgs in this mode. (We will see below that the usual signature of the top quark, $t \to b\mu^+\nu$ and $t \to be^+\nu$ are respectively a hundred and 10^7 times rarer through Higgs decay than in the conventional picture—however it is possible that a significant part of this signature might be restored by top decays to a τ subsequently producing an e or μ.) We recall that the existence of a charged Higgs with small $\tan\beta$ can also allow one to reconcile a light top quark with the current $B\bar{B}$ mixing measurements.

While the top quark remains undiscovered, the possibility remains that the $H^\pm$ is light enough to be pair produced at LEP I while the t quark is not. Limits on charged Higgses are important to validate the top limits, although unfortunately the limits that can be placed at LEP I cover only part of the range in $M_{H^\pm}$ relevant to the anticipated top quark limits from $p\bar{p}$ colliders in the near future.

We refer the reader to Refs. 6 and 4 for formulas and event rates for pair production of charged Higgses off the Z peak (where the photon exchange diagram dominates) but we do not think this will be useful at LEP I, particularly in the initial year. Again, the differential cross section goes as $\sin^2\theta$. The partial width for $Z \to H^+H^-$ is[115]

$$\Gamma(Z \to H^+H^-) = \frac{G_F M_Z^3}{6\sqrt{2}\pi}\left(\frac{1}{2} - \sin^2\theta_W\right)^2 \beta_H^3. \tag{9.7}$$

This gives a branching ratio of about 1 percent, times the kinematic suppression, or about 0.4% for a 30 GeV Higgs, 0.1% for a 40 GeV Higgs. For comparison to the previous production mode, we give the partial width to top quarks:

$$\Gamma(Z \to t\bar{t}) = \frac{G_F M_Z^3}{6\sqrt{2}\pi}\beta_t\left(\frac{1}{4}\beta_t^2 + \left(\frac{1}{2} - \frac{4\sin^2\theta_W}{3}\right)^2 \frac{3-\beta_t^2}{2}\right) \tag{9.8}$$

or about 10 percent before kinematic suppressions, 1.5% for a 35 GeV top quark, 0.1% for a 45 GeV top quark. Near $m_t = M_Z/2$ this zeroth order formula greatly underestimates the actual decay width as toponium-Z interference effects and QCD corrections must be taken into account; for details we refer to the section devoted to heavy flavor production in this workshop.[116]

For the decay widths, we give formulas in the approximation of massless decay products, since a top quark lighter than the Higgs is ruled out. We refer the reader to Ref.117 for the full formulas for massive decay products. The partial widths in Model II are then

$$\Gamma(H^+ \to \nu_l l^+) = \frac{G_F\sqrt{2}}{8\pi} M_H \tan^2\beta \; m_l^2 \tag{9.9}$$

$$\Gamma(H^+ \to u_{i=1,2}\bar{d}_{j=1,2,3}) = \frac{G_F\sqrt{2}}{8\pi} M_H 3|V_{ij}|^2 \left[\cot^2\beta \; m_i^2 + \tan^2\beta \; m_j^2\right]. \tag{9.10}$$

In Model I all $\tan\beta$'s are replaced by $\cot\beta$'s.

For $\tan\beta = 1$ in Model II, or independent of $\tan\beta$ in Model I, we expect the branching ratio to $c\bar{s}$ to be a little less than 2/3; that to $\tau^+\nu_\tau$ to be a little less than 1/3; $\mu^-\nu_\mu$ around 10^{-3}; $e^+\nu_e$ around 2×10^{-8}, and the remaining (hadronic) modes to add up to around 5%. Note that in Model II we might expect the leptonic branching ratios to be further suppressed by factors of $\sim \tan^4\beta$.

A characteristic signal is obtained when one of the produced Higgses decays to hadrons, and the other to $\tau\nu$, expected for $\sim 4/9$ of the charged Higgs pairs ($\sim \frac{4}{9}\left(\frac{3}{\tan^2\beta+2\cot^2\beta}\right)^2$ in Model II). This results in an event in which exactly half of the energy is carried off by hadrons and in which there is an energetic, well-separated τ.

ACKNOWLEDGEMENTS

We would like to thank E. Duchovni, Paolo Franzini, O. Ganel, E. W. N. Glover, E. Gross, K. I. Hikasa, G. Hulth, R. Kleiss, C. Klopfenstein, J. Lee-Franzini, A. D. Linde, G. Mikenberg, S. Narison, H. Nelson and J. J. van der Bij for useful discussions. Special thanks go to the authors of the "Higgs Hunter" — S. Dawson, J. Gunion, H. Haber, and G. Kane — for allowing us to consult preliminary drafts of their manuscript.

REFERENCES

1. R. N. Cahn, Rept. Prog. Phys. **52** (1989) 389.
2. S. Dawson, J. F. Gunion, H. E. Haber and G. L. Kane, *The Physics of Higgs Bosons: The Higgs Hunter's Guide*, to be published (1989).
3. M. S. Chanowitz, Ann. Rev. Nucl. Part. Sci. **38** (1988) 323.
4. H. Baer et al, CERN Yellow Book 86-02 (1986) 297.
5. W. Buchmüller et al, CERN Yellow Book 86-02 (1986) 203.
6. G. Barbiellini et al, DESY preprint 79/27 (1979).
7. J. Ellis, M. K. Gaillard, and D. V. Nanopoulos, Nucl. Phys. **B106** (1976) 292.
8. H. Nelson, NA31 collaboration, CERN EP preprint in preparation.
9. A. Djouadi and F. Oualitsen, Aachen preprint PITHA-89/15 (1989), and refs. therein.
10. E. Braaten and J.P. Leveille, Phys. Rev. **D22** (1980) 715. See also N. Sakai, Phys. Rev. **D22** (1980) 2220; T. Inami and T. Kubota, Nucl. Phys. **B179** (1981) 171. An extension of these calculations may be found in a more recent paper, P. Janot, Phys. Lett. **223B** (1989) 110. However, the results of this paper for the Higgs decay width appear to be in disagreement with those of the first paper above, and with the asymptotic limits given in the second two. M. Drees and K. Hikasa have repeated this calculation in a slightly different formalism and are in agreement with Braaten and Leveille. The differences seem to stem from the omission of the self-energy diagrams in the paper by Janot.
11. M. Drees and K. Hikasa, KEK/CERN preprint CERN-TH.5393/89 (1989).
12. J. Schwinger, *Particles, Sources and Fields, Vol. II* (Addison-Wesley, Reading, MA, 1973).
13. For a recent review, see W. Kwong, J. L. Rosner, and C. Quigg, Ann. Rev. Nucl. Part. Sci. **37** (1987) 325.
14. J. Ellis, M. K. Gaillard, D. V. Nanopoulos and C. T. Sachrajda, Phys. Lett. **83B** (1979) 339.
15. J. F. Gunion and H. E. Haber, Nucl. Phys. **B272** (1986) 1, Nucl. Phys. **B278** (1986) 449.
16. L. J. Reinders, H. Rubinstein and S. Yazaki, Phys. Rep. **127** (1985) 1.
17. For a review, see H. P. Nilles, Phys. Rep. **110** (1984) 1.
18. K. Griest and H. E. Haber, Phys. Rev. **B37** (1988) 719; J. F. Gunion and H. E. Haber, Nucl. Phys. **B307** (1988) 445.
19. M. B. Voloshin, Sov. J. Nucl. Phys. **44** (1986) 478 (Yad. Fiz. **44** (1986) 738).
20. M. A. Shifman, A. I. Vainshtein and V. I. Zakharov, Phys. Lett. **78B** (1978) 443.
21. V. A. Novikov and M. A. Shifman, Z. Phys. **C8** (1981) 43.

22. R. Crewther, Phys. Rev. Lett. **28** (1972) 1421; M. Chanowitz and J. Ellis, Phys. Lett. **40B** (1972) 397; J. C. Collins, A. Duncan and S. D. Joglekar, Phys. Rev. **D16** (1977) 438.

23. T. N. Truong and R. S. Willey, University of Pittsburgh Report PITT-89-05 (1989).

24. See for example Chanowitz (ref. 3) and T. P. Cheng, IASSNS/HEP-88/22 (1988).

25. R. Barbieri and G. Curci, Phys. Lett. **219B** (1989) 503.

26. B. Grinstein, L. Hall, and L. Randall, Phys. Lett. **211B** (1988) 363.

27. See for example Ref. 2 for a summary.

28. S. Raby and G. B. West, Phys. Rev. **D38** (1988) 3488.

29. E. Duchovni, E. Gross and G. Mikenberg, Phys. Rev. **D39** (1989) 365.

30. S. Narison, CERN preprint CERN-TH.5452/89 (1989).

31. S. Narison and G. Veneziano, Int. J. Mod. Phys. **A4** (1989) 2751.

32. Particle Data Group, Phys. Lett. **204B** (1988) 1.

33. See e.g. Refs. 20, 2 and 1, and references therein.

34. S. Raby, G. B. West and C. M. Hoffman, Phys. Rev. **D39** (1989) 828.

35. S. Egli et al, SINDRUM collaboration, PSI preprint PSI-PR 89-02 (1989).

36. P. Yepes, CERN preprint CERN-EP 89-68 (1989).

37. J. Lee-Franzini, CUSB collaboration, invited talk in *Proceedings of the XXIVth International Conference on High Energy Physics*, Munich, Germany, August 4-10. 1988.

38. CLEO collaboration, M. S. Alam et al, Cornell University preprint CLNS 89/888 (1989).

39. I. Beltrami et al, Nucl. Phys. **A451** (1986) 679.

40. S. L. Adler, R. F. Dashen and S. B. Treiman, Phys. Rev. **D10** (1974) 3728; the experimental references are given in this paper.

41. CUSB collaboration, M. Sivertz et al, Phys. Rev. **D26** (1982) 717.

42. Crystal Ball collaboration, C. Edwards et al, Phys. Rev. Lett. **48** (1982) 903.

43. M. I. Vystosky, Phys. Lett. **97B** (1980) 159; J. Ellis et al, ibid., **158B** (1985) 417; P. Nason, ibid., **175B** (1986) 223.

44. J. Lee-Franzini, CUSB collaboration, invited talk in *Proceedings of the INFN Eloisatron Project Higgs Workshop, Erice, Italy, July* 15 – 26, edited by A. Ali (Plenum, 1989).

45. T. E. O. Ericson and R. Barbieri, Phys. Lett. **57B** (1975) 270.

46. D. Kohler, B. Watson and J. Becker, Phys. Rev. Lett. **33** (1974) 1628; S. J. Freedman, J. Napolitano, J. Camp and M. Kroupa, Phys. Rev. Lett. **52** (1984) 240.

47. E731 collaboration, L. K. Gibbons et al, Phys. Rev. Lett. **61** (1988) 2661.

48. TASSO collaboration, M. Althoff et al, Zeit. Phys. **C22** (1984) 219.

49. JADE collaboration, W. Bartel et al, Phys. Lett. **132B** (1983) 241.

50. F. Wilczek, Phys. Rev. Lett. **39** (1977) 1304.

51. H. Goldberg and Z. Ryzak, Phys. Lett. **218B** (1989) 348.

52. I. Aznauryan, S. Grigoryan and S. Matinyan, JETP Lett. **43** (1986) 646; G. Fäldt, P. Osland and T. T. Wu, Phys. Rev. **D38** (1988) 164; see discussions in Refs. 2 and 34.

53. ARGUS collaboration, H. Albrecht et al., Zeit. Phys. **C42** (1989) 349.

54. M. Sher, Washington University preprint WU-TH-88-8, to appear in Physics Reports.

55. M. Veltman, Acta Physica Polonica **B8** (1977) 64; M. B. Einhorn and J. Wudka, Phys. Rev. **D39** (1989) 2758.

56. U. Amaldi et al, Phys. Rev. **D36** (1987) 1385; G. Costa et al, Nucl. Phys. **B297** (1988) 244.

57. A. D. Linde, JETP Lett. **23** (1976) 64.

58. A. D. Linde, Phys. Lett. **70B** (1977) 306.

59. S. Weinberg, Phys. Rev. Lett. **36** (1976) 294.

60. N. Cabibbo, L. Maiani, G. Parisi and R. Petronzio, Nucl. Phys. **B158** (1979) 295.

61. S. Coleman and E. Weinberg, Phys. Rev. **D7** (1973) 1888.

62. A. D. Linde, ICTP, Trieste preprint IC/76/26.

63. P. H. Frampton, Phys. Rev. Lett. **37** (1976) 1378.

64. A. D. Linde, Phys. Lett. **92B** (1980) 119.

65. See for example A. D. Linde, Phys. Rev. **D14** (1976) 3345.

66. K. G. Wilson, Phys. Rev. **B4** (1971) 3184; K. G. Wilson and J. Kogut, Phys. Rep. **12** (1974) 75.

67. E. Gross and E. Duchovni, Phys. Rev. **D38** (1988) 2308.

68. M. Lindner, M. Sher and H. W. Zaglauer, Fermilab preprint FERMILAB-PUB-88/206-T.

69. R. N. Cahn, M. S. Chanowitz and N. Fleishon, Phys. Lett. **82B** (1979) 112; see also J. P. Leveille, Phys. Lett. **83B** (1979) 123.

70. E. W. N. Glover, J. J. van der Bij et al, Rare Z decays, this report (1989).

71. L. Bergström and G. Hulth, Nucl. Phys. **B259** (1986) 137, Erratum ibid. **B276** (1986) 744; A. Barroso, J. Pulido and J. C. Romao, Nucl. Phys. **B267** (1986) 509; see also Ref. 2 and Ref. 70.

72. J. D. Bjorken, in *Proceedings of the 1976 SLAC Summer Institute on Particle Physics, Stanford*, edited by M. C. Zipf (Stanford Linear Accel. Center, Stanford, CA, 1977), p.1.

73. F. A. Berends and R. Kleiss, Nucl. Phys. **B260** (1985) 32.

74. J. Finjord, Physica Scripta **21** (1980) 143.

75. R. L. Kelly and T. Shimada, Phys. Rev. **D23** (1981) 1940.

76. A. Weir et al, in *Proceedings of the 2nd MARK II Workshop on SLC physics, Tahoe City, CA*, edited by K. Krieger, SLAC-Report 306 (1986) 348.

77. D. Wood, in *Proceedings of the 2nd MARKII Workshop on SLC Physics, Tahoe City, CA*, edited by K. Krieger, SLAC-Report 306 (1986) 320.

78. E. Duchovni, E. Gross and G. Mikenberg, Weizmann preprint WIS-88/39 (1988).

79. R. Kleiss, Phys. Lett. **180B** (1986) 400.

80. See for example Refs. 2 and 4, and references therein.

81. H. E. Haber, G. L. Kane and T. Sterling, Nucl. Phys. **B161** (1979) 493.

82. S. Glashow and S. Weinberg, Phys. Rev. **D15** (1977) 1958; E. A. Paschos, *ibid.* **D15** (1977) 1966.

83. H. Georgi, A. Manohar and G. Moore, Phys. Lett. **149B** (1984) 234.

84. See, for example, H.-J. Behrends et al, CELLO collaboration, Phys. Lett. **193B** (1987) 376; W. Braunschweig et al, TASSO collaboration, submitted to *XXIV International Conference on High Energy Physics*, Munich, West Germany, August 1988.

85. See references given in Ref. 2.

86. G. G. Athanasiu, P. J. Franzini, and F. J. Gilman, Phys. Rev. **D32** (1985) 3010.

87. P. J. Franzini, Phys. Rep. **173** (1989) 1.

88. This discussion is based in part on those in Refs. 86, 87 and 2.

89. ARGUS collaboration, H. Albrecht et al, Phys. Lett. **192B** (1987) 245.

90. CLEO collaboration, H. Schröder et al, in *Proceedings of the XXIVth International Conference on High Energy Physics*, Munich, Germany, August 4-10, 1988.

91. UA1 collaboration, C. Albajar et al, Phys. Lett. **186B** (1987) 247.

92. L. Maiani, in *Proceedings of the International Symposium on Lepton and Photon Interactions at High Energies*, Hamburg, Germany, 1977; L. Wolfenstein, Phys. Rev. Lett. **51** (1983) 1945.

93. G. Altarelli, N. Cabibbo, G. Corbo, L. Maiani and G. Martinelli, Nucl. Phys. **B208** (1982) 365.

94. G. Altarelli and P. J. Franzini, Z. Phys. **C37** (1988) 271.

95. J.-P. Repellin, M. Shochet, invited talks in *Proceedings of the 3rd Rencontre de Physique de la Vallée D'Aoste, La Thuile, February 26-March 4, 1989.*

96. See, for example, H. E. Haber and G. L. Kane, Phys. Rep. **117C** (1985) 75 and ref.s therein.

97. See for example G. F. Giudice and G. Ridolfi, Zeit. Phys. **41C** (1988) 447; M. Olechowski and S. Pokorski, Phys. Lett. **214B** (1988) 393 and refs. therein.

98. G. F. Giudice, Phys. Lett. **208B** (1988) 315.

99. M. Drees and K. Hikasa, CERN/KEK preprint KEK-TH-222, CERN-TH.5313/89 (to appear in Phys. Rev. **D**).

100. G. Gamberini, G. F. Giudice and G. Ridolfi, Nucl. Phys. **B292** (1987) 237.

101. H. Komatsu, Phys. Lett. **177B** (1986) 201; R. Barbieri, G. Gamberini, G. F. Giudice and G. Ridolfi, Phys. Lett. **195B** (1987) 500.

102. H. E. Haber, I. Kani, G. L. Kane and M. Quiros, Nucl. Phys. **B283** (1987) 111.

103. R. Barbieri, G. Gamberini, G. F. Giudice, and G. Ridolfi, Nucl. Phys. **B296** (1988) 75.

104. A. Bartl, W. Majerotto and N. Oshimo, Phys. Lett. **B216** (1989) 233.

105. J. Ellis, J. F. Gunion, H. E. Haber, L. Roszkowski, F. Zwirner, Phys. Rev. **D39** (1989) 844.

106. I. Antoniadis, J. Ellis, J. S. Hagelin and D. V. Nanopoulos, Phys. Lett. **194B** (1987) 231; Phys. Lett. **208B** (1988) 209; CERN preprint CERN-TH.5442 (1989).

107. D. P. Roy, *Proceedings of the 23rd International Conference on High Energy Physics*, Berkeley, July 1986, p. 387.

108. J. Ellis, K. Enqvist, D. V. Nanopoulos and F. Zwirner, Nucl. Phys. **B276** (1986) 14.

109. J. F. Gunion, H. E. Haber and L. Roszkowski, Phys. Lett. **189B** (1987) 409; Phys. Rev. **D38** (1988) 105.

110. V. Barger and K. Whisnant, Int. J. Mod. Phys. **A3** (1988) 1907.

111. E. Ma, Phys. Rev. **D36** (1987) 274; K. S. Babu, X.-G. He and E. Ma, Phys. Rev. **D36** (1987) 878.

112. S. L. Glashow and E. E. Jenkins, Phys. Lett. **B196** (1987) 233; V. Barger and R. J. N. Phillips, Univ. of Wisc. preprint MAD/PH/497 (1989).

113. See for example J. A. Grifols and A. Mendez, Phys. Rev. **D22** (1980) 1725.

114. Note that this expression is slightly different from the one given in Ref. 112; the two expressions are equivalent in the minimal case considered below.

115. Note that some earlier papers, e.g., Ref. 6, seem to have taken a coupling proportional to $\frac{1}{4} - \sin^2\theta$ rather than $\frac{1}{2} - \sin^2\theta$, which leads to a large suppression of the decay width.

116. J. H. Kühn, P. M. Zerwas et al, Heavy Flavors, this report, Vol. 1 (1989).

117. See for example H. Baer and X. Tata, Phys. Lett. **167B** (1986) 241.